ANALYSIS OF FLOW ALONG THE MEANDER PATH OF A HIGHLY SINUOUS RIGID CHANNEL

A Thesis Submitted in Partial Fulfilment of the Requirement for the Degree of

Master of Technology

In

Civil Engineering

ARPAN PRADHAN

DEPARTMENT OF CIVIL ENGINEERING

NATIONAL INSTITUTE OF TECHNOLOGY, ROURKELA

2014

ANALYSIS OF FLOW ALONG THE MEANDER PATH OF A HIGHLY SINUOUS RIGID CHANNEL

A Thesis

submitted by

ArpanPradhan

(211CE4492)

In partial fulfilment of the requirements

for the award of the degree of

Master of Technology

In

Civil Engineering

(Water Resources Engineering)

Under The Guidance of

Dr. K. K. Khatua

Department of Civil Engineering

National Institute of Technology, Rourkela

Orissa -769008, India

May 2014

DEPARTMENT OF CIVIL ENGINEERING
NATIONAL INSTITUTE OF TECHNOLOGY, ROURKELA

DECLARATION

I hereby state that this submission is my own work and that, to the best of my knowledge and belief, it contains no material previously published or written by any other person nor substance which to a substantial extent has been accepted for the award of any other degree or diploma of the university or other institute of higher learning, except where due acknowledgement has been made in the text.

ARPAN PRADHAN

DEPARTMENT OF CIVIL ENGINEERING
NATIONAL INSTITUTE OFTECHNOLOGY,ROURKELA

CERTIFICATE

This is to certify that the thesis entitled **"Analysis of Flow along the Meander Path of a Highly Sinuous Rigid Channel"** is a bonafide record of authentic work carried out by **Arpan Pradhan** under my supervision and guidance for the partial fulfilment of the requirement for the award of **Master of Technology** degree in **Civil Engineering** with specialization in **Water Resources Engineering** at the National Institute of Technology, Rourkela.

The results embodied in this thesis have not been submitted to any other University or Institute for the award of any degree or diploma.

Date:

Place: Rourkela

Prof. K.K. Khatua
Associate Professor
Department of Civil Engineering
National Institute of Technology, Rourkela

ACKNOWLEDGEMENTS

I would like to give my heart-felt thanks first to my supervisor, **Prof. K .K. Khatua**, whose profound knowledge of hydraulic engineering helped me from the first day of my research to the eventual completion of my project. His invaluable guidance, warm encouragement and continuous support have made this research easier. I know very well that without his enthusiastic supervision and hard work, it would have been impossible to finish this study on time.

I would like to extend my thanks to all the professors of Water Resources department for the kind co-operation and necessary advice they have provided whenever required. I am grateful for friendly atmosphere of the Water Resources Engineering Department. I would like to thank the staff members and students associated with the Fluid Mechanics and Hydraulics Laboratory of Civil Engineering Department for their help and support.

I extend my sincere thanks to **Ms. Saine Sikta Dash** and **Mr. Kirtikanta Sahoo**, P.hd Scholars and **Debashish**, B.Ttech Student of Civil Engineering Department for their assistance and encouragement during my work.

I wish to thank all of my friends, for their kind help and support extended during my course of study.

I would like to thank my parents and family members, for their love, patience and support, without which I could not have completed this work.

Arpan Pradhan

ABSTRACT

Despite substantial research on various aspects of velocity distribution in curved meander rivers, no systematic effort has been made to analyse the variation of velocity profile along a meander path. In this research work, variation of velocity profile along the width and depth of the channel has been methodically analysed at different cross-sections (13 sections) along a meander path of a sinuous channel of 120° cross-over angle. The meander path considered is from one bend apex to the next bend apex which changes its course at the cross-over. Bend apex is the position of maximum curvature and cross-over represents the section at which the sinuous channel changes its sign.

The study is thoroughly done to find the changes in the water surface profile throughout the meander path, where the height of water always remaining higher towards the outer wall of the curved channel. Longitudinal velocity distributions along the width and depth of the channel, i.e., the horizontal and vertical velocity profiles are investigated with the higher velocity remaining towards the inner wall of the channel unlike straight channels. As the channel changes its curvature, so does the movement of higher velocity which moves from one bank towards the other. Boundary shear stress distribution along different points of the wetted perimeter on the channel bed is also obtained at all the above sections to investigate its deviation along the meander path. This helped to compute the total shear force at each of these sections. Hence these features can be considered by engineers and researchers in the field of sediment erosion, deposition, etc.

Keywords: *bend apex, meander path, cross-over, longitudinal velocity distributions, boundary shear stress*

TABLE OF CONTENTS

LIST OF TABLES

LIST OF PHOTOS

LIST OF FIGURES

LIST OF SYMBOLS

SYMBOL	DESCRIPTION
A	Cross-sectional Area of Channel
C	Chezy's channel coefficient
C_d	Coefficient of Discharge
d	Diameter of Preston tube
f	Darcy-Weisbach Friction factor
g	Acceleration due to Gravity
h	Pressure Difference
H	Average flow Depth of water at a Section
h_w	Height of Water
H_n	Height of water above the Notch
L	Length of Channel for one Wavelength
L_n	Length of Rectangular Notch
n	Manning's Roughness Coefficient
ΔP	Differential Pressure
Q_a	Actual Discharge
Q_{th}	Theoretical Discharge
r_c	Radius of Curvature of a Sinuous Channel
ρ	Density of the Flow
S	Bed Slope of the Channel
S_r	Sinuosity
SF_{Bed}	Shear Force at the Bed of the Channel
SF_{Inner}	Shear Force at the Inner Wall of the Channel Section
SF_{Outer}	Shear Force at the Outer Wall of the Channel Section
SF_T	Total Shear Force

τ_c'	Average Shear Stress
τ	Boundary Shear Stress
υ	Kinematic Viscosity
V_w	Volume of Water
v	Point Velocity
W	Width of Channel
x^*, y^*	Non-Dimensional Parameters
λ	Wavelength of a Sinuous Channel

CHAPTER 1
INTRODUCTION

1.1 MEANDERING CHANNEL

Almost all rivers are sinuous to some extent. A river is considered straight, if its length is straight for about 10 to 12 times its channel width, which is not usually possible in natural conditions. Sinuosity is defined as the ratio of valley slope to channel slope. Rivers having sinuosity greater than 1.5 are considered to be meandering.

River defines its own path. Meandering of a river is a very complicated process involving flow interaction during bends, erosion and sediment transport. **Inglis (1947)** stated that river bends erode during floods due to excess turbulent energy for which it widens and shoals. With fluctuating discharges and silt formation, there is a tendency for silt to deposit at one bend and move towards the other. **Levliasky (1955)** suggested the centrifugal force to be the factor causing meandering of a river, due to the helicoidal cross-current formation. **Chang (1984)** suggested that "as a general rule, the channel slope cannot exceed the valley slope under the state of equilibrium. If the discharge and load are such that the channel slope so produced exceeds the valley slope, the dynamic changes in the form of aggradations will occur, resulting in steepening of the valley slope. As the channel slope cannot exceed the valley slope under the state of equilibrium, it must either be equal or less than the valley slope. The meander channel pattern represents a degree of channel adjustment so that a river with a flatter channel slope can exist in a steeper valley slope".

River continuously adjusts itself with respect to its ability to balance the water discharge and sediment load supplied from the watershed. These adjustments, likely changes in the channel geometry, side slope, meandering pattern, roughness etc., are made such that the river undergoes minimum energy expenditure in transportation of its load.

1.2 MEANDER PATH

Meander path is a flow path undertaken by a river. The meander path under study is taken from one bend apex to the next bend apex. Bend apex or the axis of bend is the section at which the river has the maximum curvature. A channel while moving from one bend apex to the other passes through the cross-over. Cross-over is a section at the point of inflection where the meander path changes its course as shown in Fig. 1.1. The concave bank or the outer bank becomes the convex bank or the inner bank after the cross-over and similarly the convex bank or the inner bank becomes the concave bank or the outer bank. In the Fig.1.1 W represents the width of the channel, λ represents the wavelength, L represents the length of channel for one wavelength and r_c represents the radius of the channel.

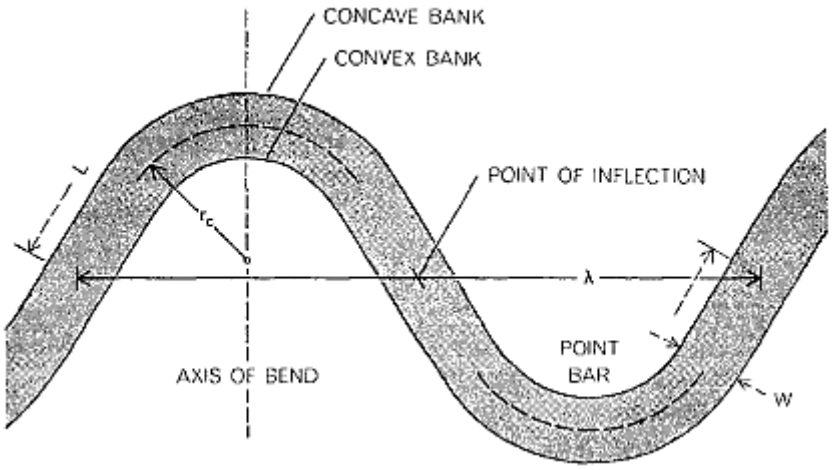

Fig. 1.1: Properties of River Meander (Leopold and Langbein, 1966)

1.3 VELOCITY DISTRIBUTION

Velocity distribution helps to identify the velocity magnitude at each point across a flow section. Numerous researcheshas been doneon various aspects of velocity distribution in curved meander rivers, but no systematic effort has been made to study the variation of velocity along a meander path. In straight channel velocity distribution varies with different width-depth ratio, whereas in meandering channel velocity distribution varies with aspect

ratio, sinuosity, etc. making the flow more complex to investigate. In laminar flow max stream wise velocity occurs at water level; for turbulent flows, it occurs at about 5-25% of water depth below the water surface **(Chow, 1959)**.Typical stream wise velocity contour lines (isovels) for flow in various cross sections are shown in Fig. 1.2.

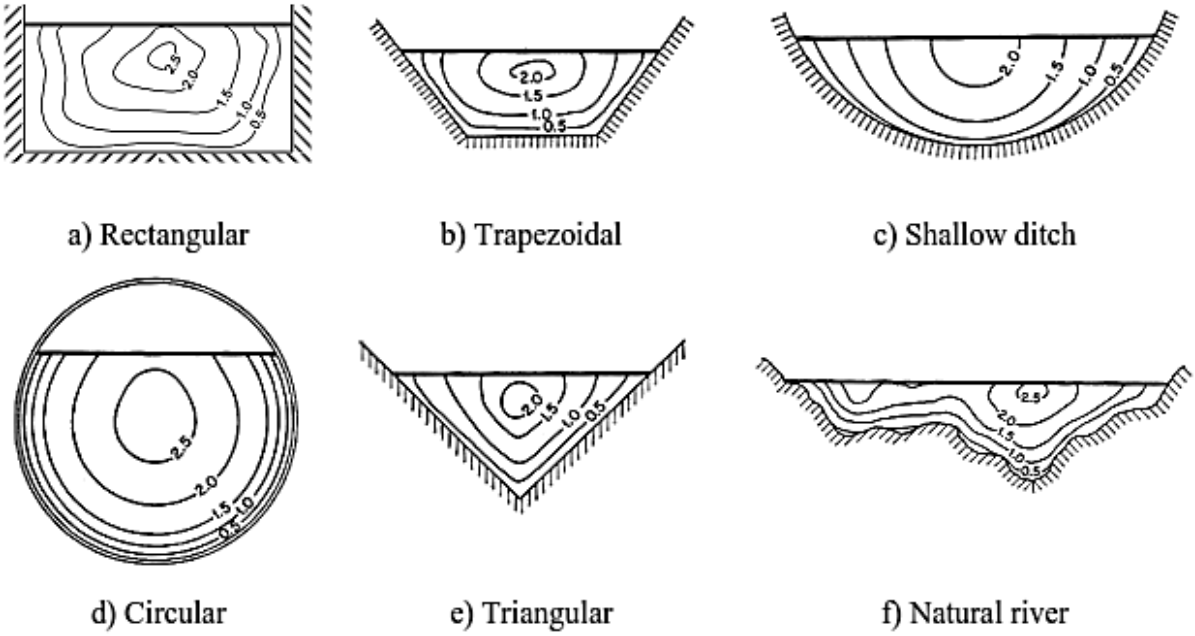

Fig.1.2: Contours of constant velocity in various open channel sections (Chow, 1959)

The above velocity contours satisfy for straight channels as the maximum velocity is considered to be present somewhere in the middle of the cross-section below the free water surface. This condition is not true in the case of meandering river as the local maximum velocity is seen to occur at the inner wall or the convex side of the channel. In this project the experimental channel under study changes its course, and both the clockwise and anticlockwise curves of the meandering channel are analysed. Hence the movement of velocity can be studied from one bank of the channel to the other bank. The detailed investigation of velocity distribution along the depth and width of a channel is also essential in many hydraulic engineering studies involving bank protection, sediment transport, conveyance, water intakes and geomorphologic investigation.

1.4 BOUNDARY SHEAR

Water flowing in an open channel is opposed by resistance from the bed and side slopes of the channel. This force of resistance is apparently the boundary shear force. Boundary shear stress is the tangential component of the hydrodynamic forces acting along the channel bed. Flow characteristics of an open channel flow are directly dependent on the boundary shear force distribution along the wetted perimeter of the channel.

Computation of bed form resistance, channel migration, side wall correction, sediment transport, dispersion, cavitations and conveyance estimation, etc. can be studied and analysed by the boundary shear stress distribution.

The shear force, for steady uniform flow is related to bed slope, hydraulic radius and unit weight of fluid. However in a practical point of view, these forces are not uniform even for straight prismatic channels. The non-uniformity of shear stress is mainly due to secondary currents formed by the anisotropy between vertical and transverse turbulent intensities, given by **Gessner (1973)**. **Tominaga *et al.* (1989)** and **Knight and Demetriou (1983)** demonstrated that boundary shear stress increases when the secondary currents flow towards the wall and shear stress decreases when it flows away from the wall. The presence of secondary flow cells in main channel affects the distribution of shear stress along the channel's wetted perimeter which is illustrated in Fig. 1.3. Other factors affecting the shear stress distribution are the shape of channel cross-section, depth of flow, later-longitudinal distribution of wall roughness and sediment concentration. For the case of meandering channels, the factors increase even more due to the nature of flow of water in such channels. Sinuosity in the case of meandering channel is regarded to be a critical parameter in the shear stress distribution along the channel bed and walls.

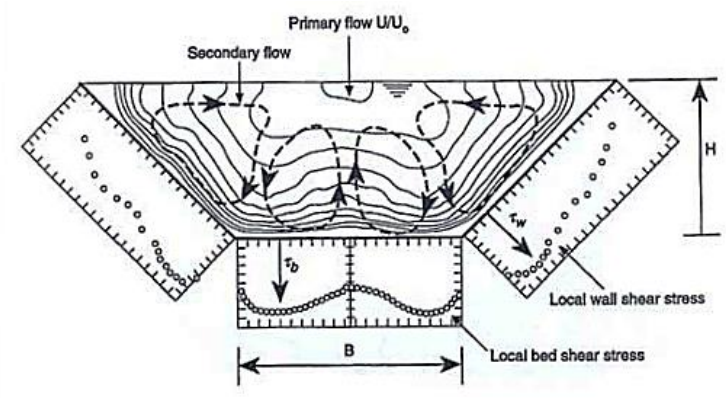

Fig.1.3: Schematic influence of secondary flow cells on boundary shear distribution in a trapezoidal section (Knight *et al.*, 1944)

1.5 OBJECTIVES OF THE RESEARCH

The current work is intended to examine the various flow characteristics of a meandering path of a 120°cross-over angle meandering channel. Although considerable research has been carried out on flow characteristics of open channel curves with different angles, but not much research has been done along a path of meandering channel which is preceded and followed by the meandering channel of same sinuosity. The path being a part of a longer meandering channel helps to acquire more precise information about its characteristics which can then be applied to real field conditions.

The objectives of the present work are summarized as:

- Study of change in the water surface profile as the water moves in the meander path, changing its course of travel at the cross-over.
- Determination of horizontal profile of longitudinal velocity along the width of channel. The horizontal profiles are studied at the bed, 0.4*H*, 0.6*H* and 0.8*H* above the channel bed. *H* being the average depth of flow of water at the corresponding section. The horizontal profile helps to analyse the movement or position of maximum velocity at every section along the meander path.

- Determination of vertical profile of longitudinal velocity along the depth of channel. The vertical profiles are studied at equal intervals of 4cm along the width of the channel at every section. The study helps to understand the detailed characteristic of velocity distribution throughout the channel section and also along the meander path.
- Analysis of boundary shear stress along the bed and side slopes of every channel section along the meander path. The study helps to determine the variation of shear stress at a section and how it changes along the path of the channel.
- Study of distribution of boundary shear force along the channel bed and the side slopes at every section. This examines the sharing of shear force between the bed and the side slopes at an individual section and how the sharing changes along the meander path.

1.6 THESIS STRUCTURE

The thesis consists of five chapters. General introduction is provided in Chapter 1, Chapter 2 contains literature survey, experimental work and the methodology is described in Chapter 3, experimental results are illustrated and analysis of results are done in Chapter 4, Chapter 5 contains the conclusions drawn from the analysis and then the references are presented.

Chapter 1 represents a general view about meandering channels and about meander path. Concept of velocity distribution and boundary shear is also described.

Chapter 2 gives detailed literature study by other researcher on velocity distribution and boundary shear. The previous research works arranged according to the year of publication with the latest work at the latter.

Chapter 3 gives details about the construction of the channel and the apparatus and equipments used. The methodology adopted for obtaining velocity distribution, boundary shear stress and boundary shear force is also discussed.

Chapter 4 illustrates the experimental results which are then analysed. The results discussed are the water surface profile, the horizontal velocity distribution, the vertical velocity distribution, and the boundary shear stress distribution at thirteen different sections along the meander path of the highly sinuous channel

Finally Chapter 5 summarizes the conclusions reached by the research and the recommendations for further work are listed.

Reference made in the subsequent chapters is provided at the end of the thesis.

CHAPTER 2
LITERATURE REVIEW

2.1 OVERVIEW

In this chapter a detailed literature survey is prerequisite to any expressive and successful research in any subject. The present work is no exception and hence a focused and intensive review of literature was carried out covering various aspects concerning the meandering channels. In the literature review the researchers' studied mainly on hydraulic engineering problem which was related to the behaviour of rivers and channels collected to obtain the various features and characteristics of meandering rivers. Almost river systems, analysis of its velocity distribution, boundary shear distribution along its meander path study is very critical. In ariverthe flow characteristics is overbearing for different conditions such as flood control, channel design, and renewal projects include the transport of pollutants and sediments. Flow in meandering channels is common for natural rivers, and research work was conducting in this type of channel for flood control, discharge estimation and stream restoration.

Flow structure in meandering channels is erratic as compared to straight channels. This is due to the velocity distributions in meandering paths as demonstrated by researchers.The degree of meandering was calculated by the term of sinuosity, which is defined as the ratio of channel length to valley length. **Chow (1959)** described the degree of meandering as follows:

Table 2.1:-Degree of meandering

Sinuosity ratio	Degree of meandering
1.0 - 1.2	Minor
1.2 - 1.5	Appreciable
1.5 and greater	Severe

In a meander path the flow analysis is not only limited to its velocity distribution but also the shear force variations for the bed is also studied to get an outline of the shear force sharing in meander path of different section in between them. This chapter is therefore divided into sections related to the previous research carried out on velocity distributions and boundary shear force distribution of meandering channels.

The prediction of the flow characteristics in meandering channels is a challenging task for rivers engineers due to the three-dimensional nature of flow. The dominant feature consists of the interaction effect between the fast moving flows in the meandering channel. This results in a high shear layer at the meandering channel, leading to the generation of large-scale vortices with vertical axes, and depth-scale vortices with longitudinal axes. However, the focus of the current work is on modelling flow in meandering channels.

2.2 PREVIOUS RESEARCH ON LONGITUDINAL VELOCITY DISTRIBUTION

The longitudinal velocity represents the speed at which the flow is moving in the stream wise direction. If a number of velocity measurements are taken throughout the depth across the channel, it is possible to produce a distribution of the isovels that represents contour lines. Each of these lines stands for the same velocity magnitude across the channel. The isovels reach values as low as zero in the vicinity of the channel perimeter and increase to a maximum value below the water surface in the area surrounding the centre of the channel. These isovels are affected by the secondary currents that result in a bulge in their distribution.

Thomson (1876) studies concerning the flow in meandering channels are mentioned for they provide insight to the nature and characteristics of flow and associated mechanisms occurring in a simple meandering channel where the course of river or flume keeps on changing along its path.

Coles (1956) proposed a semi-empirical equation of velocity distribution, which can be applied to outer region and wall region of plate and open channel.

The Soil Conservation Service (1963) proposed an empirically-based model which gives to account for meander losses by adjusting the basic value of Manning's *n* using sinuosity of the channel only. The adjusted value of Manning's *n* was proposed for three different ranges of sinuosity.

Toebes and Sooky (1967) conducted experiments in a small laboratory channel with sinuosity 1.09. From the experimental results they concluded that energy loss per unit length for meandering channel was up to 2.5 times as large as those for a uniform channel of same width and for the same hydraulic radius and discharge. They proposed an adjustment to the roughness *f* as a function of hydraulic radius below a critical value of the Froude number.

Chang (1983) investigated energy expenditure in curved or meandering channels and derived an analytical model for obtaining the energy gradient, based on fully developed secondary circulation. By making simplifying assumptions he was able to simplify the model for wide rectangular sections.

Johannesson and Parker (1989a) presented an analytical model for calculating lateral distribution of depth averaged primary flow velocity in meandering rivers. Using an approximate "moment method" they accounted for the secondary flow in the convective transport of primary flow momentum, yielding satisfactory results of the redistribution of primary flow velocity.

James (1994) reviewed the various methods for bend loss in meandering channel proposed by different investigators. He tested the results of the methods using the data of FCF, trapezoidal channel of Willets, at the University of Aberdeen, and the trapezoidal channels measured by the U.S. Army Corps of Engineers at the Waterways Experiment Station, Vicksburg. He proposed some new methods accounting for additional resistance due to bend by suitable modifications of previous methods. His modified methods predicted well the stage discharge relationships for meandering channels.

Shiono, *et. al*. (1999) investigated the effect of sinuosity and bed slope on the discharge assessment of a meandering channel. Dimensional analysis was used to derive the conveyance capacity of a meandering channel which facilitated in finding the stage-discharge

relationship for meandering channels. The study showed that the discharge increased with an increase in bed slope and decreased with increase in sinuosity for the same channel.

Sarma, *et al*. (2000) tried to formulate the velocity distribution law in open channel flows by taking generalized version of binary version of velocity distribution, which combines the logarithmic law of the inner region and parabolic law of the outer region. The law developed by taking velocity-dip in to account.

Patra, Kar and Bhattacharya (2004) demonstrated the longitudinal velocity distribution for meandering channels are strongly considered by flow interaction. By taking all the interaction effect, they proposed empirical equations which were found to be in natural rivers. Here experimental results are validating with other smooth and rough sections of symmetrical and unsymmetrical channels.

Wilkerson, *et al*. (2005) developed two models which is predicting depth-averaged velocity distributions using data from previous investigators forstraight trapezoidal channels. The 1st model gives velocity data for calibrating the model coefficients, and 2nd model used for prescribed coefficients. When depth-averaged velocity data are available that time 1st model is recommended. When predicted depth-averaged velocities are expected to be within 20% of actual velocitiesthen 2nd model is used.

Patra and Khatua (2006) observed roughness coefficient that Manning's *n*, Chezy's C, Darcy's *f* not only denotes the roughness characteristics of a channel but also the energy loss in the flow of channels.

Afzal *et al*. (2007) analyzed power law velocity profile in fully developed turbulent pipe and channel flows in terms of the envelope of the friction factor. This model gives good approximation for low Reynolds number in designed process of actual system compared to log law.

Khatua (2008) gives the result of energy loss in a meandering channel. It is calculated in different depth of flow which gives the resistance factors Manning's *n*, Chezy's *C*, and Darcy-Weisbach *f* for meandering channel. Stage-discharge relationship from in-bank to the over-bank flow is given.

Pinaki (2010) analysed a series of laboratory tests for smooth and rigid meandering channels and developed mathematical equation using dimension analysis to evaluate roughness coefficients of smooth meandering channels of less width ratio and sinuosity.

Seo and Park (2010) carried out laboratory and numerical studies to find the effects of secondary flow on flow structures and dispersion of pollutants in curved channels. Primary flow is found to be skewed towards the inner bank at the bend while flow becomes symmetric at the cross-over.

Absi (2011) analytic solution of the Reynolds-Averaged Navier-Stokes equation was carried out to get ordinary differential equation for velocity distribution in open channel. The proposed equation was helpful in predicting the maximum velocity below the free surface. Two different degrees of approximation was done. A semi-analytical solution of the proposed ordinary differential equation for the full dip-modified-log-wake law and another simple dip-modified-log-wake law. Numerical solution of the ordinary differential equation and velocity profiles of the two laws are compared with the previously published experimental data.

Bonakdri *et. al*. (2011) studied numerical analysis of a flow field of a 90° bend. Prediction of data was carried out by using Artificial Neural Network and Genetic Algorithm. CFD model was used to investigate the flow patterns and the velocity profiles. ANN was used to predict data at locations were experimental data was not available.

Baghalian *et. al.* (2012) studied the velocity field in a 90° bend channel. Investigations were carried out by using artificial intelligence, analytic solutions and numerical methods.

Experimental results were compared with the models with ANN and numerical methods which gave better performance than analytic solutions.

Khatua and Patra (2012) developed a mathematical model using dimension analysis by taking series of experiments data to evaluate roughness coefficientsfor smooth and rigid meandering channels. The vital variables are required for stage-discharge relationship such as velocity, hydraulic radius, viscosity, gravitational acceleration, bed slope, sinuosity, and aspect ratio.

Khatua *et. al.* (2013) proposed a discharge predictive method for meandering channels taking into account the variation of roughness with depth of flow. The performance of the model was evaluated by comparing with several other models of different researchers.

Dash (2013) analysed the important parameters affecting the flow behaviour and flow resistance in term of Manning's*n* in a meandering channel. Factors affecting roughness coefficient are non-dimensionalized to predict and find their dependency with different parameters. A mathematical model was formulated to predict the roughness coefficient which was applied to predict the stage-discharge relationship.

Mohanty (2013) predicted lateral depth-averaged velocity distribution in a trapezoidal meandering channel. A nonlinear form of equation involving overbank flow depth, main channel flow depth, incoming discharge of the main channel and floodplains etc. was formulated. A quasi1D model Conveyance Estimation System (CES) was applied to the same experimental compound meandering channel to validate with the experimental depth averaged velocity.

2.3 PREVIOUS RESEARCH ON BOUNDARY SHEAR

In straight channels, the longitudinal velocity in the channel is generally faster. This causes a shear layer at the interface of straight channel. Due to the presence of this shear layer, the flow in the straight channel decreases due to the effects of the faster flow. This result gives

that the flows decreases the whole discharge of the cross section, **Knight and Mohammed (1984)**. **Wormleaton (1996)** stated that the effects of this shear layer extend across the width of the floodplain and it decreases to reach zero toward the outer edges of the floodplain. **Myers (1978)** found that the effects of the shear layer were greater at lower overbank flow depths and decrease as the flow increases. **Rajaratnam and Ahmadi (1981)** showed that the boundary shear stress reduces from the centre of the meandering channel toward the edge of the meandering channel. Then it sharply increases at the interface with the edges, afterwards it decreases and levels off for most of the width and finally decreases near the wall. They also concluded that the effect of the meandering channel is to reduce the boundary shear stress. This is a direct effect of the reduction of velocity in the meandering channel resulting from the slow moving flow towards wall. This shear stress is highly affected by the secondary currents since according to **Tominaga *et. al.* (1989)** and **Knight and Demetriou (1983)**, it increases where the secondary currents flow toward the wall and decreases when they flow away from the wall. Many other aspects affect the boundary shear stress distribution across the channel. In fact, **Rhodes and Knight (1994)** stated that the bank slope had significant effects on the boundary shear stress distribution at the interface between the main channel and floodplain. Adopting a model that predicts accurately the boundary shear stress distribution across the channel is crucial for river engineers since it governs sediment transport, bank erosion and morphology.

Leighly (1932) studied the boundary shear stress distribution in open-channel flow by using conformal mapping. He pointed out that, in the absence of secondary currents, the boundary shear stress acting on the bed must be balanced by the downstream component of the weight of water contained within the bounding orthogonal shear layer

Cruff (1965) estimate the boundary shear stress by the use of the Preston tube technique as well as the Karman-Prandtl logarithmic velocity-law from uniform flow in a rectangular

channel. Though he did not calculate boundary shear stresses distribution in a rectangular channel with overbank flow, mainly his work was known for a method which was help to calculate the apparent shear stress and momentum transfer between a channel and its flood plain.

Ghosh and Jena (1972) gives the boundary shear distribution for rough and smooth in a compound channel. Using the Preston tube technique combined with the Patel calibration, they found the boundary shear distribution along the wetted perimeter of the total channel for various depths of flow. From the analysis, it is clearly shows that the maximum shear stress on the channel bed and approximately midway between the centre line and corner.

From the experimental analysis the shear distribution is probable to estimate τ_c' the average shear stress in the channel. It is analysed that roughening the total periphery of the boundary shear in the meandering channel could be redistributed with the maximum shear at the channel bed.

Rajaratnam and Ahmadi (1979) were doing experimental work in a channel 18.29 meters long, 1.22 meters wide and 0.9 meters deep. Here, they recorded the velocity traverses and boundary shear stresses. They analysed velocity profiles at different depths in the channel exhibited similarity.

Bathurst *et al.* (1979) obtainable the field data for calculating the bed shear stress in a curved river and it is obtained that the bed shear stress distribution is affected by both the location of core of the main velocity and the structure of secondary flows.

Knight and Demetriou (1983) carried out series of experiments in straight symmetrical compound channels to find the characteristics of discharge, boundary shear stress and boundary shear force distributions. Equations to calculate the percentage of shear force carried by the floodplain were being proposed. The apparent shear force was observed to be

higherat the lower flow depth. For high floodplain widths for vertical interface between main channel and floodplain the apparent shear force was also found to be higher.

Knight and Patel (1985) take the laboratory experiments results which concerning the boundary shearsdistribution in smooth rectangular cross section for different aspect ratios between 1 and 10. The boundary shear distributions were shown to be subjective by the number and shape of the secondary flow cells, which, was depended mainly on the aspect ratio. Equations were given for the maximum, centreline and mean boundary shear stresses on the channel walls in terms of the aspect ratio.

Knight, Yuan and Fares (1992) gives the experimental data of SERC-FCF about the boundary shear stress distributions in meandering channels through the path of one complete wave length. They also reported the experimental data on surface topography, velocity vectors, and turbulence for meandering channels. They studied the effects of channel sinuosity, secondary currents, and cross section geometry on the value of boundary shear in meandering channels and presented a momentum-force balance for the flow.

Shiono, Muto, Knight and Hyde (1999) presented the secondary flow and turbulence data using two components Laser- Doppler anemometer. They developed the turbulence models, and studied the behaviour of secondary flow for both in bank and over bank flow conditions. They divided the channel into three sub areas, namely (i) the main channel below the horizontal interface (ii) the meander belt above the interfaces and (iii) the area outside the meander belt of the flood plain. They investigated the energy losses for compound meandering channels resulting from boundary friction, secondary flow, turbulence, expansion and contraction. They reported that the energy loss at the horizontal interface due to shear layer, the energy loss due to bed friction and energy loss due to secondary flow in lower main channel have the significant contribution to the shallow over-bank flow. They also concluded

that the energy loss due to expansion and contraction in meander belt have the significant contribution to the high over-bank flow.

Knight and Sterling (2000) analysed the boundary shear distribution in a circular channels flowing partially full with and without a smooth flat bed using Preston-tube technique. The results have been analysed that the variation of local shear stress with perimeter distance and the percentage of total shear force acting on wall or bed of the channel. The %SFW results have been validating with Knight's (1981) empirical formula for prismatic channels.

Patra and Kar (2000) reported the test results concerning the boundary shear stress, shear force, and discharge characteristics of compound meandering river sections composed of a rectangular main channel and one or two floodplains disposed of to its sides. They used five dimensionless channel parameters to form equations representing the total shear force percentage carried by floodplains. A set of smooth and rough sections were studied with aspect ratio varying from 2 to 5. Apparent shear forces on the assumed vertical, diagonal, and horizontal interface plains were found to be different from zero at low depths of flow and changed sign with increase in depth over floodplain. They proposed a variable-inclined interface for which apparent shear force was calculated as zero. They presented empirical equations predicting proportion of discharge carried by the main channel and floodplain.

Jin *et. al.* (2004) proposed a semi analytical model for prediction of boundary shear distribution in straight open channels. Secondary Reynolds stress terms were involved to develop the simplified stream-wise vorticity equation. An empirical model was generated for computing the effect of the channel boundary on shear stresses.In the calculation of the boundary shear distribution in trapezoidal open channels, the model predictionswere in good agreement with the experimental data.

Duan (2004) found that a 2D model could be better because of being computationally cost-effective for parametric analyses needed by policy and management planning as well as

preliminary design applications. Because they compared the flow analysis in mildly and sharply curved or meandering channels through the use of depth averaged 2-D model and full 3-D model and established that the last one is more skilled than the previous in taking the flow fields in meandering channels. Finally the author concluded that the 1D, 2D and 3D numerical models should be integrated and cost effectiveness.

Patra and Kar (2004) reported the test results concerning the flow and velocity distribution in meandering compound river sections. Using power law they presented equations concerning the three-dimensional variation of longitudinal, transverse, and vertical velocity in the main channel and floodplain of meandering compound sections in terms of channel parameters. The results of formulations compared well with their respective experimental channel data obtained from a series of symmetrical and unsymmetrical test channels with smooth and rough surfaces. They also verified the formulations against the natural river and other meandering compound channel data.

Khatua (2008) extended the work of **Patra and Kar (2000)** to meandering compound channels. Using five parameters (sinuosity S_r, amplitude, relative depth, width ratio and aspect ratio) general equations representing the total shear force percentage carried by floodplainwaspresented. The proposed equations are simple, quite reliable and gave good results with the observed data for straight compound channel of **Knight and Demetriou (1983)** as well as for the meandering compound channel.

Khatua (2010) reported the distribution of boundary shear force for highly meandering channels having distinctly different sinuosity and geometry. Based on the experimental results, the interrelationship between the boundary shear, sinuosity and geometry parameters has been shown. The models are also validated using the well published data of other investigators.

Patnaik (2013) studied boundary shear stress at the bend apex of a meandering channel for both in bank and overbank flow conditions. Experimental data were collectedunder different discharge and relative depths maintaining the geometry, slope and sinuosity of the channel.Effect of aspect ratio and sinuosity on wall (inner and outer) and bed shear forces were evaluated and equation was developed to determine the percentage of wall and bed shear forces in smooth trapezoidal channel for in bank flows only. The proposed equations were compared with previous studies and the model was extended to wide channels.

CHAPTER 3
EXPERIMENTAL SETUP AND PROCEDURE

3.1 OVERVIEW

Experimental work on natural rivers is very complicated; hence the flow characteristics of a river can be analysed by studying them on a model designed close to natural rivers. Rivers are generally meandering in nature, having different sinuosity throughout their path. Flow patterns are studied on experimental models for different sinuosity and can then be used to model them on natural channels.

To study the flow patterns and characteristics of meandering rivers, a highly sinuous channel is constructed and the different velocity and shear changes are measured for the entire meander path. The study helps to analysis the movement of rivers in natural meanders.

3.2 DESIGN AND CONSTRUCTION OF CHANNEL

Experimental channel was built in a large tilting flume of 4m wide and 15 long. The flume has an arrangement of hydraulic jacks to produce different bed slopes on tilting. This total arrangement is made available at the Fluid Mechanics and Hydraulics Laboratory of NIT, Rourkela. A meandering channel has been built within the tilting flume with Perspex sheets to carry out the experimentations. The Perspex sheets are of 6mm to 10mm thick.

The meandering channel is constructed having a bank full depth of 0.065m with a bottom width of 0.33m and 1:1 side slopes.Fig. 3.1 illustrate the schematic view of the channel setup. The main channel is a sinuous channel, similar to a sine curve of one and half wave length. The total wavelength being λ = 2.162m which is preceded and followed by a bell mouth section for proper flow field development at the experimental which is from the second bend apex to the next bend apex of the central curve.

Water into the channel is circulated from an underground sump to an overhead tank with the help of centrifugal pumps. Overhead tank is helpful in maintaining a constant head of water, where the excess water is allowed to flow back into the sump.

Water comes into the flume from the overhead tank through adjustable pipes which can be used to maintain a desired quantity of discharge. This water falling into the flume is first held in a stilling tank. Then it is directed through an adjustable vertical gate into a series of baffle wall suitable ahead of the rectangular notch. These arrangements are done to reduce the turbulence of the incoming water. Water from the notch falls over a wire mesh placed just below the notch, to further steady the flow.Water then flows into the main channel through a smooth bell mouth transition section so as to achieve a more steady flow in the channel. The flow attains a Quasi-Uniform flow.

Water flows in the channel due to gravity, accomplished by providing a slight slope to the tilting flume. The flow of water after running through the main channel is directed into a volumetric tank through an adjustable tailgate. The volumetric tank is connected to the underground sump. The volumetric tank is utilized to measure the actual discharge of flow; otherwise the water is allowed to move into the underground sump. Hence a complete recirculation of water is achieved.

All the measurements are observed from the second bend apex to the next corresponding bend apex of the experimental channel from the upstream end. Observations are recorded under steady and uniform conditions. A moving bridge arrangement is provided along the width of the channel of around 1.2m width by 4m length across the channel. The measuring instruments such as point gauges and Pitot tubes are arranged on the bridge such that each section along the meander path is accessible for measurements.

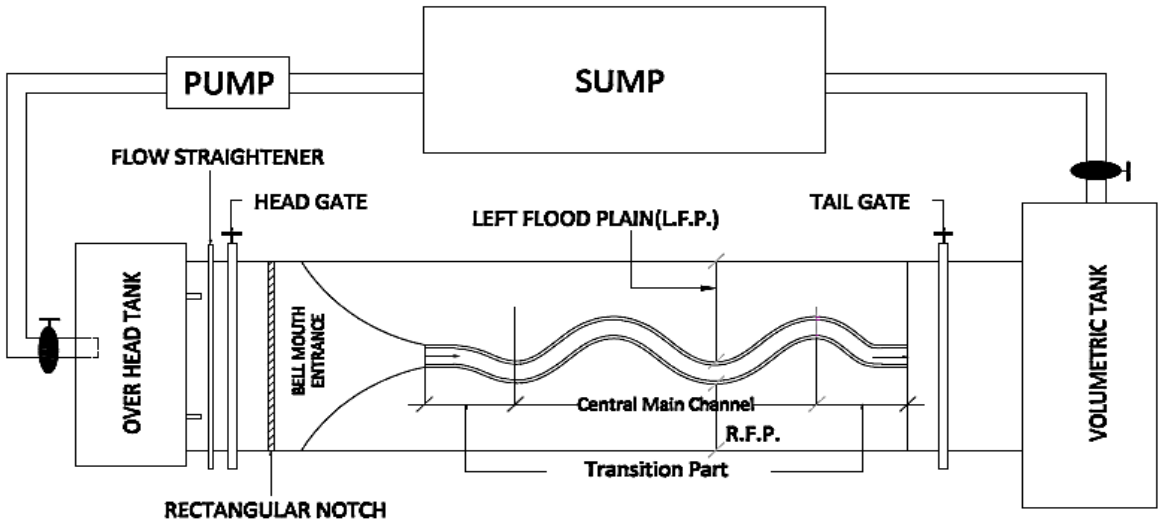

Fig.3.1. Schematic Diagram of Experimental Meandering Channels with Setup

3.3 APPARATUS AND EQUIPMENTS USED:-

The moving bridge arrangement is fitted with five Pitot tubes which are unequally spaced with an external diameter of 4.7mm along with a pointer gauge of least count 0.1mm. The moving bridge is traversed across the meander path to every section and respective readings are taken. The pointer gauge is utilized to find out the water surface profile across the channel width at every section. The set of Pitot tubes measure the pressure difference at every predefined location across every section. Velocity at those points is the calculated from the pressure difference. All the Pitot tubes are connected to five different manometers which are arranged on a vertical board having a spirit level. The spirit level helps to maintain the verticality of the manometers. A rectangular notch arrangement is provided at the upstream section to maintain and calculate the discharge of water into the meandering channel. The following photographs show the measuring devices used for data collection.

Photo 3.1: PitotTube Arrangement

Photo 3.2: Manometer Arrangement

Photo 3.3: Point Gauge at Notch

Photo 3.4: Rectangular Notch

Photo 3.1 – 3.4: Photographs of Different Experimental Equipments.

3.4 EXPERIMENTAL PROCEDURE

3.4.1 EXPERIMENTAL CHANNEL

The meandering main channel constructed has a sinuosity of 4.11 with a one and a half wavelength of 2.162m. The main channel is a trapezoidal section of 1:1 side slopes and having a bottom width of 0.33m and top width of 0.46m with the bank full depth of 0.065m.The detailed geometric parameters of the meandering channel are illustrated in the following tabulation.

Table 3.1: Details of Geometrical Parameters of the Channel

Sl No	Parameter	Description
1	Type of Channel	Simple Meandering
2	Flume Dimension	4.0m×15m×0.5m Long
3	Meandering Channel Geometry	Trapezoidal with side slopes 1:1
4	Type of Bed Surface	Rigid and Smooth Bed
5	Section of Channel	0.33m at Bottom and 0.46 m at Top
6	Bank Full Depth	0.065m
7	Bed Slope of the Channel	0.00040146
8	Sinuosity of the Channel	4.11
9	Amplitude of the Meandering Channel	1.555 m
10	Wave length of the Meandering Channel	2.162 m

Photo 3.5: Meandering Channel

Photo 3.6: Moving Bridge Arrangement

Photo 3.7: Meander Path

Photo 3.8: Stilling Chamber

Photo 3.9: Volumetric Tank

Photo 3.10: Tail Gate

Photo 3.5-3.10 Meandering Channel inside the Flume with Requisite Arrangements

3.4.2 POSITION OF MEASUREMENT

All observations are recorded along a meandering path from the second bend apex to the next bend apex passing through the cross-over of the meandering channel. A section at crossover perpendicular to both the inner and outer curves of the meandering channel is drawn and extended unto the extended bend apex line, as shown in Fig. 3.2. An angle of 120^0 is formed for both the curves. This is the cross-over angle or the arc angle. The curves are divided into 6 equal sections of 20^0 each to the centreline of the meandering channel. Channel sections along the width i.e. perpendicular lines drawn to both the curvesfrom these points. Sections A and M are the bend apex while section G is the cross-over section.The sections A through M are considered for measurement of the velocity profiles.

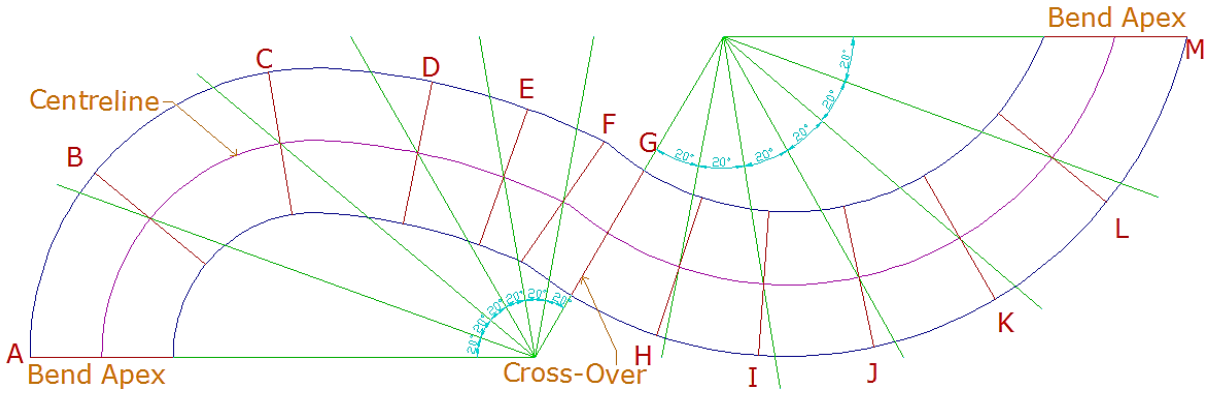

Fig.3.2 Plan Geometry of the Meandering Path.

A constant discharge is maintained while taking the readings for the entire meandering path. Series of Pitot-tubes with moving bridge arrangement are made to measure the velocity at different points of the flow passage of the channel. The measurements are taken at different reaches along the meander path for every section. Data are observed from left edge to the right edge of the main channel in the direction of flow. The lateral spacing of the grid points has been taken as 4cm on either side of the centreline. The Pitot tube is traversed upwards from the bed of the channel. The bed of the channel represented here is the position of radius of the Pitot tube which is 0.2385cm from the bed. This is achieved by placing the Pitot tube at the surface of the channel. Readings are taken atthe bed and then moved up by 0.4*H*, 0.6*H*, and 0.8*H* from the bed. *H* here is the average depth of water at the every corresponding section along the meander path. Fig.3.3 shows the grid diagram used for the experiments.

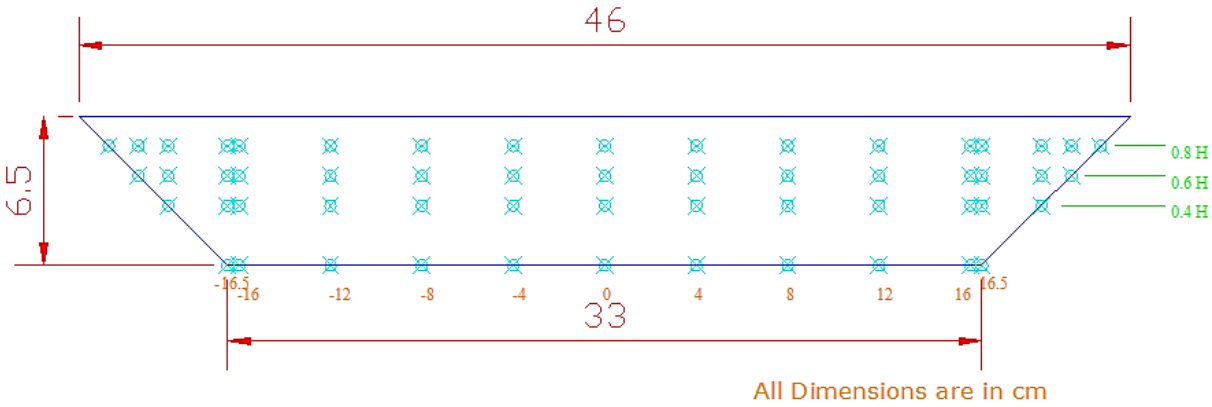

Fig.3.3 Grid Arrangement of Points for Velocity Measurementacross a Channel Section.

3.4.3 MEASUREMENT OF BED SLOPE

For measurement of bed slope, water level piezometric tube is used. Water level with respect to the bed of the channel at the upstream and then at the downstream of the flume is taken which are about 15m apart. The water level taken is from the bed of the flume without considering the thickness of the Perspex sheet. Difference in the two corresponding points was measured. Slope is measured by dividing this level difference with the distance between the observed points. Five such readings are taken and averaged for accuracy. The slope

calculated is 0.00165 which is the slope of the flume or the valley slope. To calculate the slope of the main channel, which is meandering in nature, the sinuosity of the main channel is divided from the slope of the flume which gives the channel slope. The sinuosity of the meandering channel being 4.11, the channel slope of the main channel is found to be 0.00040146.

3.4.4 NOTCH CALIBRATION

Rectangular notch provided at the upstream section of the flume is utilized to calculate the theoretical discharge into the channel. Before calculating the discharge, the notch needs to be calibrated with respect to actual discharge from the volumetric tank at the downstream section. The volumetric tank has a cross-sectional area of 208666cm^{2}and has a piezometer attached to it for measurement of the rate of rise in water level. Actual discharge is calculated by recording the time taken for rise in unit increase in height of water level in the piezometer.

The volume of water collected at the volumetric tank is given by,

$$V_w = Ah_w \qquad \text{Eq. 3.1}$$

Actual discharge of water collected at the volumetric tank is given by,

$$Q_a = V_w/t \qquad \text{Eq. 3.2}$$

For theoretical discharge, the height of water over the rectangular notch is measured by a point gauge arrangement. Theoretical discharge is given by,

$$Q_{th} = \frac{2}{3} L_n \sqrt{2g} H_n^{3/2} \qquad \text{Eq. 3.3}$$

The coefficient of discharge for each run is calculated as per equation given below,

$$C_d = \frac{Q_a}{Q_{th}} \qquad \text{Eq. 3.4}$$

Where, Q_a is the actual discharge, Q_{th} is theoretical discharge, A is the area of volumetric tank, V_w volume of water, t time in sec, C_d is the coefficient of discharge calculated from

notch calibration, h_w is the height of water in the volumetric tank, L_n is the length of the notch (3.4 m in this case), H_n is the height of water above the notch and g is the acceleration due to gravity.

From the notch calibration, coefficient of discharge 'C_d' of rectangular notch was found to be 0.66. The discharge is maintained at 5.2 x 10^{-3} m^3/s throughout the experiment.

3.4.5 MEASUREMENT OF LONGITUDINAL VELOCITY

Pitot tubes are utilized for the measurement of velocity. Five Pitot tube arrangements are used for measurement of the pressure difference at every predefined point on the channel cross-section throughout the meander path. The Pitot tubes have an external diameter of 4.7mm. The Pitot tubes are attached to individual manometers placed on a vertical board. The vertical board has a spirit level to keep the manometers in vertical level. The connections between the Pitot tubes and the manometer are made by long transparent PVC tubes of small diameters. Extra care is taken to drive out any air bubbles inside the tubes.

Pitot tubes are placed against the direction of flow perpendicular to it. The pressure difference at every pre-defined grid of the channel section along the meander path is achieved. The point form velocity is measured by $v=\sqrt{2gh}$, where g is the acceleration due to gravity and h is the pressure difference. Here the tube coefficient is taken as unit and the error due to turbulence considered negligible while measuring velocity.

The velocity data are taken at the bed (0.2385cm from bed) and then moved up by 0.4H, 0.6H and 0.8H from the bed. Here H is the averageflow depth of water at the every corresponding section along the meander path. While representation of vertical velocity profile, the velocity value at the surface is assumed to be zero considering the no slip condition.

3.4.6 MEASUREMENT OF BOUNDARY SHEAR STRESS

Measurement of shear stress in open channel flow helps in understanding Shear bed load transport, momentum transfer, channel migration; etc.The shear forces at the bed are handy in the examination of bed load transfer whereas shear forces at the walls give a general overview of channel migration pattern. Although there are several methods to evaluate bed and wall shear, Preston-tube method being an indirect estimate, is broadly used for experimental observations.

Preston (1954) developed a simple technique for measuring local shear stress on smooth boundaries using a Pitot tube in contact with the surface. His method was basedon theassumption of an inner law relating the boundaryshear stress to the velocity distribution near the wall.Preston presented a non-dimensional relationship between thePreston tube differential pressureΔP, and the boundary shear stress,τ, of the form:

$$\left(\frac{\tau d^2}{4\rho\upsilon^2}\right) = F\left(\frac{\Delta P d^2}{4\rho\upsilon^2}\right) \qquad \text{Eq. 3.5}$$

where d is the outer diameter of the Preston tube, ρ is the density of the flow, υ is the kinematic viscosity of the fluid , and F is an empirical function. **Patel (1965)** further extended the research and his calibration is given in terms of two non dimensional parameters x^* and y^* which are used to convert pressure readings to boundary shear stress, where

$$x^* = \log_{10}\left(\frac{\Delta P d^2}{4\rho\upsilon^2}\right) \text{ and } y^* = \log_{10}\left(\frac{\tau d^2}{4\rho\upsilon^2}\right) \qquad \text{Eq. 3.6}$$

In the form

For $y^* < 1.5$ $\qquad y^* = 0.5x^* + 0.037$ $\qquad$ Eq. 3.7

For $1.5 < y^* < 3.5$ $\qquad y^* = 0.8287 - 0.1381x^* + 0.1437x^{*2} - 0.006\,x^{*3}$ $\qquad$ Eq. 3.8

and

For $3.5 < y^* < 5.3$ $\qquad x^* = y^* + 2\log_{10}(1.95y^* + 4.10)$ $\qquad$ Eq. 3.9

In the present case, all shear stress measurements are taken at all the thirteen sections throughout the meander path between the two bend apexes. The pressure readings were taken using pitot tubes along the predefined points across all the sections of the channel along the bed and side slopes. The manometers attached to the Pitot tubes provide the head difference between the dynamic and static pressures. The differential pressure is then calculated from the readings on the vertical manometer by,

$$\Delta P = \rho g \Delta h \qquad \text{Eq. 3.10}$$

where Δh is the difference between the two readings from the dynamic and static, g is the acceleration due to gravity and ρ is the density of water. Here the tube coefficient is taken as unit and the error due to turbulence is considered negligible while measuring velocity.

Accordingly out of the Eq. 3.6-3.9, the appropriate one was chosen for computing the wall shear stress based on the range of x^* values. After that the shear stress value was integrated over the entire perimeter to calculate the total shear force per unit length normal to flow cross-section carried by the meandering section. The total shear thus computed was then compared with the resolved component of weight force of the liquid along the stream-wise direction to check the accuracy of the measurements.

CHAPTER 4
RESULT AND DISCUSSION

4.1 OVERVIEW

Chapter 3 represents the different experimental procedures which have been carried out on the series of experiments conducted throughout the meandering path of the sinuous channel. This chapter will now present the results of the tests conducted in form of water surface profile plots, velocity distributions along the width and depth and boundary shear stress along the wetted perimeter of the channel section.

4.2 TRANSVERSE WATER SURFACE PROFILE

A single discharge is maintained at a time and the surface profile data at different sections throughout the meandering path along the channelare obtained. The constant discharge of $5.2x10^{-3}$ m^3/s throughout the experiment is maintained.

At every section, point gauge is used to take the depth of water along the width at 11 positions across the channel section. The data are taken at 4cm intervals on either side of the centreline of the meandering channel along with the corner edges of the side walls.

The readings are taken from the left bank towards the right bank of the channel section and the water surface profile are analysed. The surface profile seems to change its course at the cross-over. The water height usually remains higher towards the outer wall and lower at the inner wall.

The figure 4.1 to 4.13 illustrates the transverse water surface profile data at all the 13 different sections along the meander path of the highly sinuous channel.

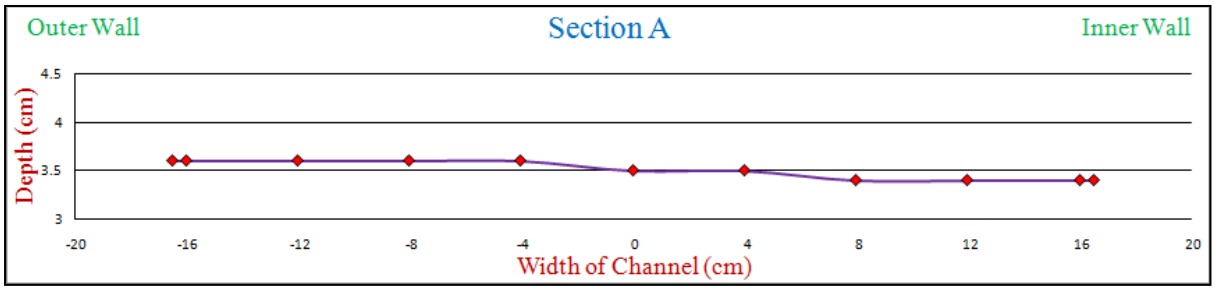

Figure 4.1.1

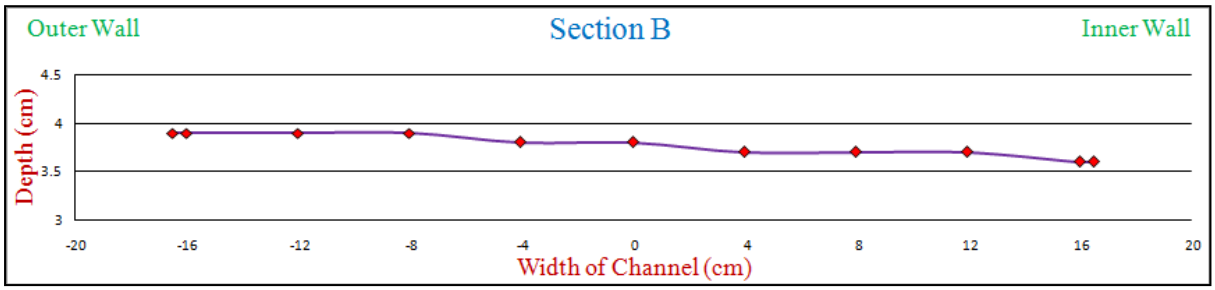

Figure 4.1.2

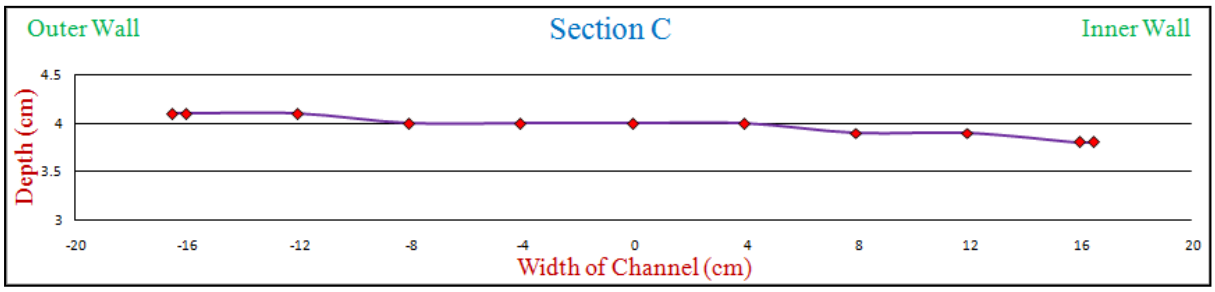

Figure 4.1.3

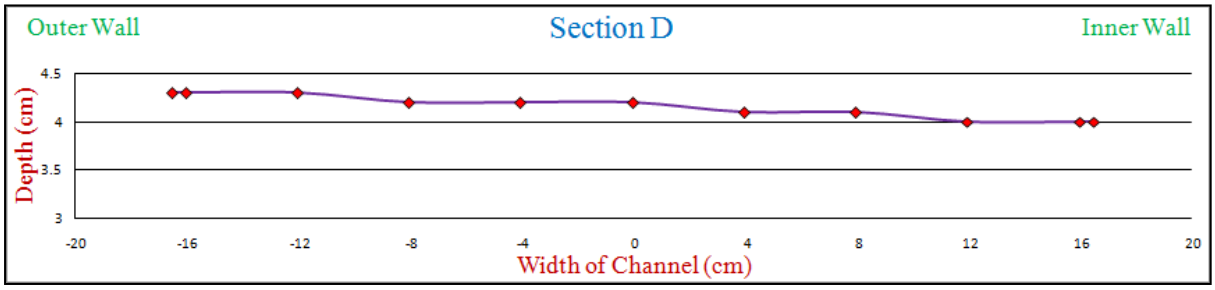

Figure 4.1.4

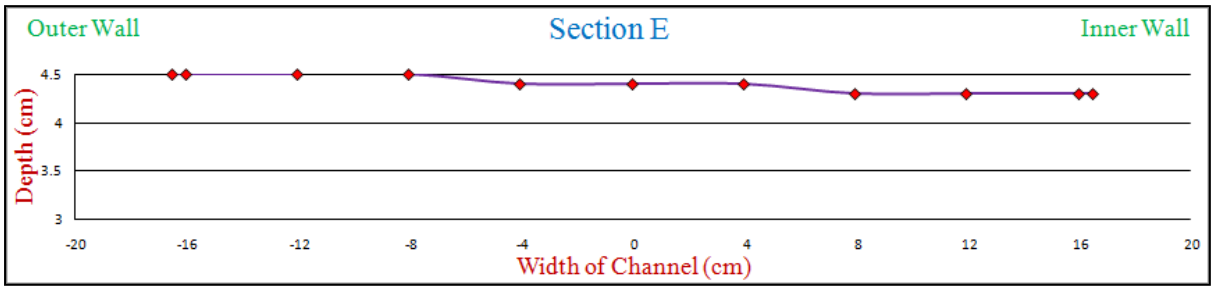

Figure 4.1.5

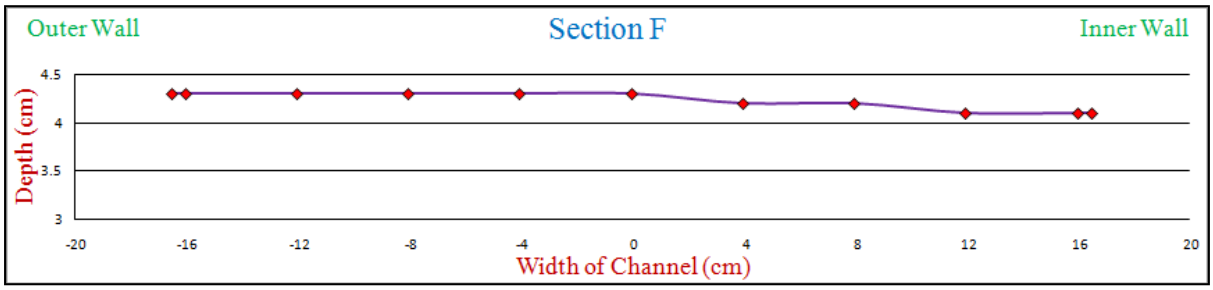

Figure 4.1.6

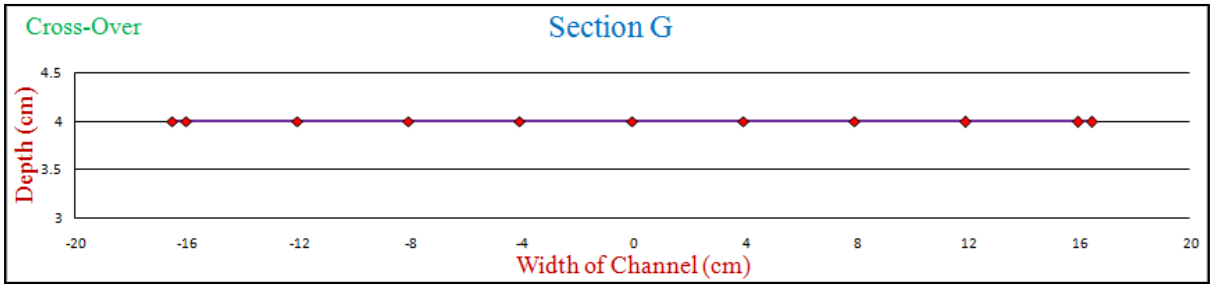

Figure 4.1.7

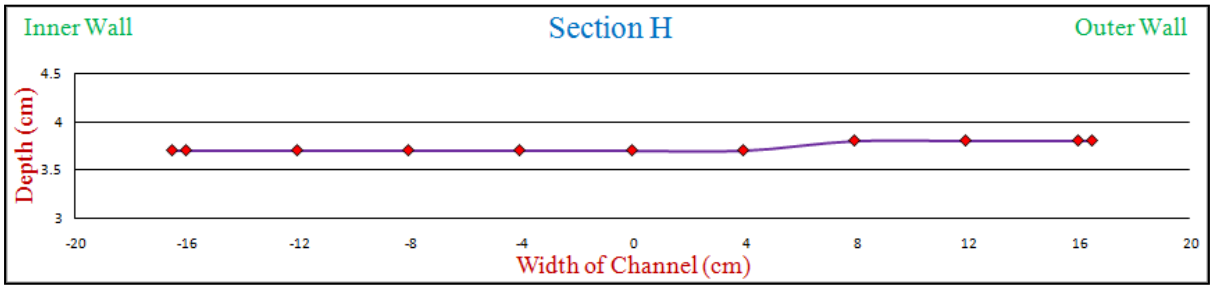

Figure 4.1.8

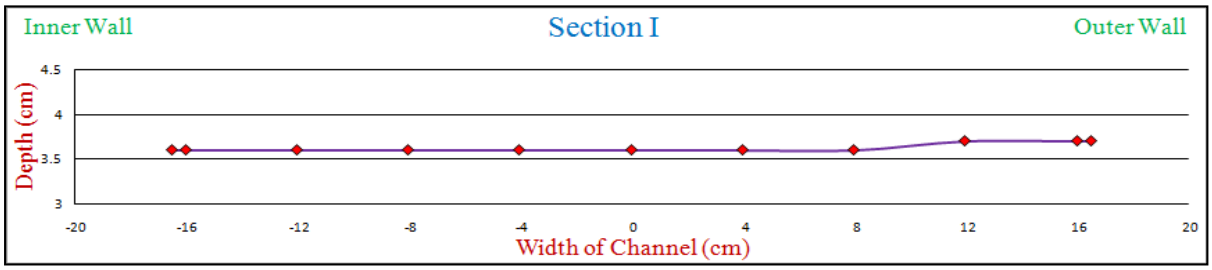

Figure 4.1.9

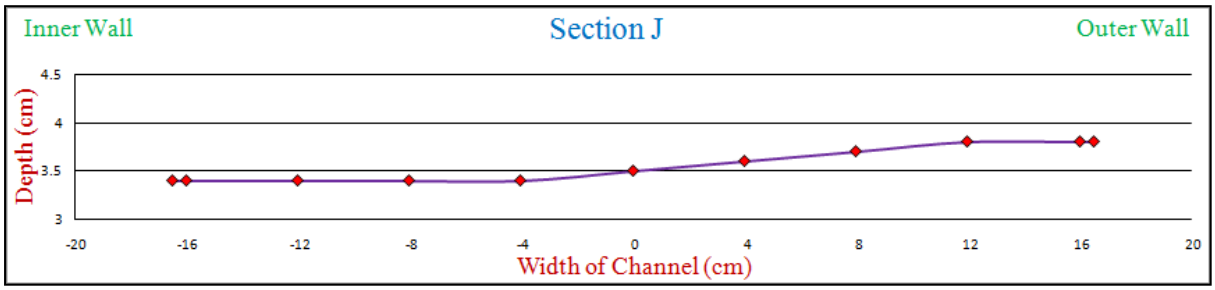

Figure 4.1.10

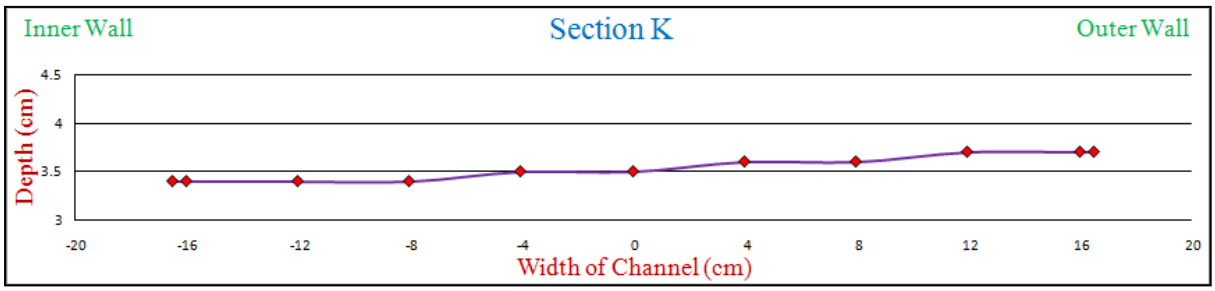

Figure 4.1.11

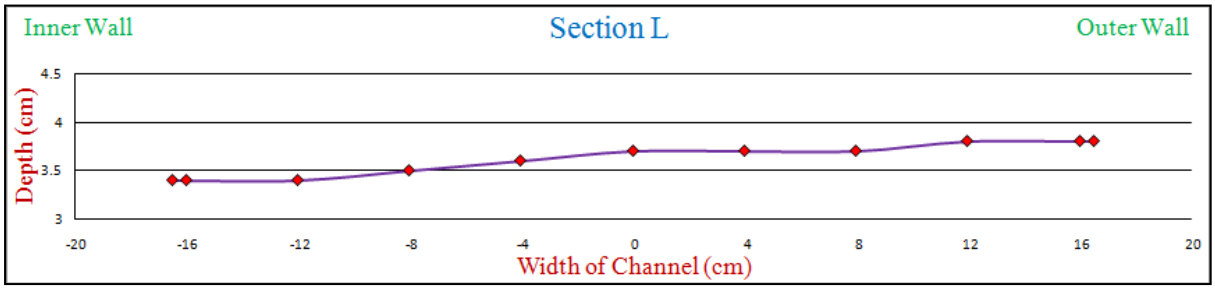

Figure 4.1.12

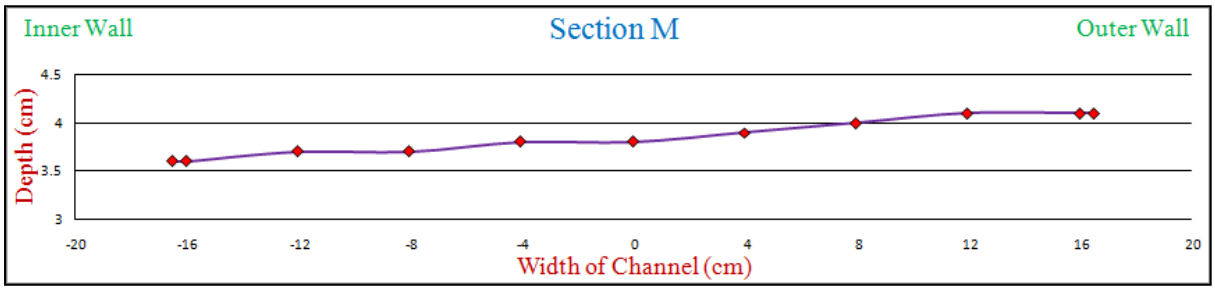

Figure 4.1.13

Figure 4.1.1 to 4.1.13: Water Surface Profile at Sections along the Meander Path

The following inferences can be made from the above water surface profile graphs

1. At the initial sections, i.e. at the bend apex A, the height of water remains higher on the outer wall which is at the left bank.
2. The height of water in section A through F remains higher on the left bank of the channel, which is the outer wall for the clockwise curve of the meandering channel.
3. The water surface profile levels itself at the section G, which is the cross-over section. Similar observations are usually recorded for straight channels, where the water surface profile is same throughout the width of the channel.
4. The cross-over section, G is assumed to behave similar to a straight channel.
5. At the sections E, F, H, and I; the difference in water surface profile between the inner and outer walls is not so prominentbecause the sections lie close to the cross-over where the surface profile levels itself.
6. The water surface profile is found to increase slowly in the consequent sections after the cross-over from the left bank towards the right bank of the channel section.
7. The surface profile in the sections H through M remains higher on the right bank of the channel which is apparently the outer wall for the anti-clockwise curve of the meandering channel after the cross-over.
8. The height of the water at both the bend apex sections, i.e. A and M, remains significantly high on the outer wall.Bend apex is the section of maximum curvature, and the experimental channel precedes and continues as a sinuous channel. Therefore, due to the curvature at both the bend apexes, the variation of water surface profile at sections A and M is significant.
9. The water surface profile is always observed to remain higher on the outer wall than at the inner wall at every channel section across the meandering path.

4.3 LONGITUDINAL VELOCITY DISTRIBUTION

The discharge of 5.2 x 10^{-3} m^3/s is maintained for the entire experiment and the velocity data are obtained for the meandering path along the channel at every cross-section.

A set of Pitot tube are arranged unequally and are moved across the channel section from the left bank toward the right bank. The velocity data are recorded at 4cm intervals on either side of the centreline of the meandering channel for the bed and depths of 0.4*H*, 0.6*H* and 0.8*H*. *H* being the average flow depth of water at a corresponding section.

The velocity data are analyzed along the width and depth of the channel section to better understand the characteristic of flow through the meander path of the sinuous channel.

4.3.1 LONGITUDINAL VELOCITY DISTRIBUTION IN THE CHANNEL WIDTH AT DIFFERENT SECTIONS ALONG THE MEANDER PATH

The longitudinal velocity distribution is analyzed along the width of the channel at the bed, at 0.4*H*, at 0.6*H* and at 0.8*H* from the channel bed. *H* here is the averaged flow depth of water at a corresponding section.

The following figures from 4.2.1 to 4.2.13 represent the horizontal velocity profile along the channel width close tochannel bed at all the sections of the meandering path. Figure 4.3 represents the contour plot of horizontal velocity distribution at the bed of the meander path.

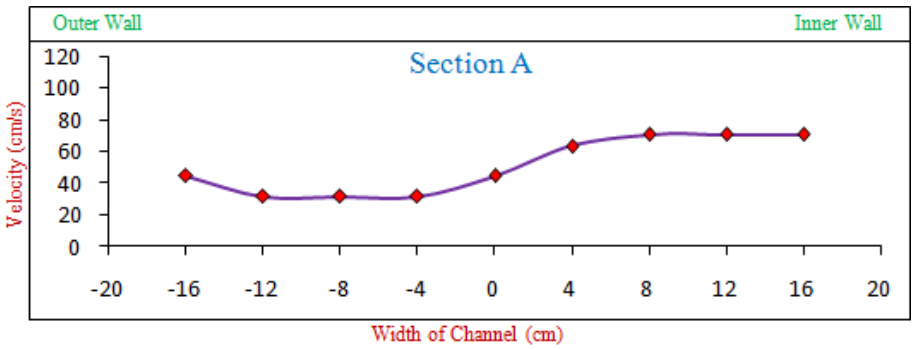

Figure 4.2.1

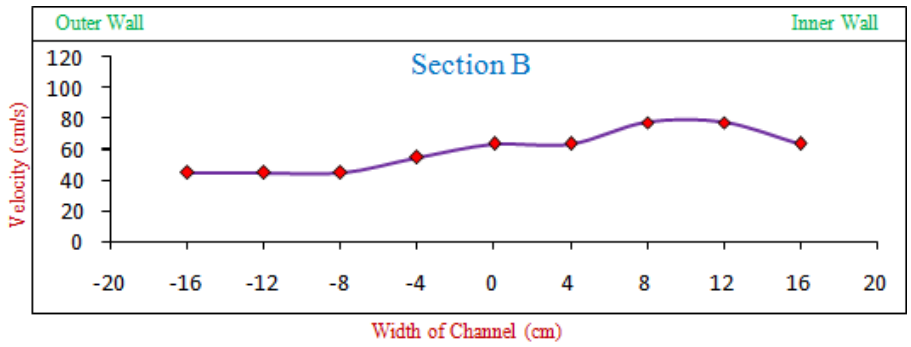

Figure 4.2.2

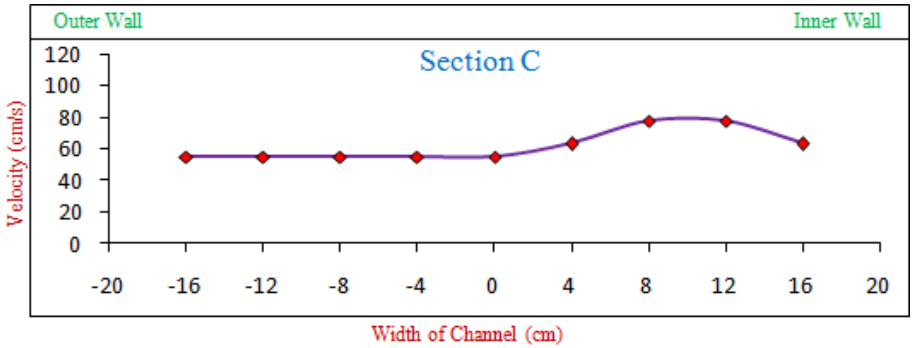

Figure 4.2.3

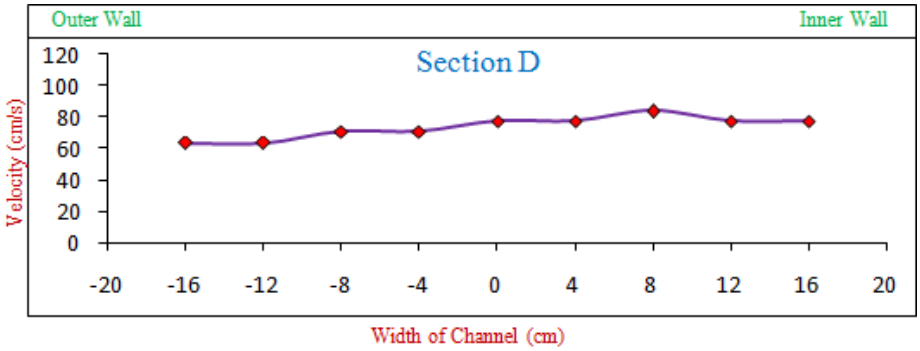

Figure 4.2.4

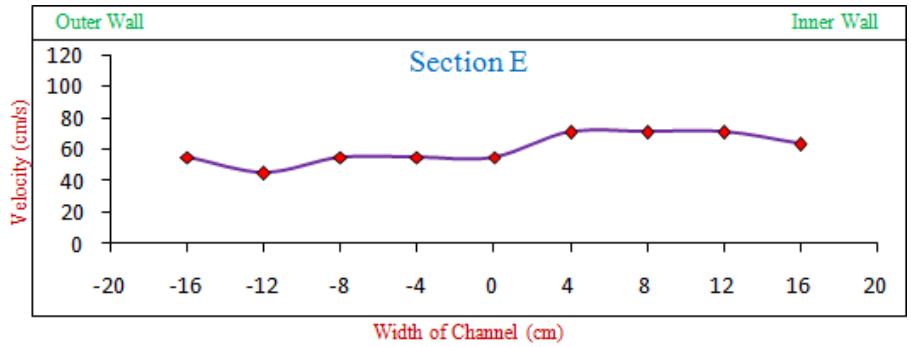

Figure 4.2.5

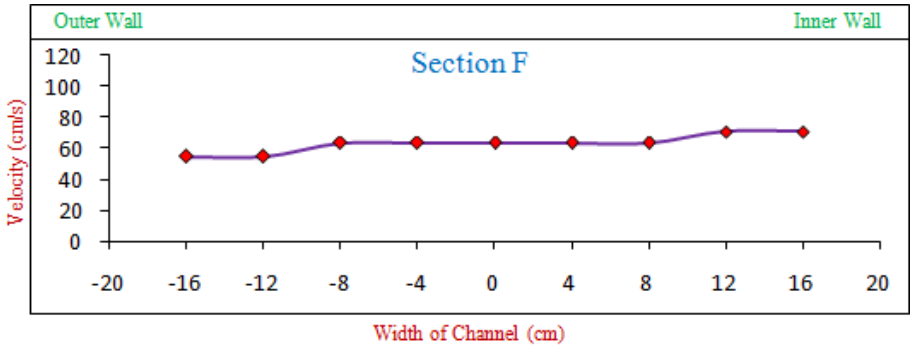

Figure 4.2.6

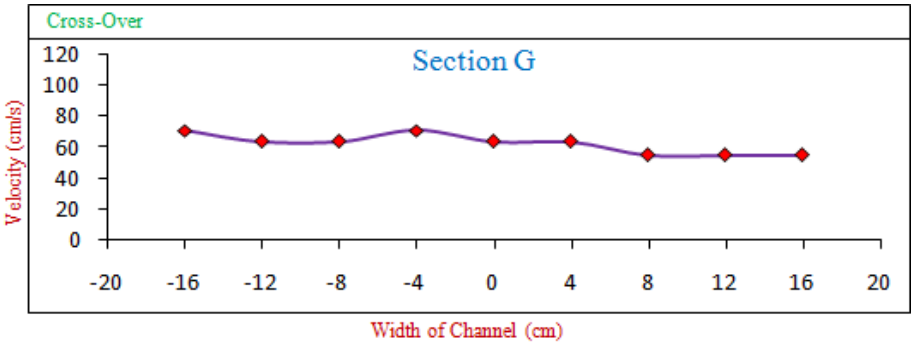

Figure 4.2.7

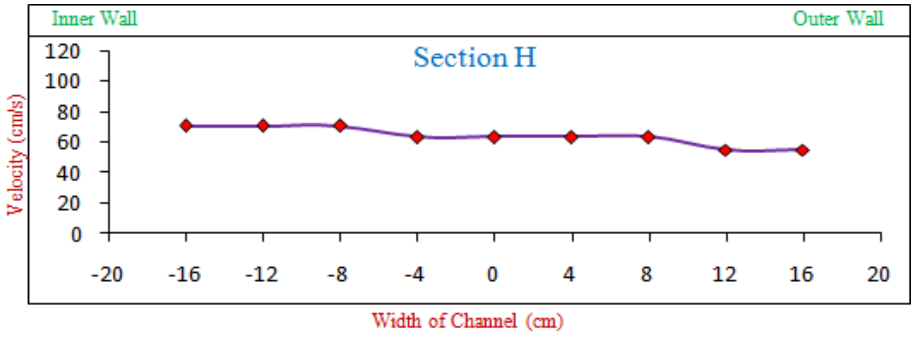

Figure 4.2.8

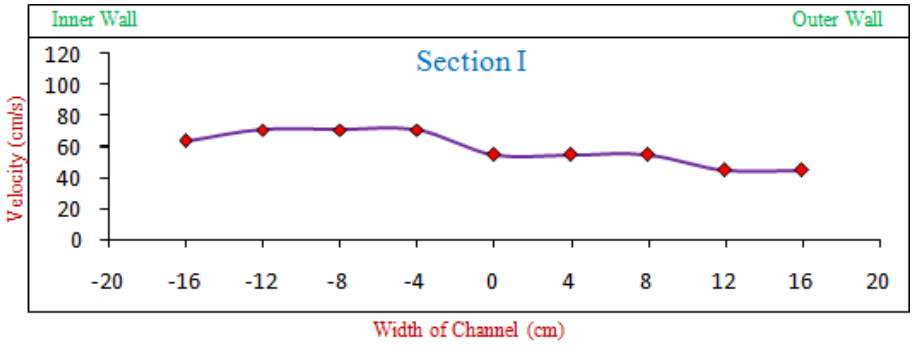

Figure 4.2.9

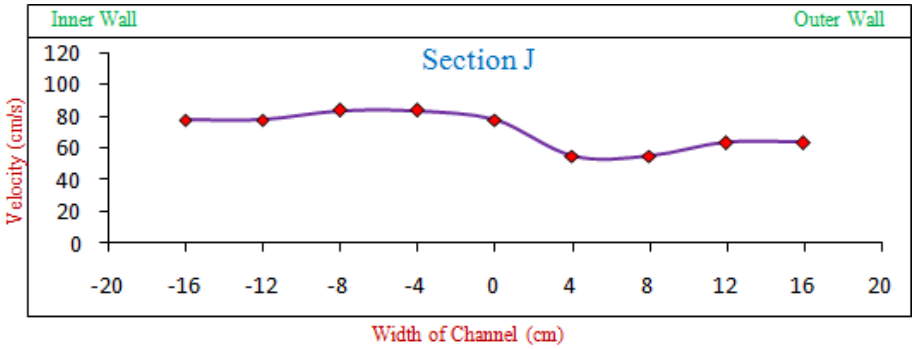

Figure 4.2.10

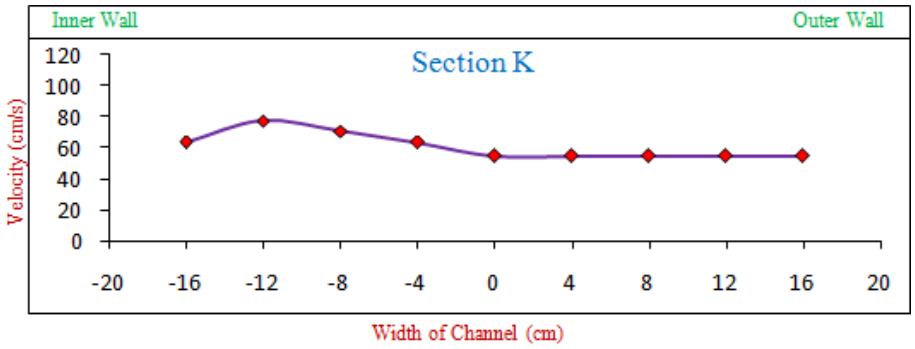

Figure 4.2.11

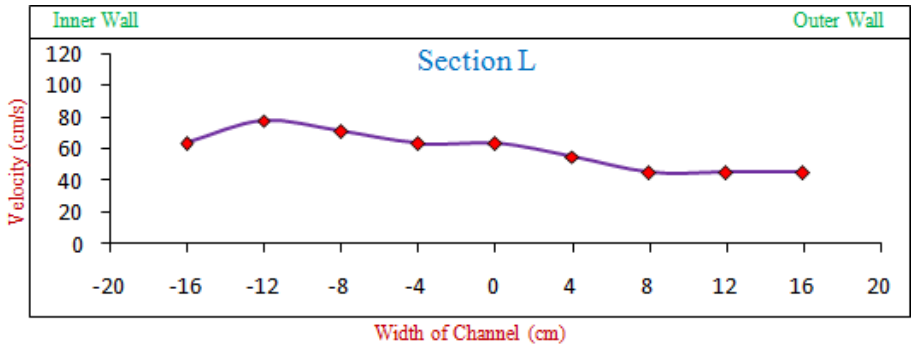

Figure 4.2.12

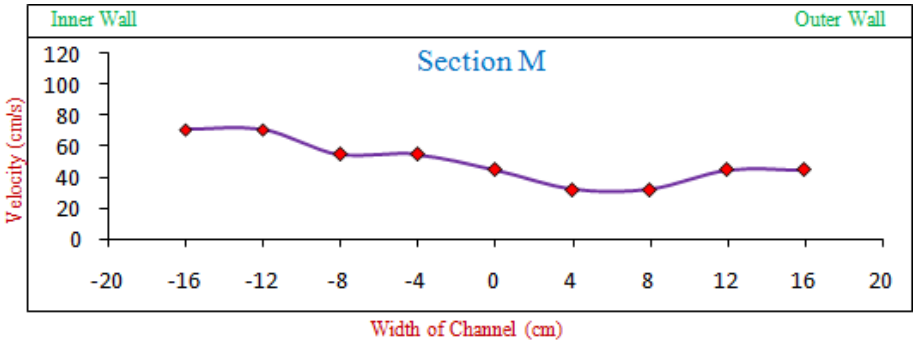

Figure 4.2.13

Figure 4.2.1 to 4.2.13: Horizontal Velocity Profile at the bed of the Channel Section along the Meander Path

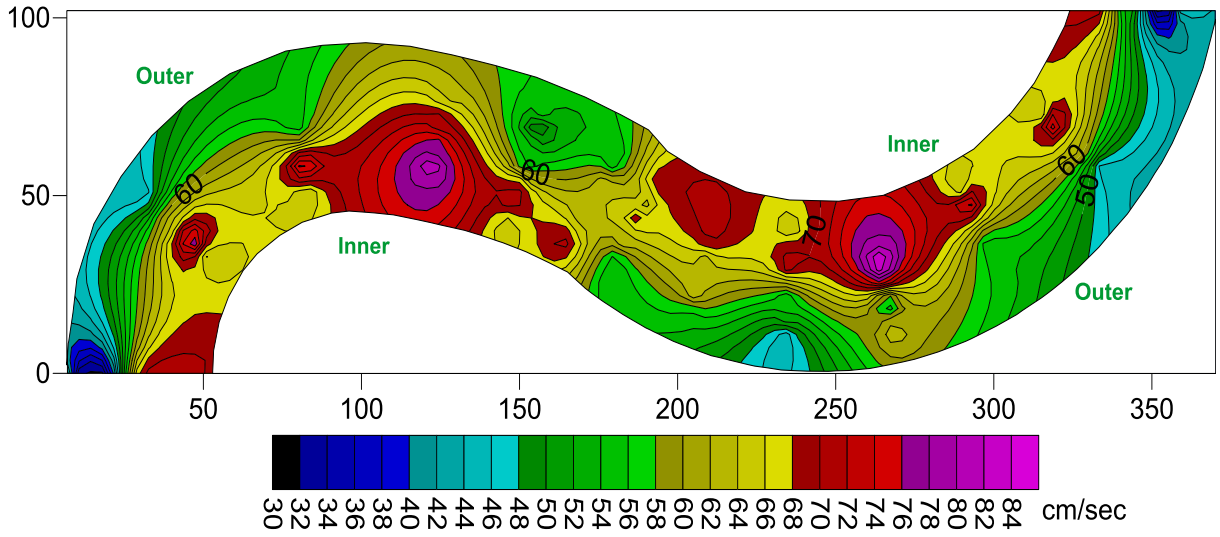

Figure 4.3: Contour Plot of Horizontal Velocity at bed of the Channel Section along the Meander Path

The following figures from 4.4.1 to 4.4.13 represent the horizontal velocity profile at 0.4*H* from the bed of the channel, where *H* is the average flow depth of water at the corresponding section. The graphs represent all the sections along meandering path. Figure 4.5 represents the contour plot of horizontal velocity distribution at 0.4*H* from the bed of the meander path.

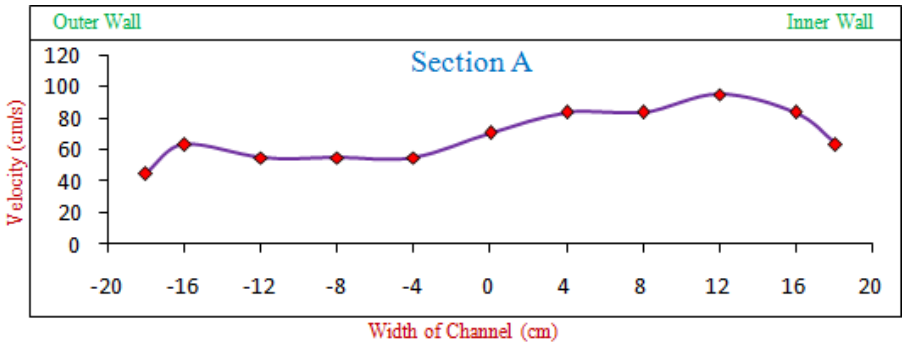

Figure 4.4.1

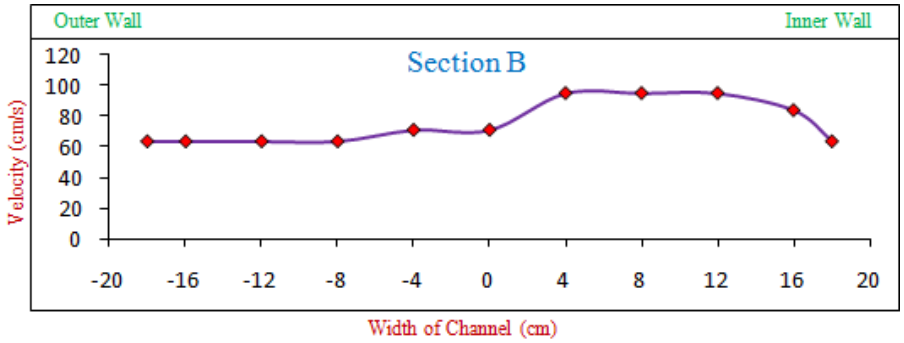

Figure 4.4.2

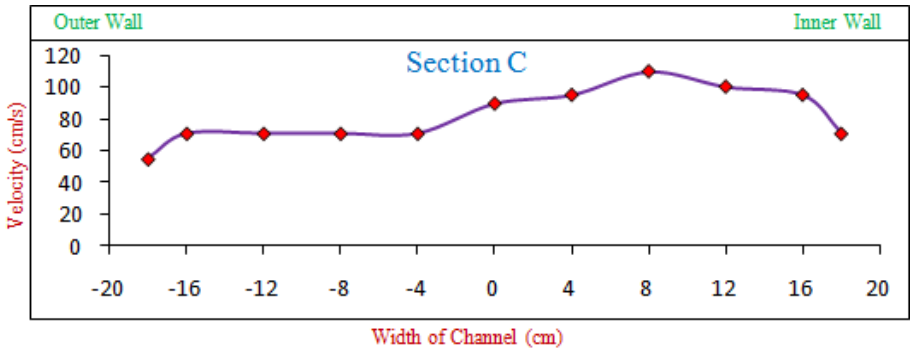

Figure 4.4.3

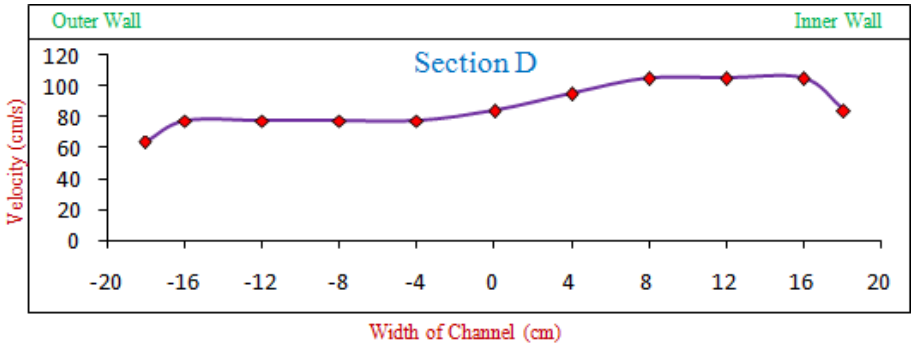

Figure 4.4.4

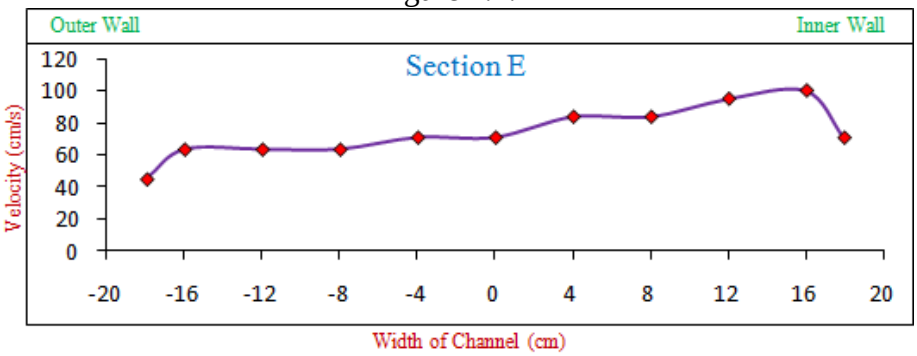

Figure 4.4.5

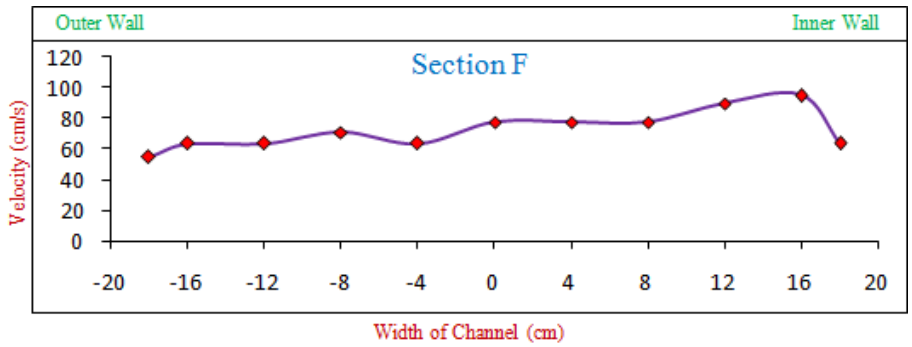

Figure 4.4.6

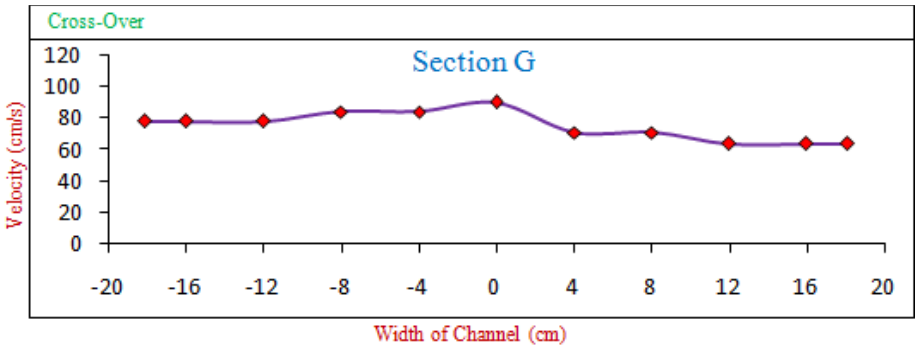

Figure 4.4.7

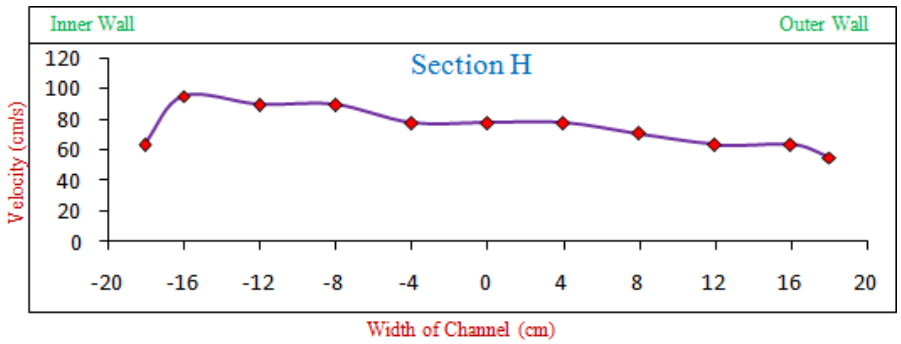

Figure 4.4.8

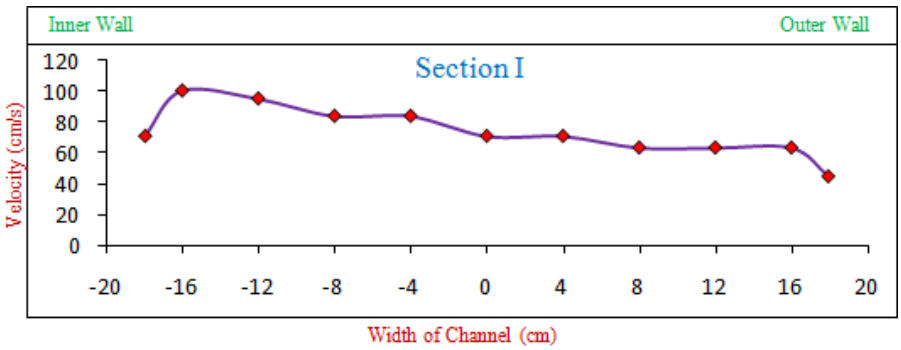

Figure 4.4.9

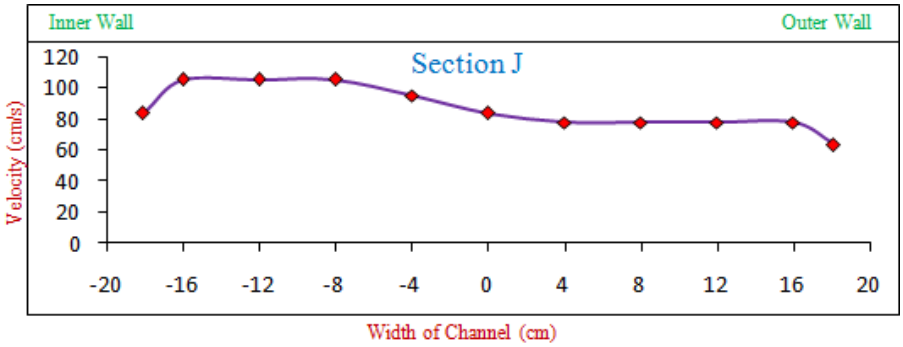

Figure 4.4.10

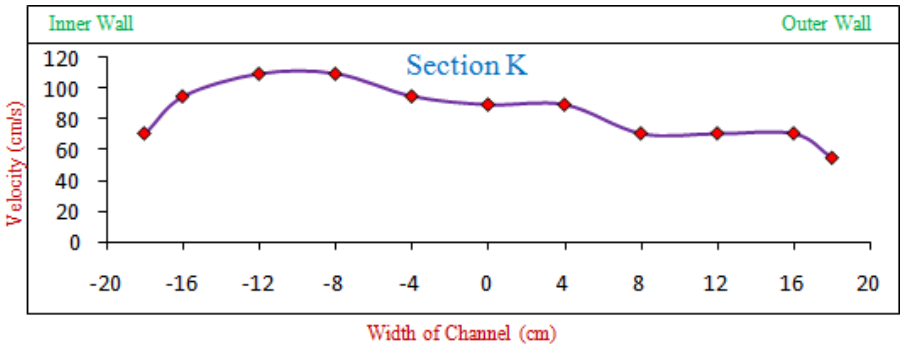

Figure 4.4.11

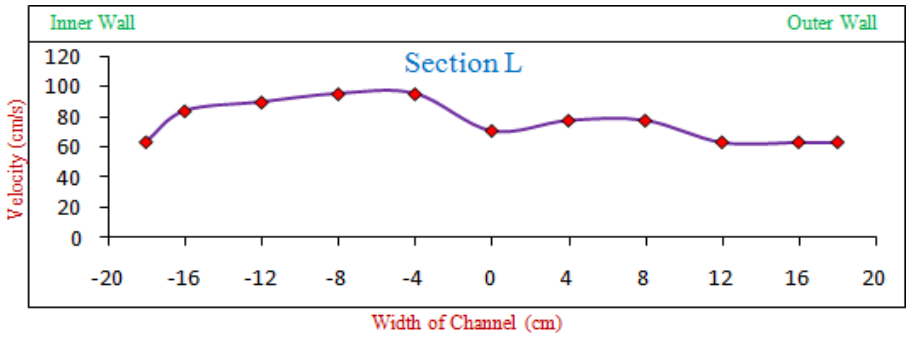

Figure 4.4.12

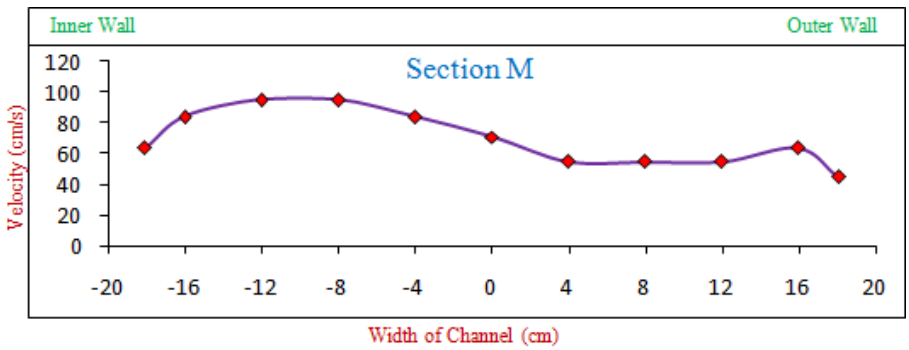

Figure 4.4.13

Figure 4.4.1 to 4.4.13: Horizontal Velocity Profile at 0.4*H* from the bed of the Channel Section along the Meander Path

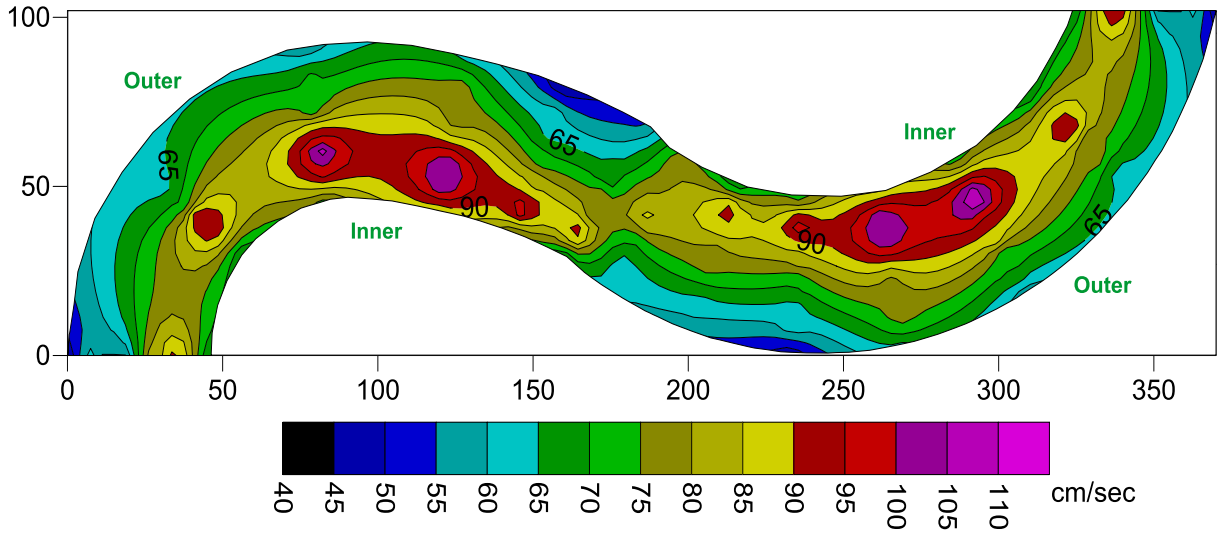

Figure 4.5: Contour Plot of Horizontal Velocity at 0.4*H* from the bed of the Channel Section along the Meander Path

The following figures from 4.6.1 to 4.6.13 represent the horizontal velocity profile at 0.6*H* from the bed of the channel, where *H* is the average depth of flow at the corresponding section. The graphs represent all the sections along meandering path. Figure 4.7 represents the contour plot of horizontal velocity distribution at 0.6*H* from the bed of the meander path.

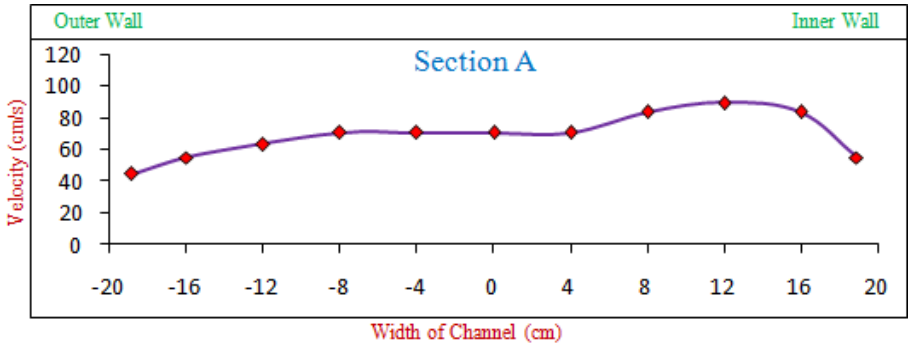

Figure 4.6.1

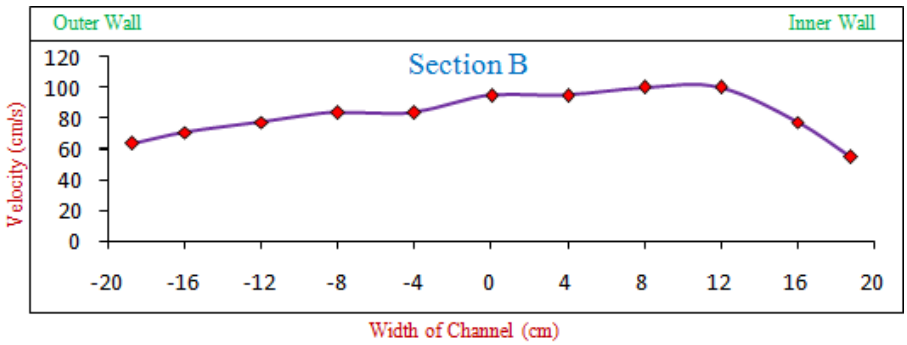

Figure 4.6.2

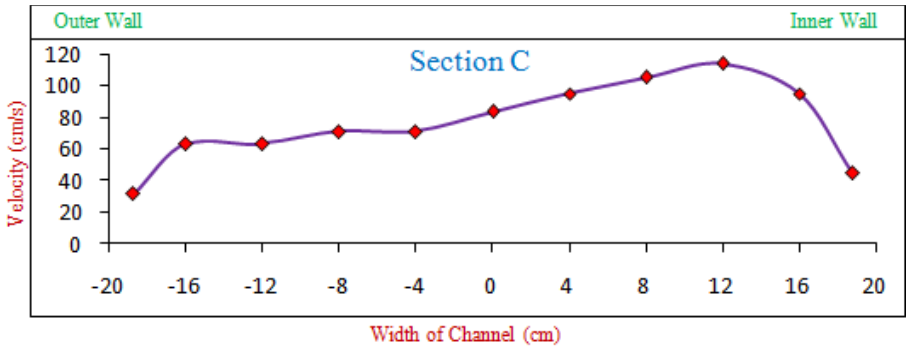

Figure 4.6.3

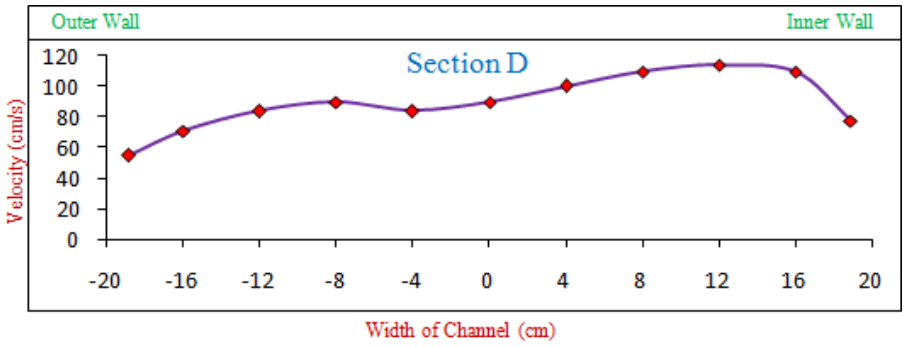

Figure 4.6.4

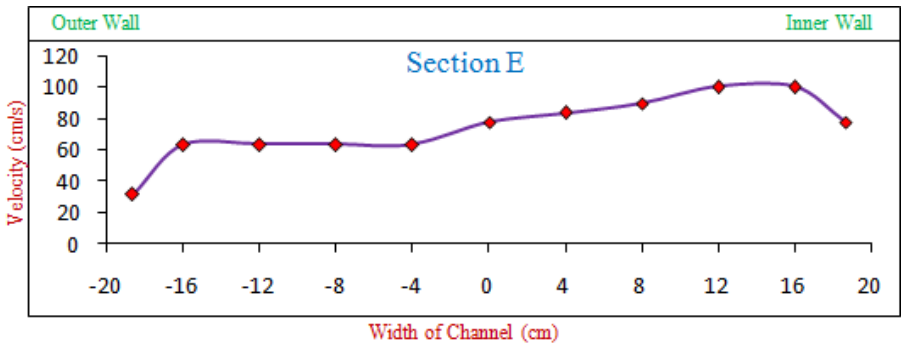

Figure 4.6.5

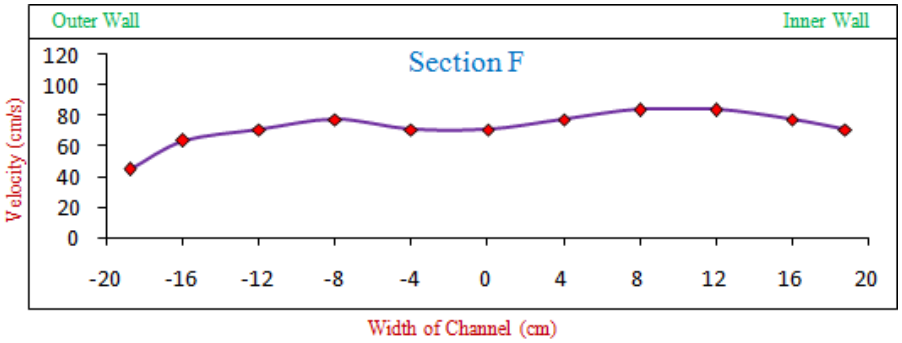

Figure 4.6.6

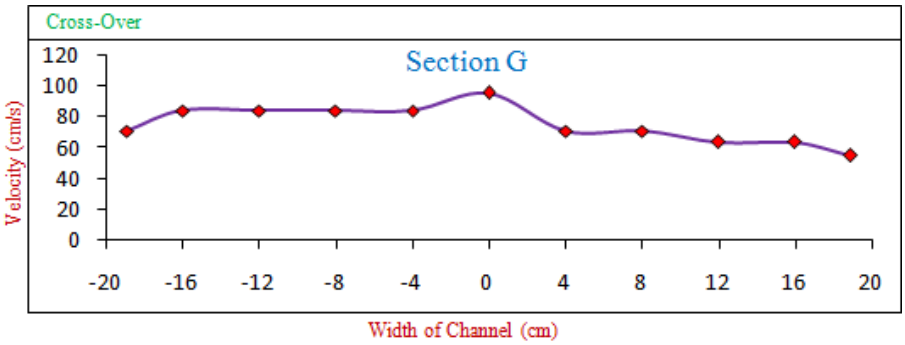

Figure 4.6.7

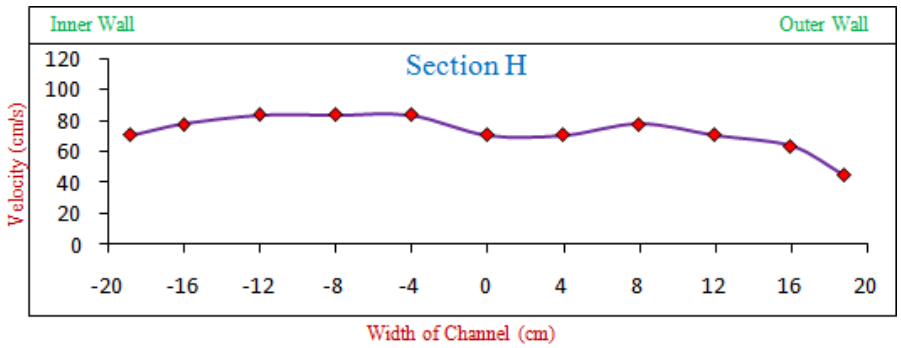

Figure 4.6.8

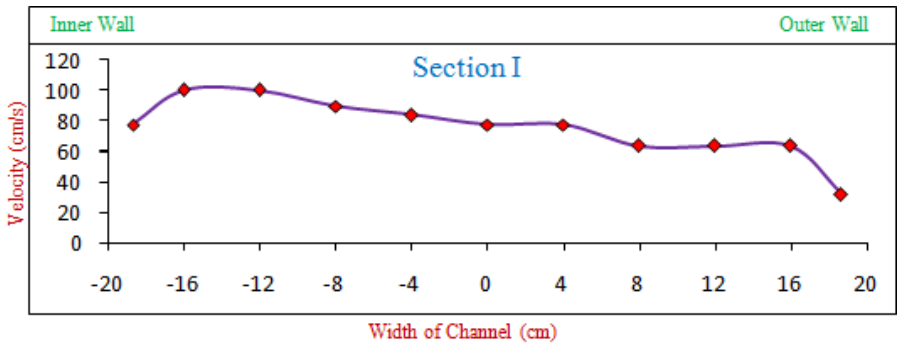

Figure 4.6.9

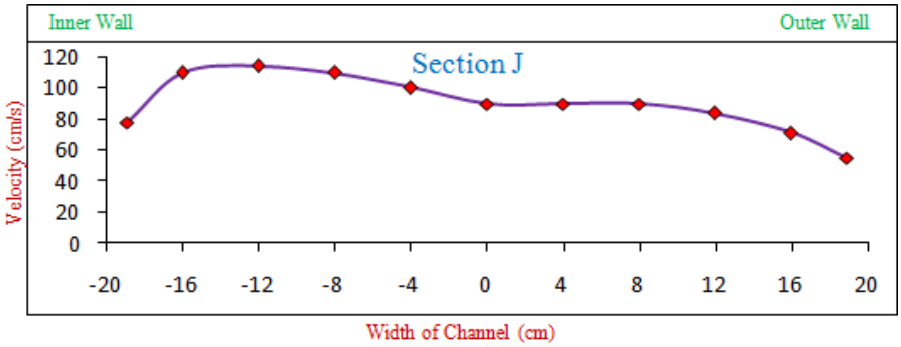

Figure 4.6.10

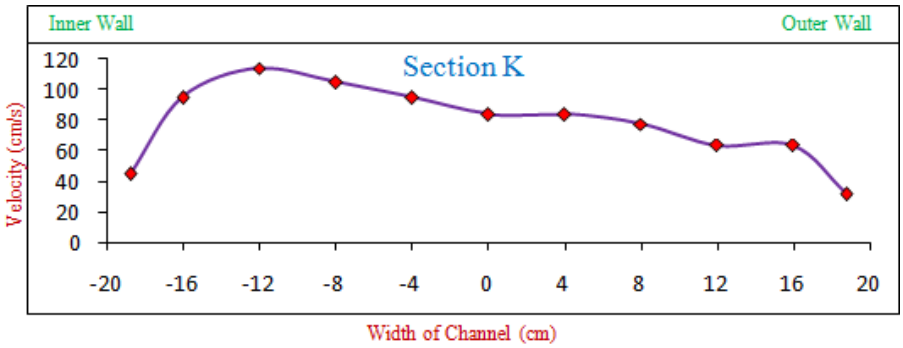

Figure 4.6.11

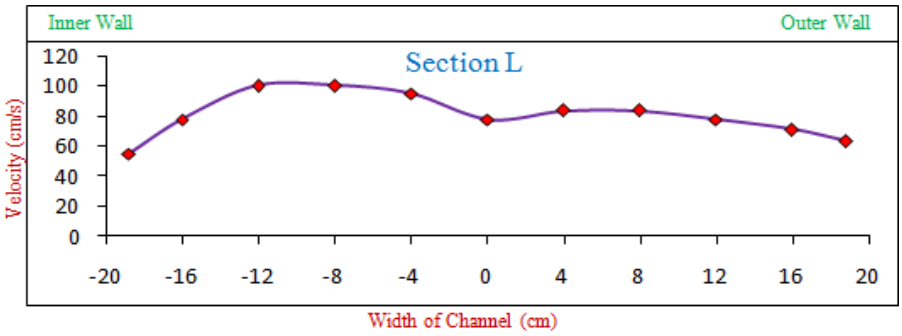

Figure 4.6.12

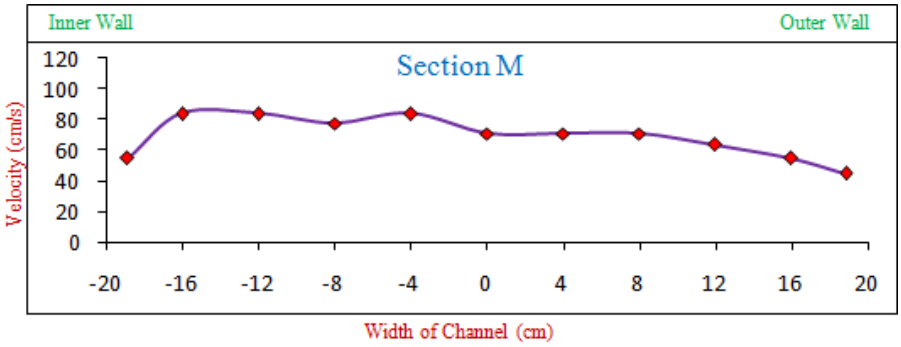

Figure 4.6.13

Figure 4.6.1 to 4.6.13: Horizontal Velocity Profile at 0.6*H* from the bed of the Channel Section along the Meander Path

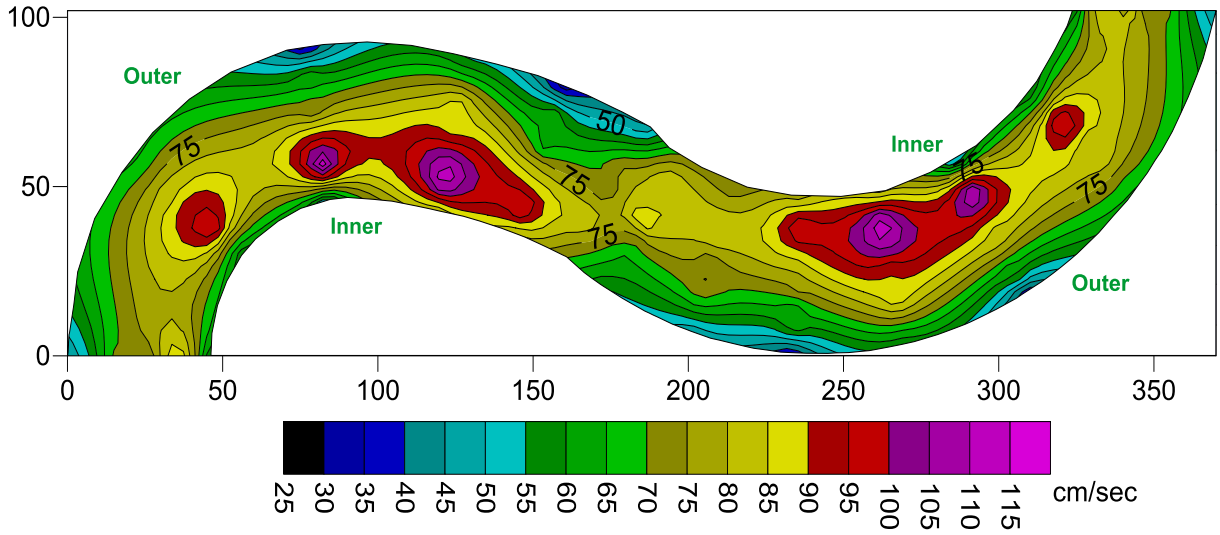

Figure 4.7: Contour Plot of Horizontal Velocity at 0.6*H* from the bed of the Channel along the Meander Path

The following figures from 4.8.1 to 4.8.13 represent the horizontal velocity profile at 0.8*H* from the bed of the channel, where *H* is the average depth of flow at the corresponding section. The graphs represent all the sections along meandering path. Figure 4.9 represents the contour plot of horizontal velocity distribution at 0.8*H* from the bed of the meander path.

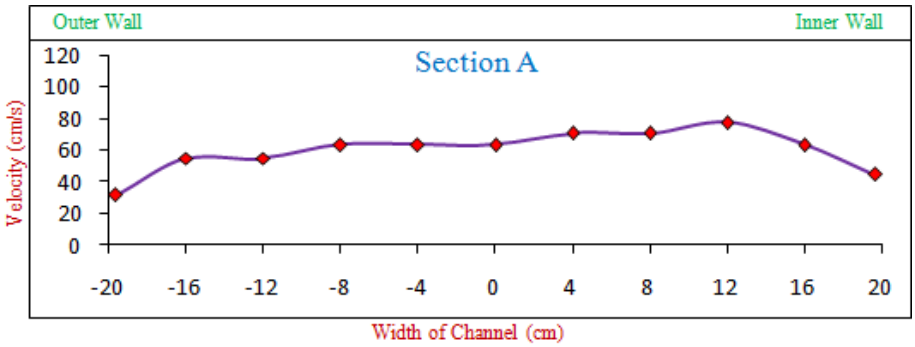

Figure 4.8.1

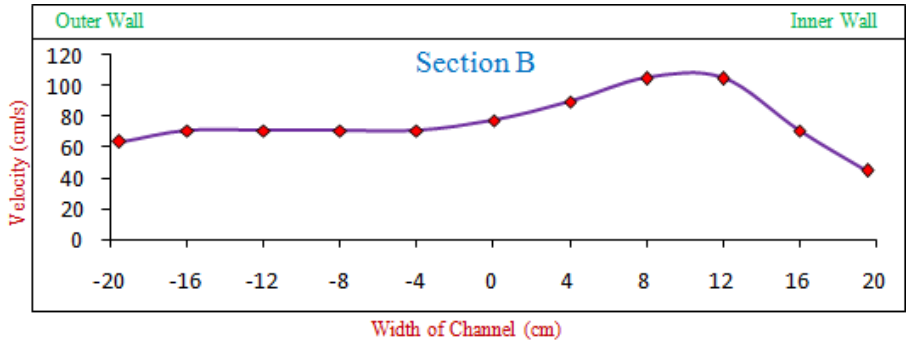

Figure 4.8.2

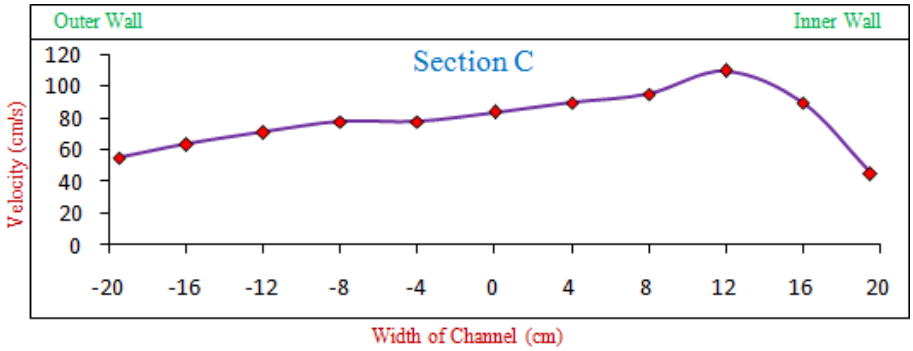

Figure 4.8.3

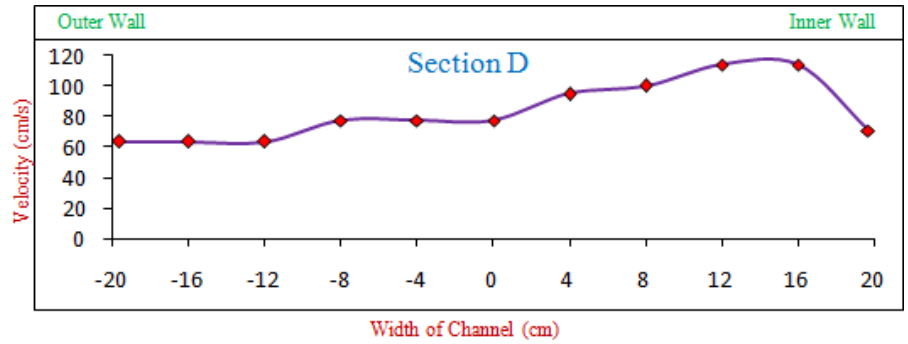

Figure 4.8.4

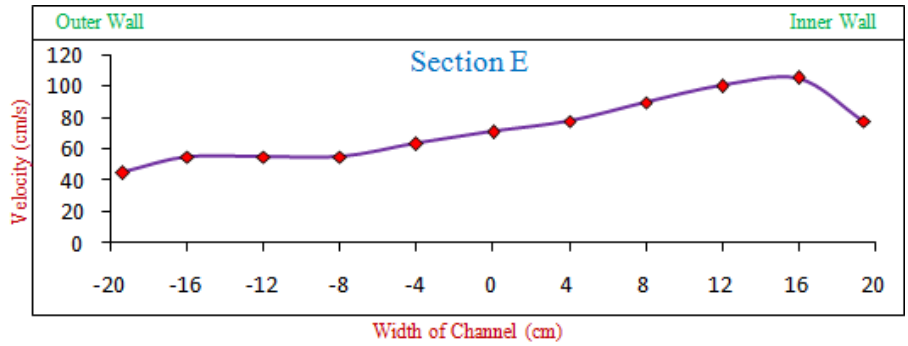

Figure 4.8.5

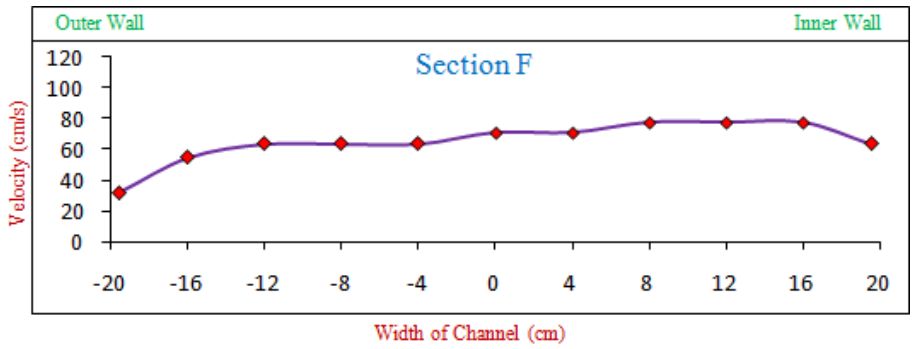

Figure 4.8.6

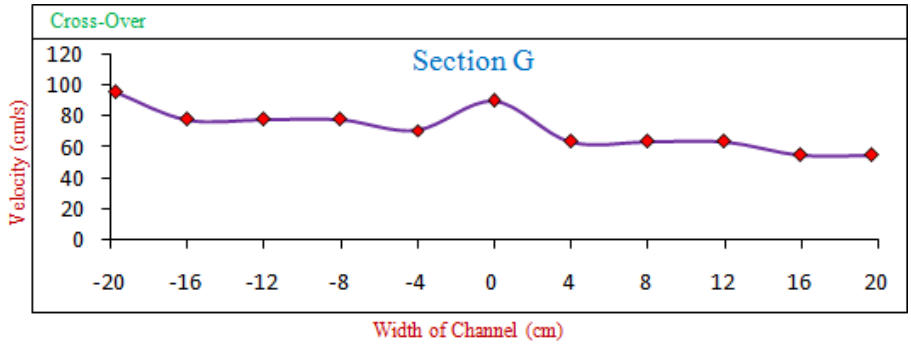

Figure 4.8.7

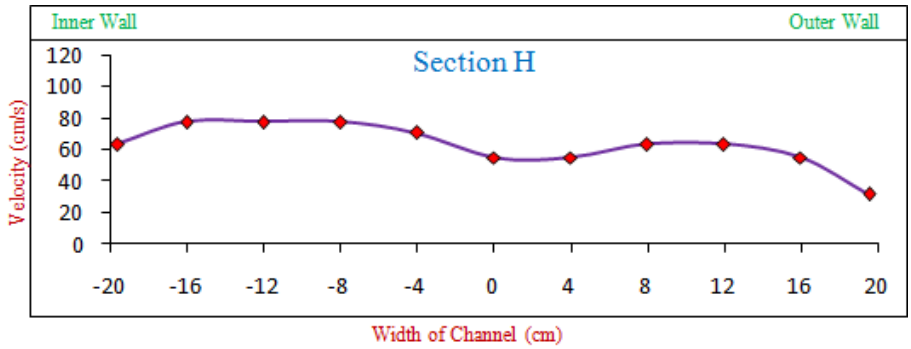

Figure 4.8.8

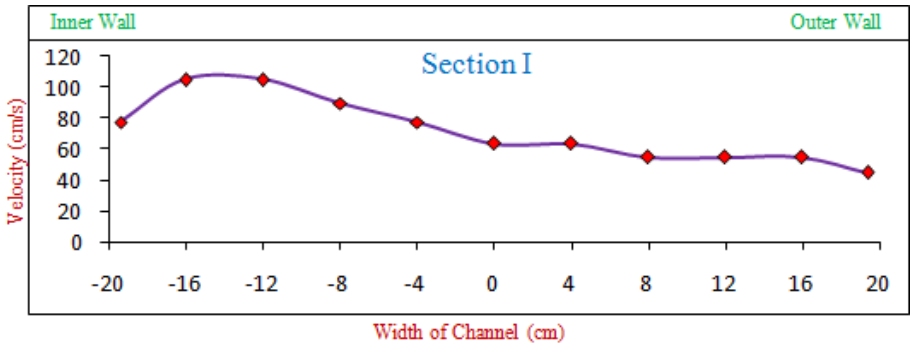

Figure 4.8.9

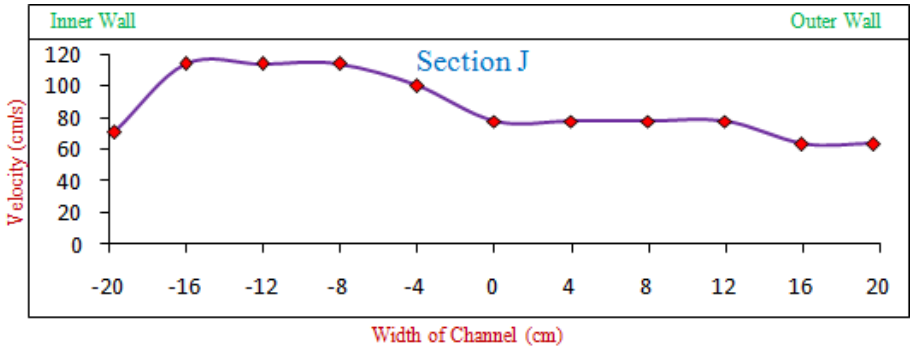

Figure 4.8.10

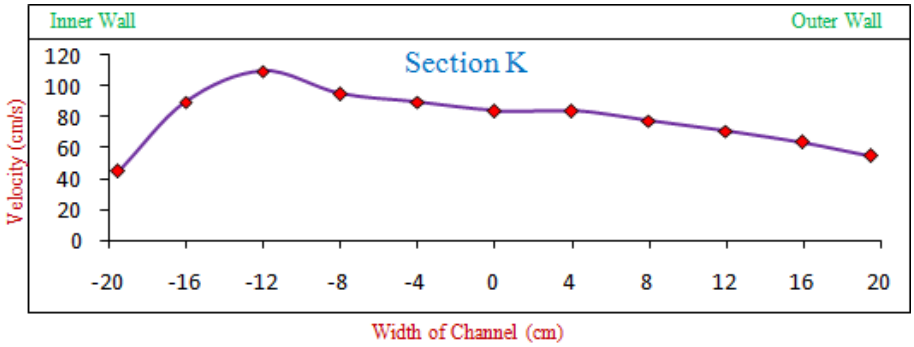

Figure 4.8.11

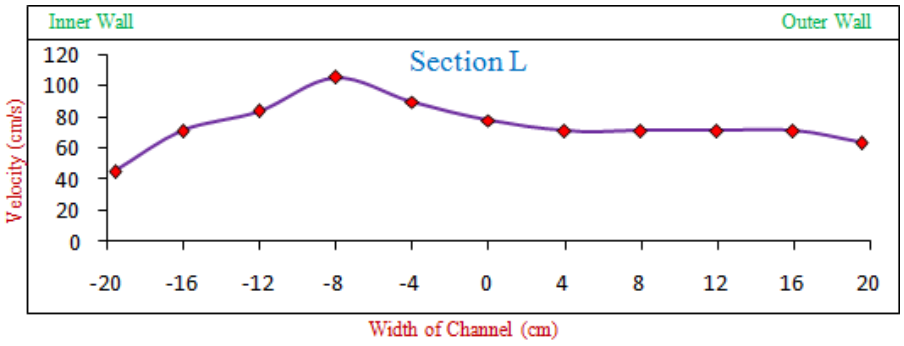

Figure 4.8.12

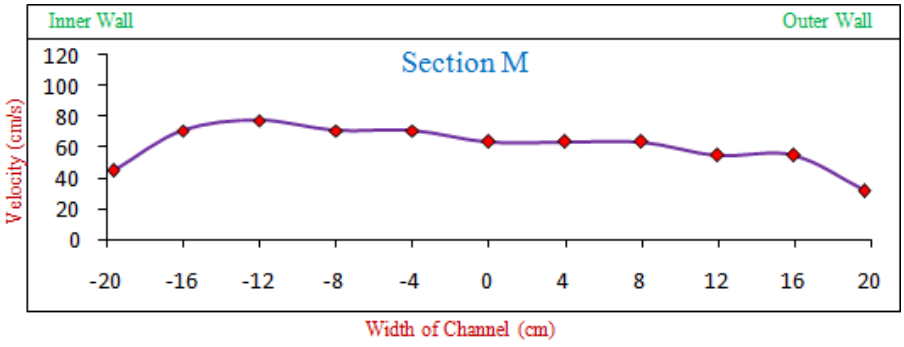

Figure 4.8.13

Figure 4.8.1 to 4.8.13: Horizontal Velocity Profile at 0.8*H* from the bed of the Channel Section along the Meander Path

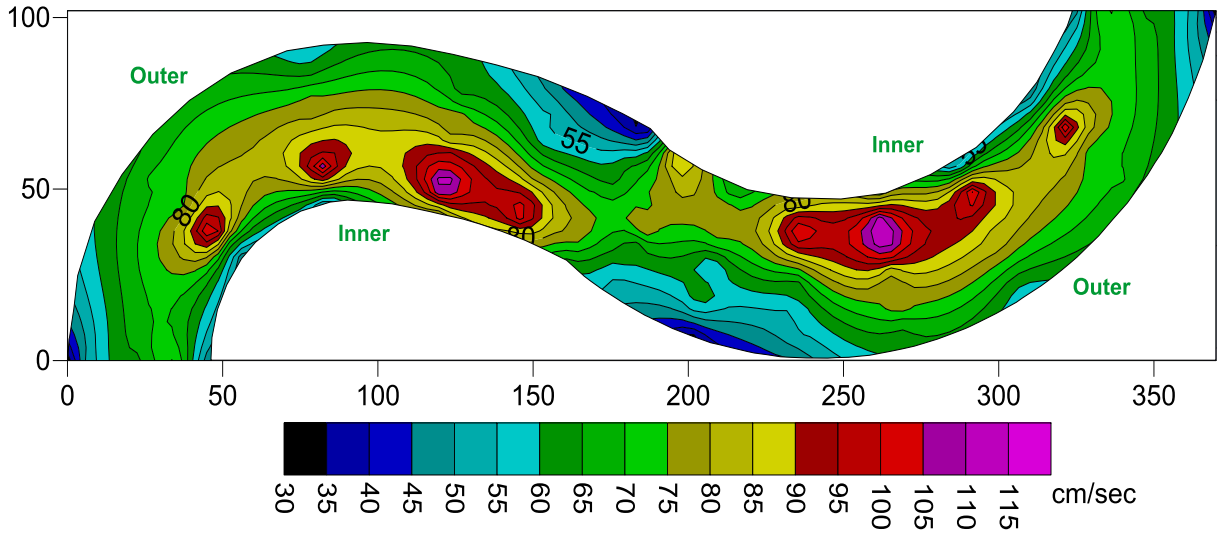

Figure 4.9: Contour Plot of Horizontal Velocity at 0.8*H* from the bed of the Channel Section along the Meander Path

From the above horizontal profile study at different levels, the following deductions can be made

1. The horizontal velocity profiles at the bed of the channel in section A (bend apex) remains higher at the inner wall i.e. the right bank and there is a drastic difference in velocity between the inner and outer walls as seen in Fig. 4.2.1. The highest velocity remains close to 80cm/s
2. On moving at the bed from the initial bend apex region towards the cross-over (Section G) as seen in Fig. 4.2.2 to 4.2.6; there is a gradual change in the horizontal velocity profile along the width of the channel, with higher velocity remaining at the inner wall.
3. As seen in Fig. 4.2.7, at the bed of the cross-over section G, the maximum velocity moves towards the centre of the channel section, with gradual variation of velocity towards the inner and outer walls. The maximum velocity at the bed of the cross-over being about 70cm/s

4. In the following sections, from Fig. 4.2.8 to Fig. 4.2.12, on moving from cross-over towards the other bend apex, the higher velocity at the bed moves towards the left bank which is the inner wall as the curvature of the meandering channel changes its course.
5. Fig. 4.2.13 depicts the variation of velocity at the bed of the section M, with considerable difference in velocity between the inner and outer walls.
6. Fig. 4.3 shows the contour plots of the velocity variation at the bed of the channel along the meander path. The maximum velocity as seen from the contours is around 80cm/s.
7. It is observed from the contour plots in Fig.4.3 that the horizontal velocity profiles at different sections before the cross-over remains similar (mirror image) after the cross-over.
8. Fig. 4.4.1 depicts the velocity variation at the bend apex section A at the depth of 0.4*H* from the bed. Here the horizontal velocity profile shows a gradual variation with higher velocity at the right bank i.e. the inner wall of the section. Here the highest velocity remains close to 95cm/s.
9. Fig. 4.4.2 to 4.4.6 show similar variations as seen at the bed of the channel, with the highest velocity remaining at the inner wall of the channel.
10. At the section G, as shown in Fig. 4.4.7, local highest velocity lies at the centre of the channel with a value of less than 100cm/s.
11. Fig. 4.4.3, i.e. section C shows the presence of highest velocity of around 110cm/s (10 percent more than cross-over) close to the inner wall at 0.4*H* from the bed. Hence, it can be concluded that higher velocity is achieved somewhere in-between the bend apex and the cross-over.
12. Fig. 4.4.11 i.e. the section K for the anti-clockwise curve of the meander path shows similar characteristics as in section C for the clockwise curvature. The maximum local

velocity in section K is also found to be around 110cm/s in the inner wall which lies at the left bank.

13. Sections preceding and following the section K i.e. from Fig. 4.4.8 to 4.4.13 show gradual variation with highest velocity towards the left bank or the inner wall of the channel.
14. Fig. 4.5 shows the horizontal velocity contour at 0.4*H* from the bed of the channel. It is observed that the maximum value of velocity is around 110cm/s.
15. Fig. 4.6.1 to 4.6.13 and Fig. 4.8.1 to 4.8.13 depict the horizontal velocity plots at 0.6*H* and 0.8*H* from the bed of the channel respectively. The pattern seen is found to be similar to the previous water levels.
16. The velocity values at 0.6*H* and 0.8*H* levels are usually less as compared to the level of 0.4*H* from the bed. But it is observed that in both the levels, the local maximum velocity in sections C, D, J and K (see Fig. 4.6.3, 4.6.4, 4.6.10, 4.6.11,4.8.3, 4.8.4, 4.8.10, 4.8.1) is close to 115cm/s the values of which at the same section is less as compared to the corresponding value at 0.4*H*water level.
17. The local maximum velocity at the cross-over which lies at the centre of the channel section is found to be highest at the 0.6*H* level from the bed with a velocity of around 95cm/s.
18. Fig. 4.7 and 4.9 represent the horizontal velocity contours of 0.6*H* and 0.8*H* level from the bed of the channel. Both the contours show similar pattern with the maximum velocity being close to 115cm/s.

4.3.2 LONGITUDINAL VELOCITY DISTRIBUTION IN THE CHANNEL DEPTH AT DIFFERENT SECTIONS ALONG THE MEANDER PATH

The longitudinal velocity distribution is analyzed along the depth of the channel at 9 positions along the width of the channel. The vertical sections are taken at 4cm intervals from the centreline of the meandering channel. The profiles are analyzed at all the 13 sections along the meander path.

The following figures from 4.10.1 to 4.10.13 represent the contour plots at all the sections along the meander path. Figures 4.11.1 to 4.11.13 represent the velocity profiles at every section along the meander path. Each section has the vertical velocity profiles at 9 positions across the channel section taken 4cm from either side of the centreline.

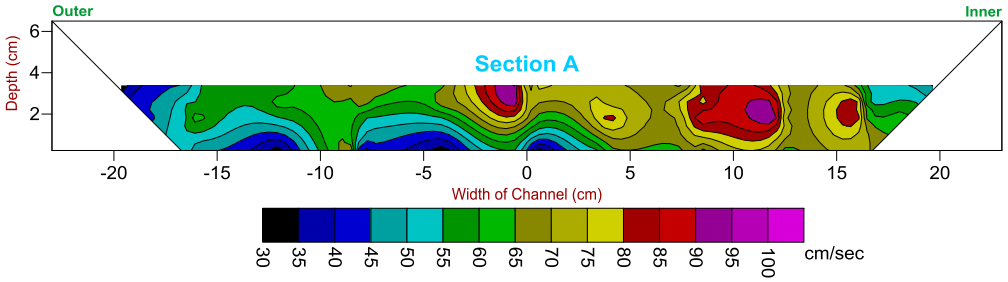

Figure 4.10.1

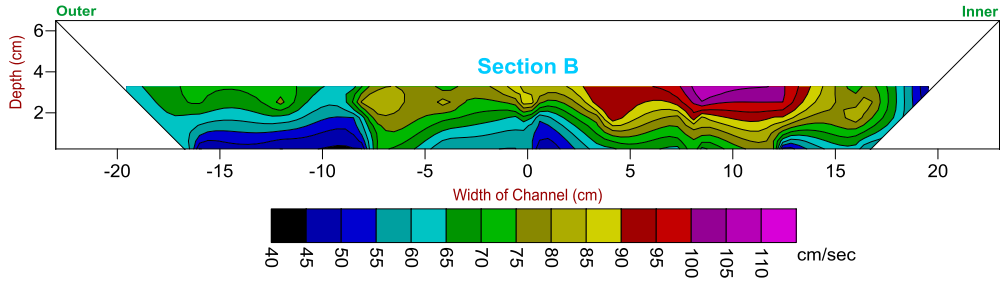

Figure 4.10.2

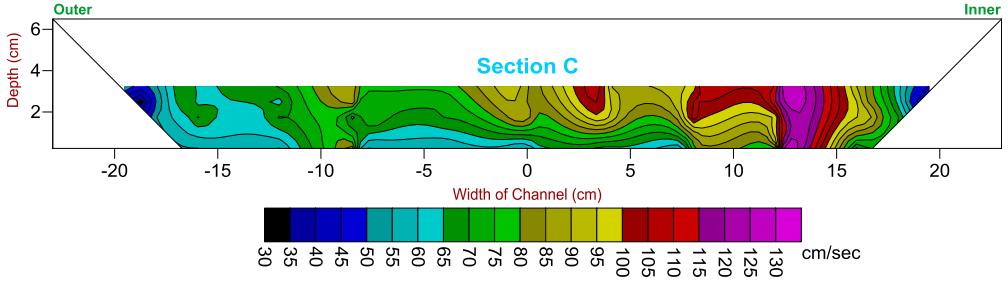

Figure 4.10.3

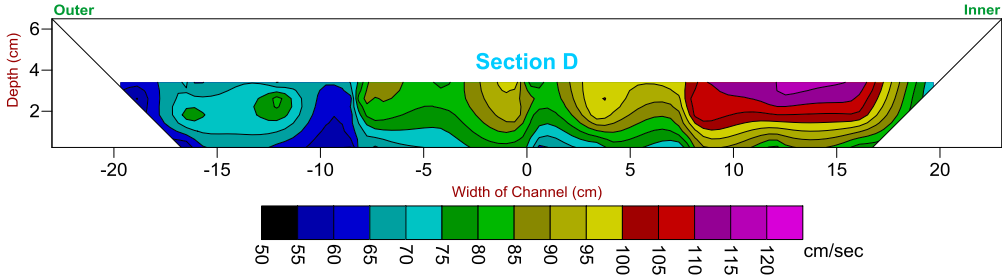

Figure 4.10.4

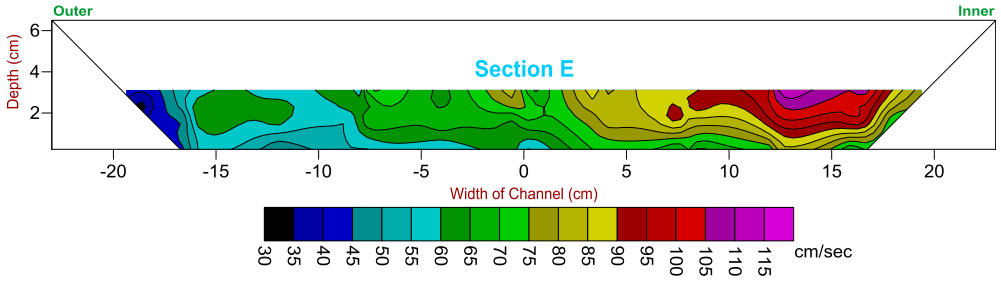

Figure 4.10.5

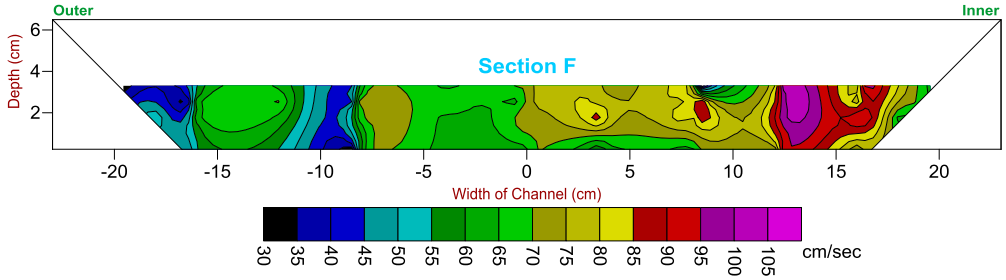

Figure 4.10.6

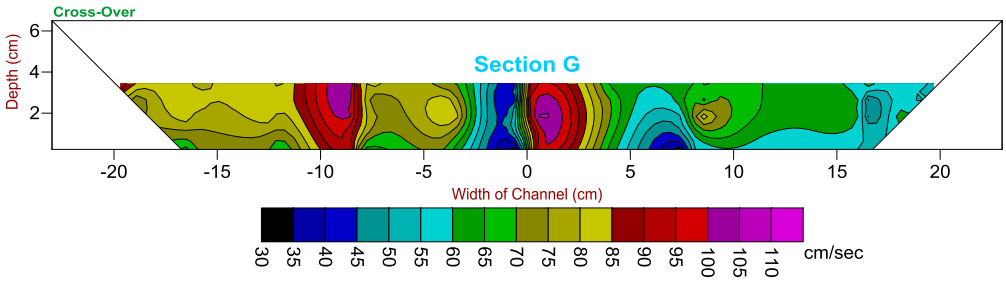

Figure 4.10.7

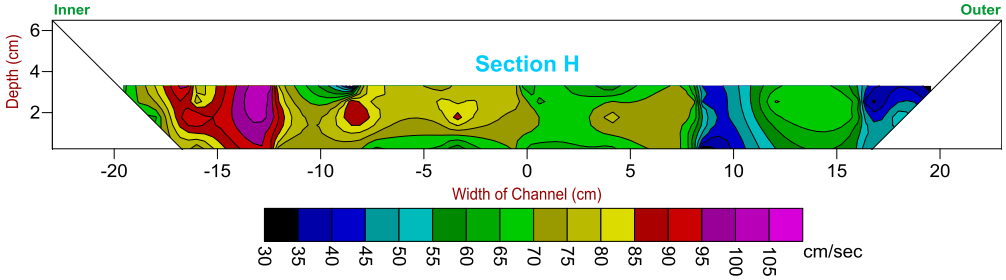

Figure 4.10.8

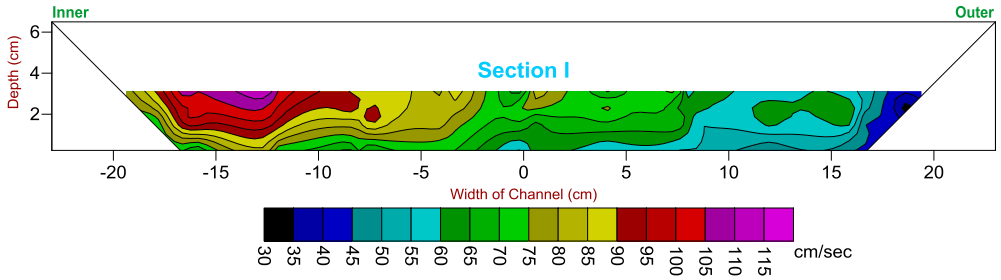

Figure 4.10.9

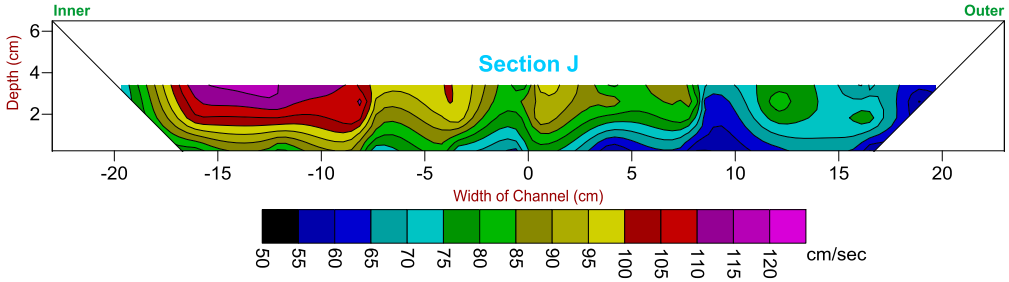

Figure 4.10.10

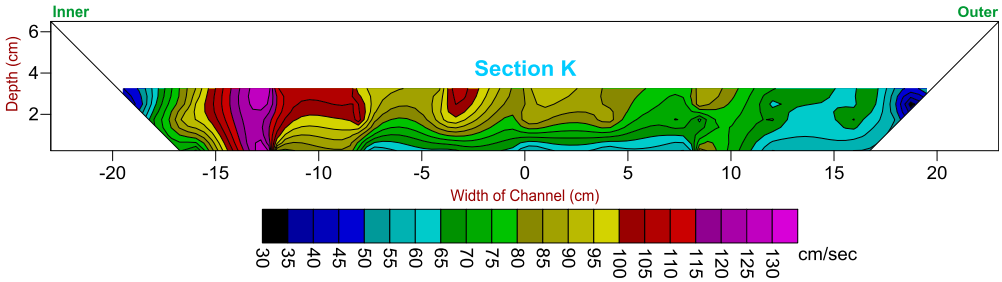

Figure 4.10.11

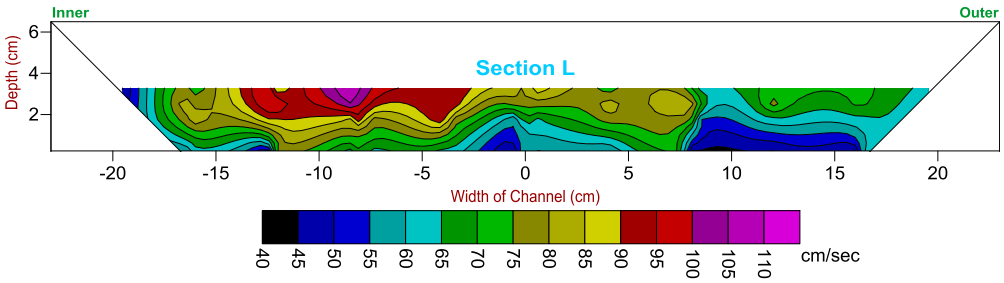

Figure 4.10.12

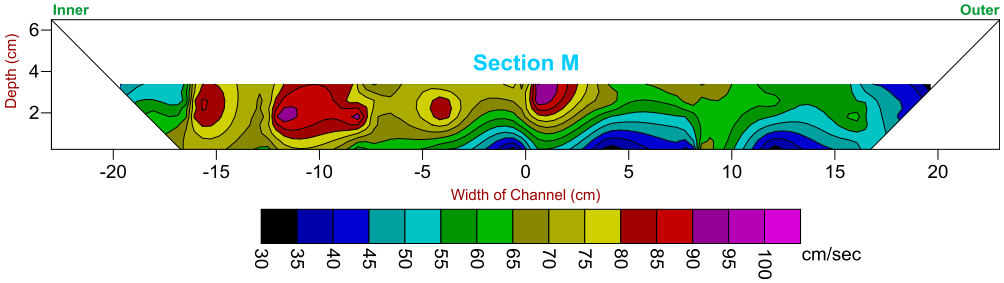

Figure 4.10.13

Figure 4.10.1 to 4.10.13: Vertical Velocity Contours for all 13 Sections along the Meander Path

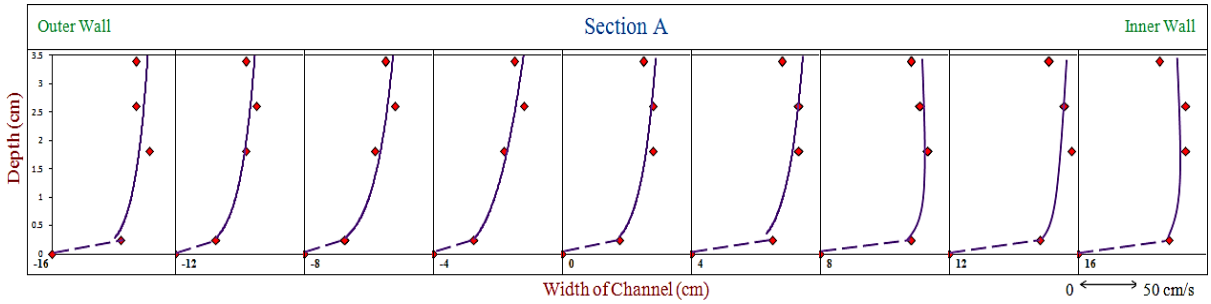

Figure 4.11.1

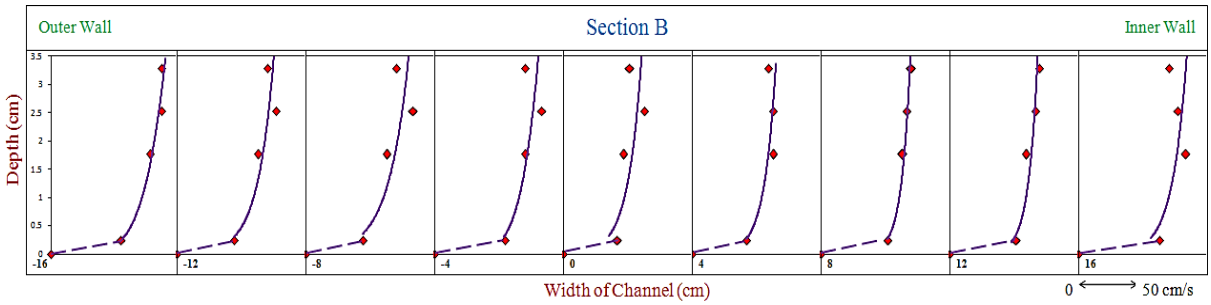

Figure 4.11.2

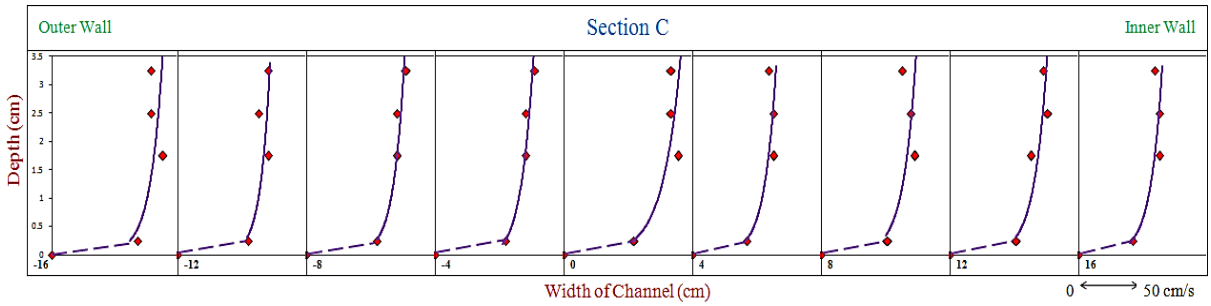

Figure 4.11.3

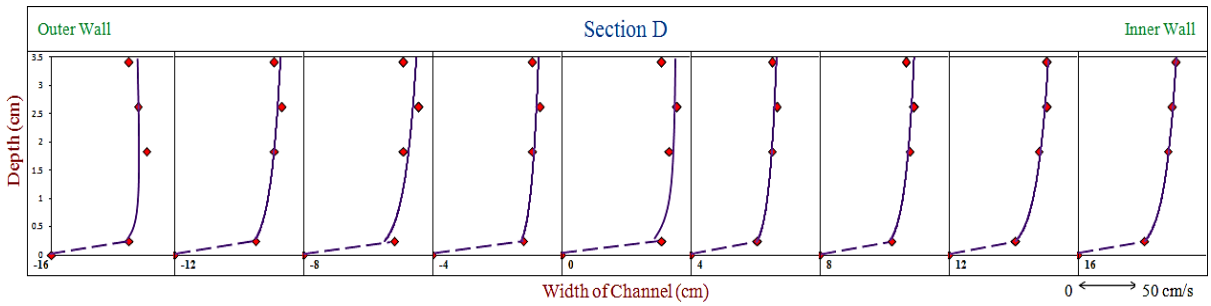

Figure 4.11.4

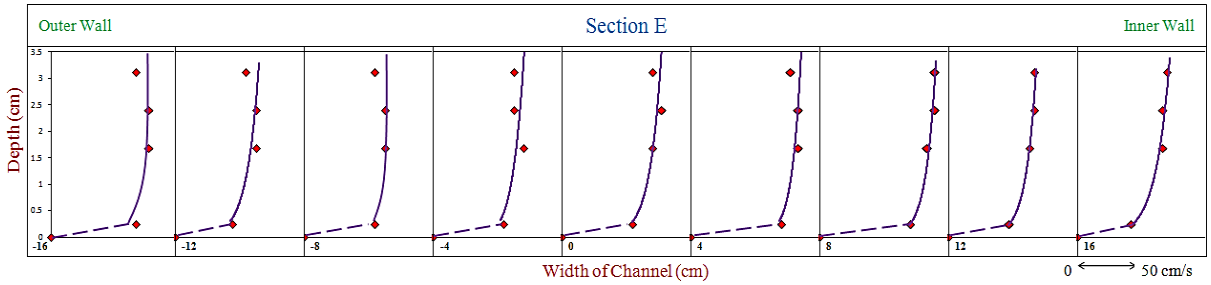

Figure 4.11.5

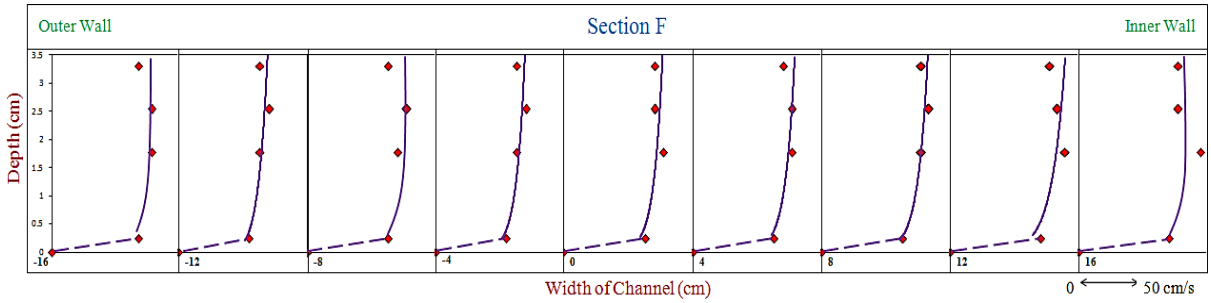

Figure 4.11.6

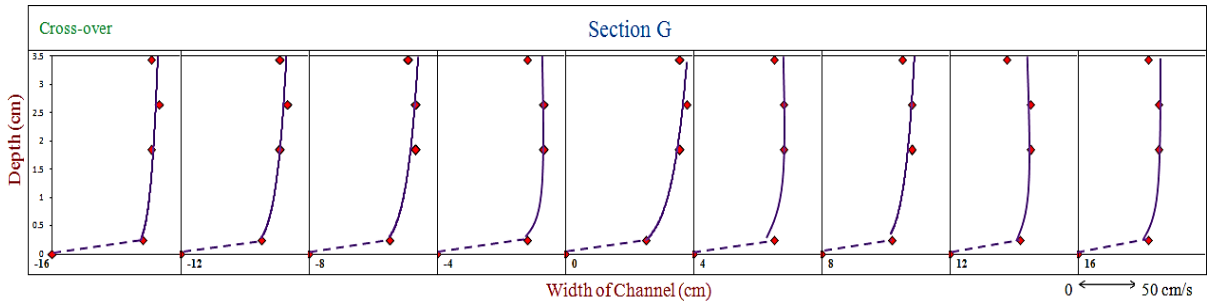

Figure 4.11.7

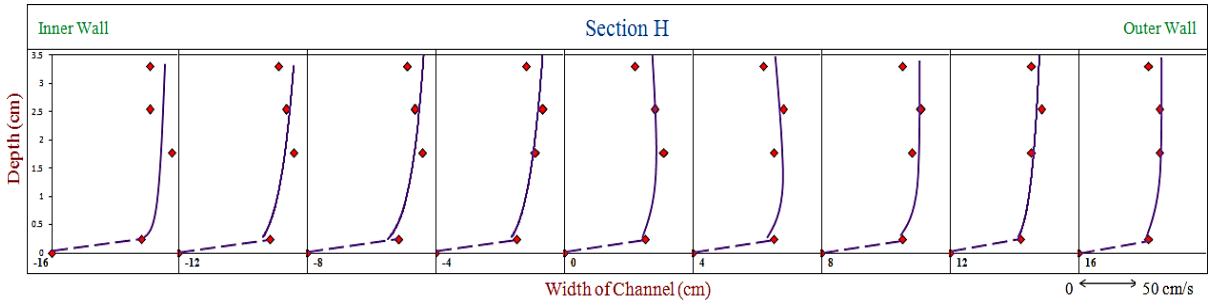

Figure 4.11.8

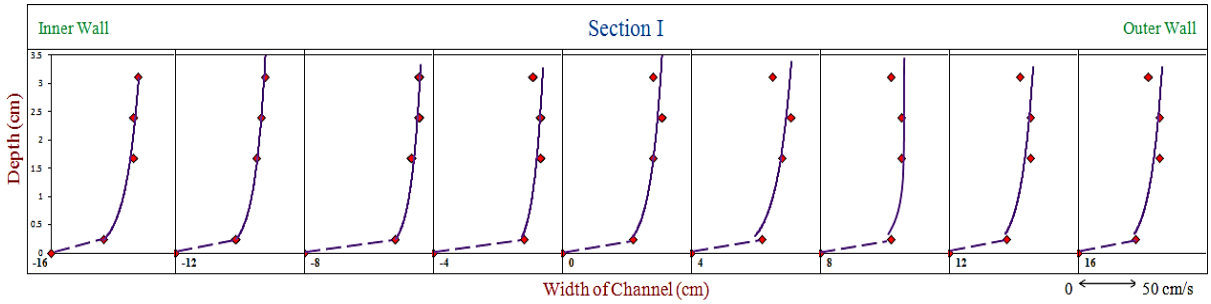

Figure 4.11.9

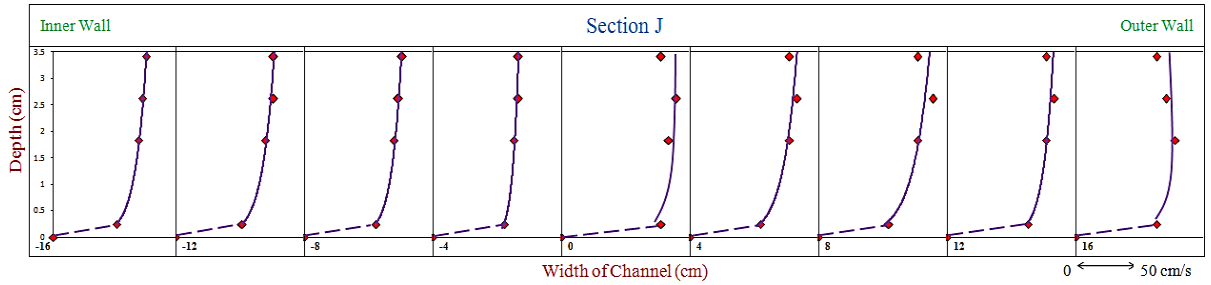

Figure 4.11.10

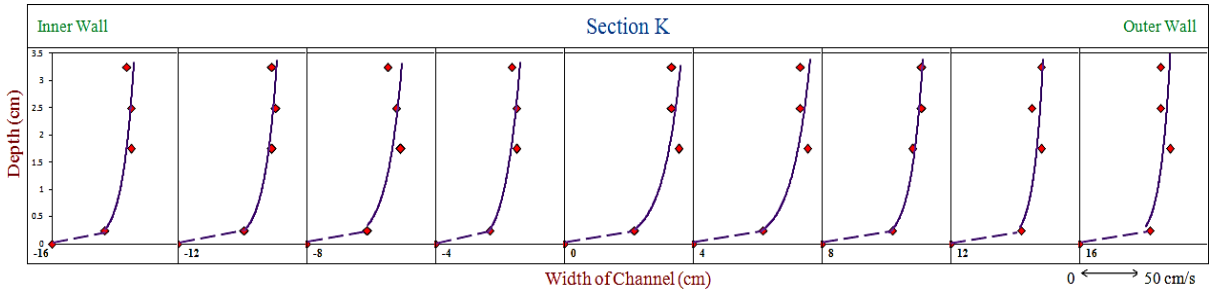

Figure 4.11.11

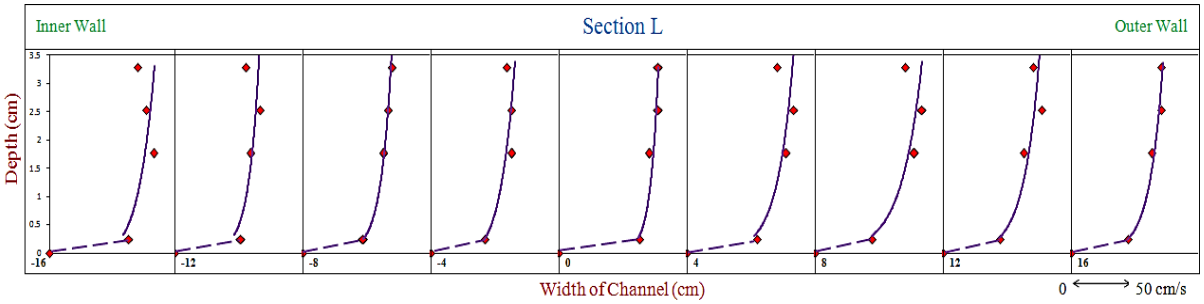

Figure 4.11.12

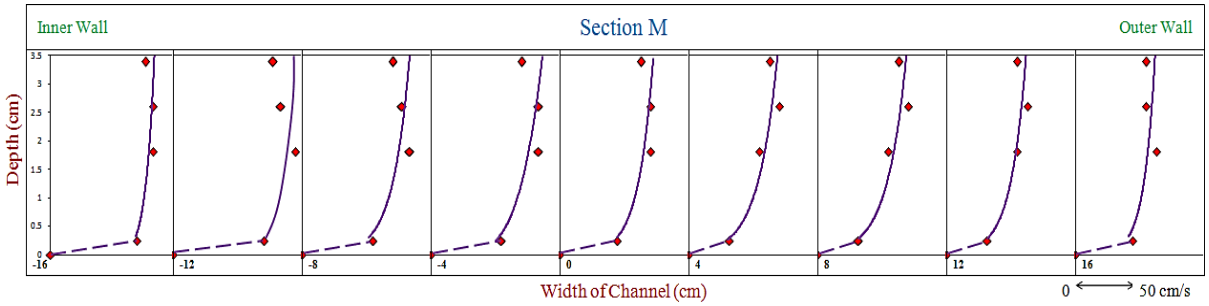

Figure 4.11.13

Figure 4.11.1 to 4.11.13: Vertical Velocity Profile plots for all 13 Sections along the Meander Path

The following inferences can be made from the vertical velocity profile plots

1. The velocity contour diagram of section A, as given in Fig. 4.10.1 shows that higher longitudinal velocity lies towards the right bank or the inner wall of the channel section. The vertical velocity profiles at the same section (Fig. 4.11.1), depicts the similar pattern. The vertical velocity profile sections closer to the inner wall are observed to be bulgier than at the outer wall.
2. It is observed in the contour plots of Fig. 4.10.1 to 4.10.3 that the maximum velocity from inner bank of section A moves towards the central region of section C. The

maximum local velocity initially moves close to the surface, which latter moves towards the bed of section C.

3. The maximum velocity at section C is found to be always higher, i.e. close to 130 cm/s as compared to the other sections for the entire clockwise curvature of the meandering channel, until the cross-over.The presence of maximum velocity at section C depicts that the velocity of flow increases while moving in the curvature from the bend apex to the cross-over. As the water negotiates the curvature, the velocity remains high.
4. The longitudinal velocity profiles in Fig. 4.11.1 to 4.11.6, i.e. at section A to F, show that the velocity remains higher towards the inner wall as compared to the outer wall while moving in the curved path of the meandering channel. Non-uniformity in velocity distribution is seen in these sections.
5. Fig. 4.10.7 and 4.11.7 show that the variation of velocity between the inner and outer walls is very less at the cross-over section G. However, the local maximum velocity of about 110 cm/s is found to be somewhere near the central region. The contour plot in Fig. 4.10.7 shows that the maximum velocity lies close to the bed.
6. Fig. 4.10.8 through 4.10.13 demonstrates that the maximum velocity moves from the central region at the cross-over towards the left bank or the inner wall of the corresponding anti-clockwise curvature. The maximum velocity initially moves close to the bed and then shifts closer to the free surface.
7. The bend apex sections A and M have the maximum degree of curvature and the channel continues as a sinuous channel at both these sections. Hence the local maximum velocities at these sections lie close to the inner wall.
8. The sections C and K as seen in Fig. 4.10.3 and 4.10.11, have highest maximum velocity throughout the channel, close to 130 cm/s. Such observation is due to the curvature of the meander path, moving towards the cross-over.

4.3.3 OCCURANCE OF MAXIMUM DEPTH AVERAGED VELOCITY

Depthaveraged velocity is considered to be the average velocity at anyvertical section of a channel cross-section.The occurrence of this velocity is generally trusted to be found at 0.4*H* from the bed of the channel. *H* being the flow depth of water at that section. Here we have taken the readings of depth averaged velocity at different vertical sections of a cross-section. The process is repeated for thirteen cross-sections along the meander path. At every cross-section the occurrence of maximum depth averaged velocity along the meander path are found and plotted. Figure 4.12 demonstrates the movement of local maximum depth averaged velocity at every section along the meander path of the meandering channel.

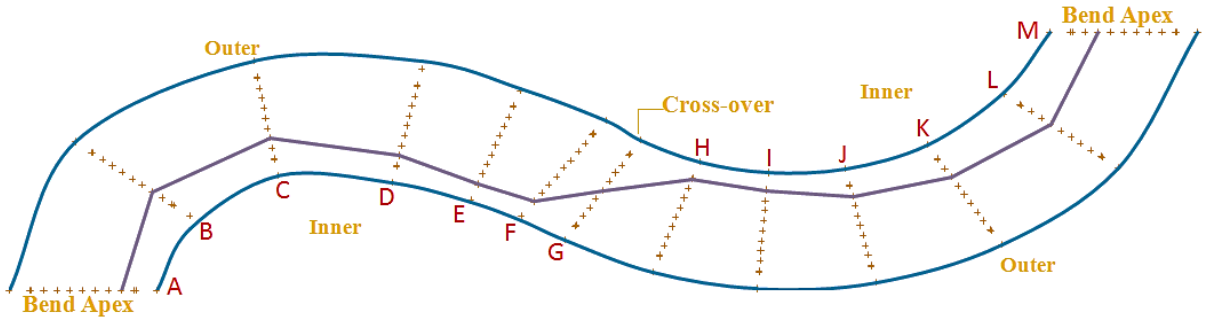

Figure 4.12: Occurrence of Maximum Depth Averaged Velocity along the Meander Path

From the above figure, the following inferences can be made

1. The maximum depth-average velocity remains at the inner wall throughout the meander path.
2. The maximum depth averaged flow velocity remains closer towards the inner wall at sections nearer to the cross-over.
3. Then the local maximum depth averaged velocity moves towards the centre of the cross-over section.There is a direct movement of local maximum depth averaged velocity from the inner wall of the section F towards inner wall of section H passing through the centre of the cross-over section G.

4.4 BOUNDARY SHEAR STRESS DISTRIBUTION AT DIFFERENT SECTIONS ALONG THE MEANDER PATH

Boundary shear measurements are carried out at different sections from one bend apex to another bend apex through the cross-over. Total 13 reaches of boundary shear measurements are carried out.

The figure 4.13.1 to 4.13.13 illustrates the boundary shear stress distributions across the channel bed and the side slopes at the inner and outer walls for all the 13 reaches of measurement.

The shear stress profiles along the rigid surface of the channel are represented by showing the stress curves perpendicular to all the three sides of the channel; namely the bed, the inner wall and the outer wall. Hence the figures give a clear demonstration about the boundary shear stress distribution throughout the channel section.

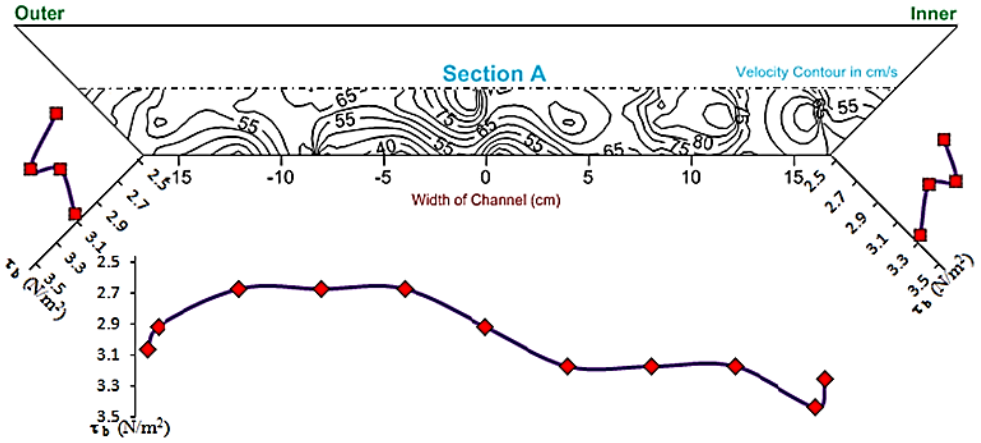

Figure 4.13.1

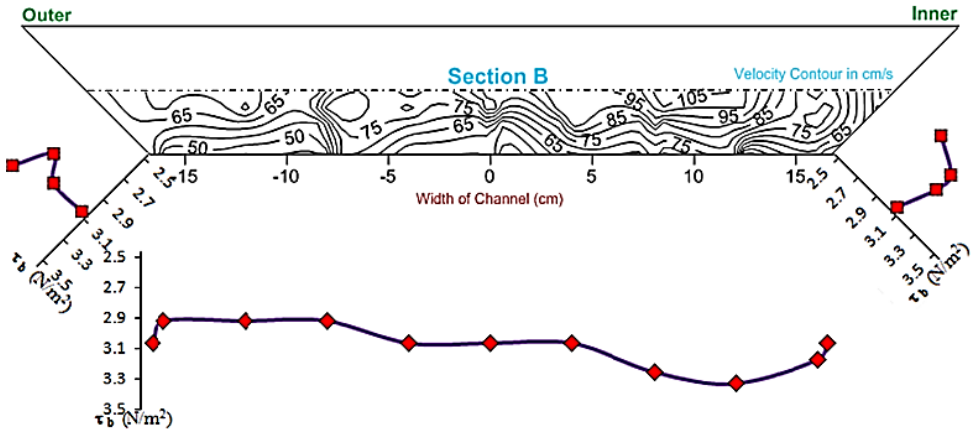

Figure 4.13.2

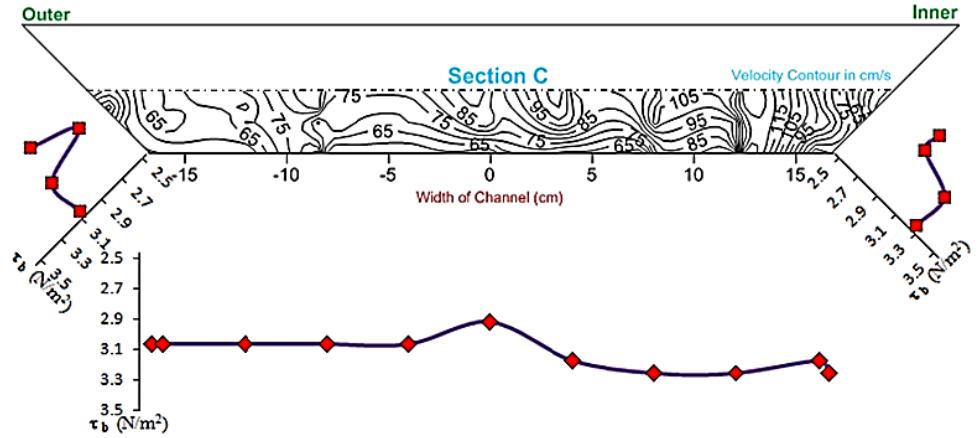

Figure 4.13.3

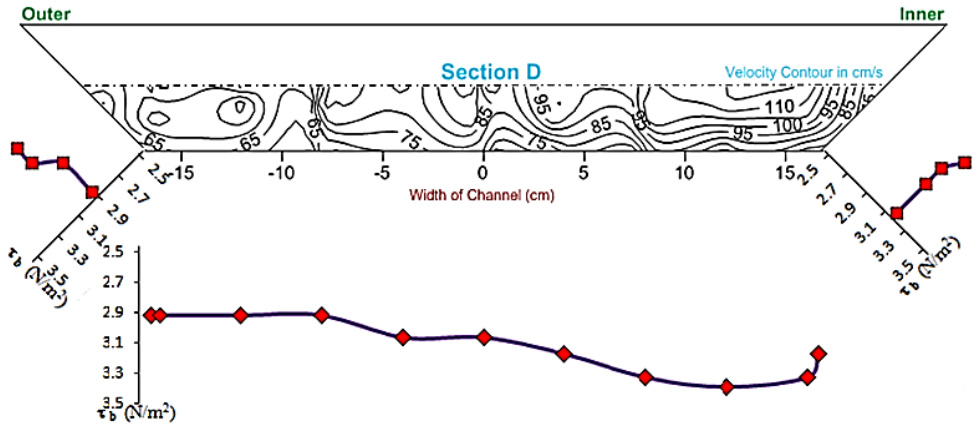

Figure 4.13.4

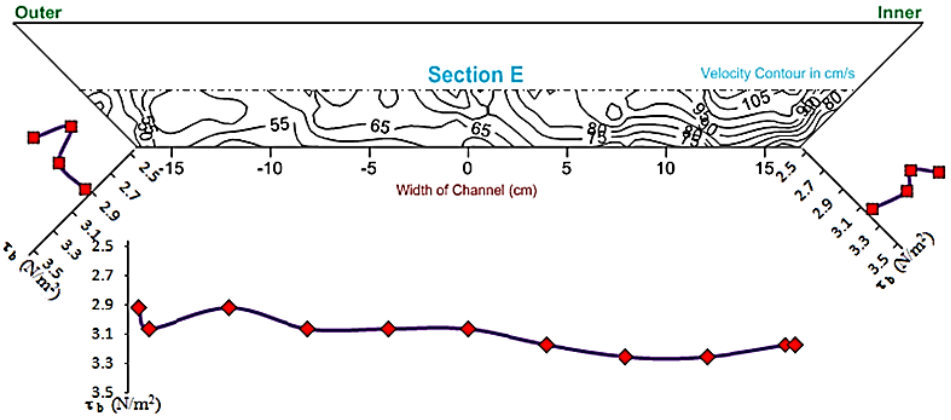

Figure 4.13.5

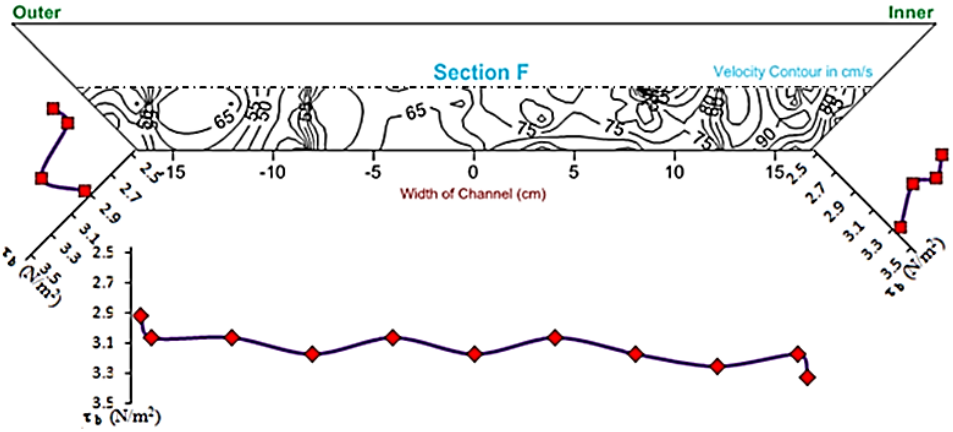

Figure 4.13.6

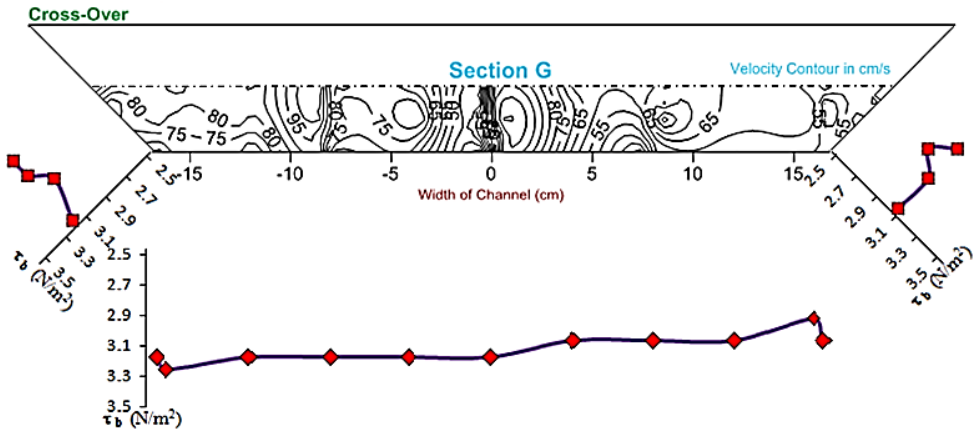

Figure 4.13.7

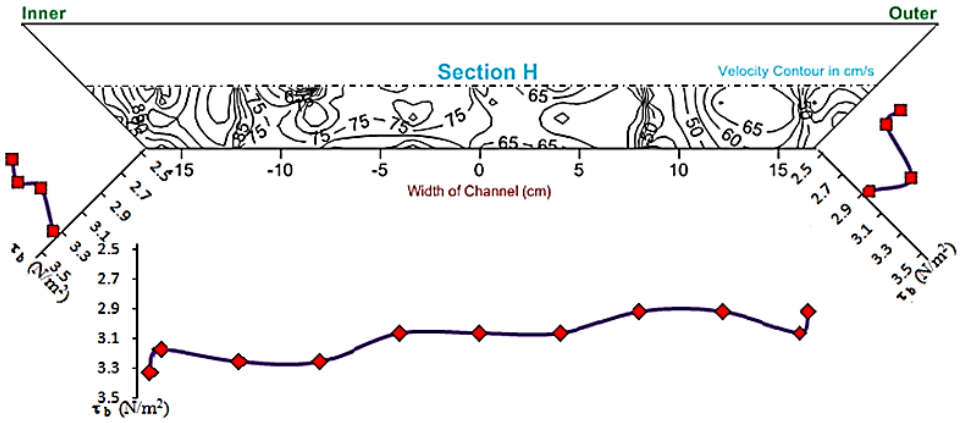

Figure 4.13.8

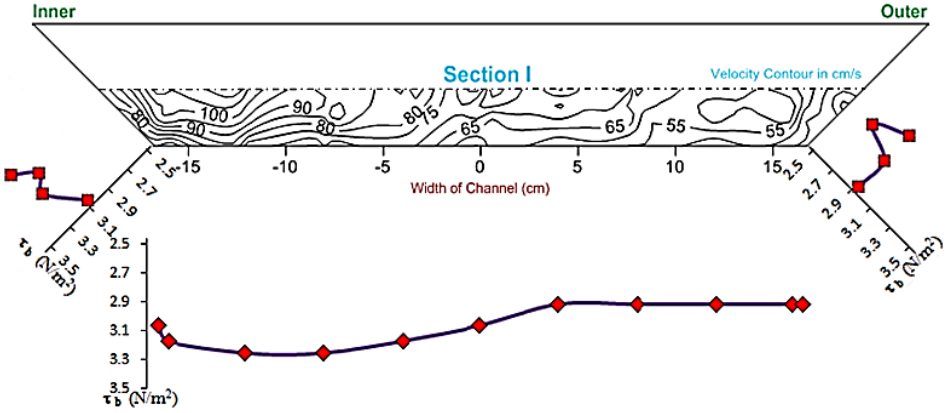

Figure 4.13.9

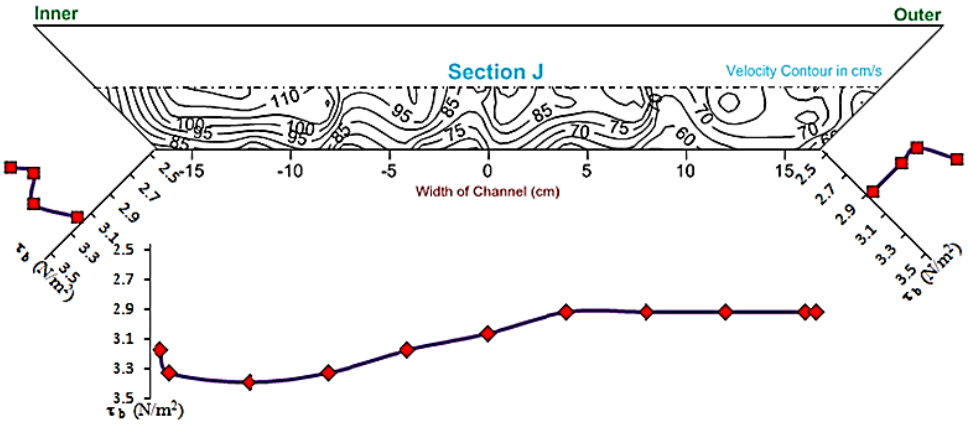

Figure 4.13.10

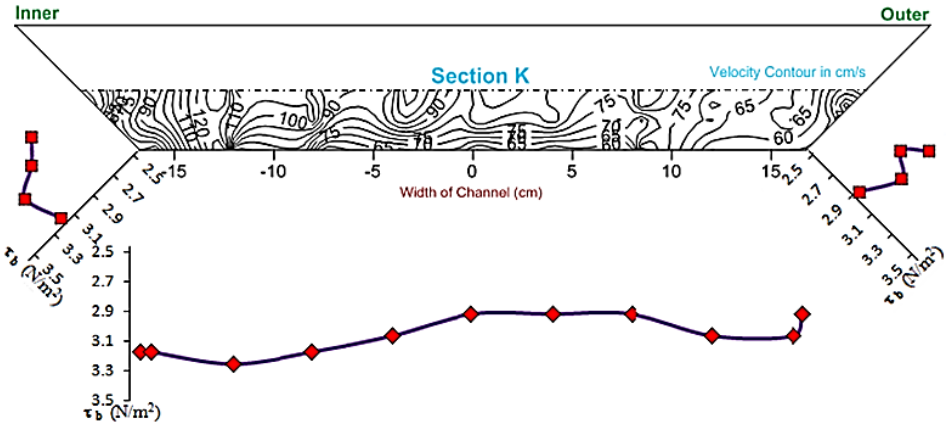

Figure 4.13.11

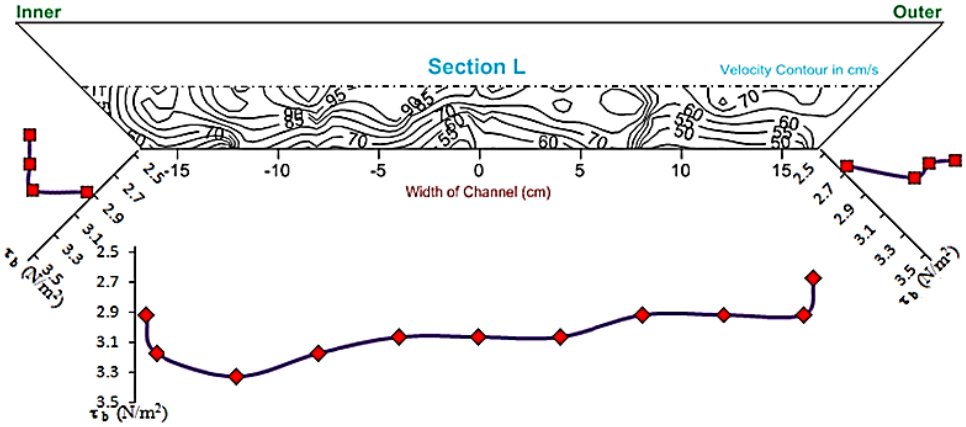

Figure 4.13.12

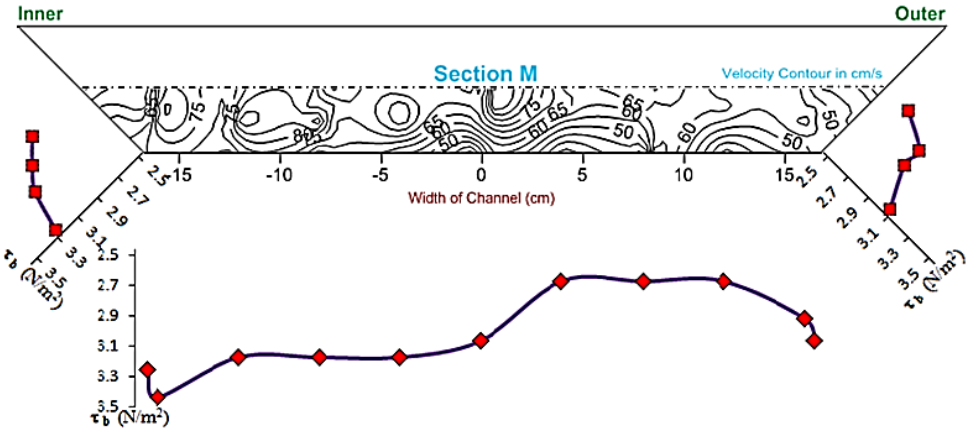

Figure 4.13.13

Figure 4.13.1 to 4.13.13: Boundary Shear Stress Plots across all 13 Sections along the Meander Path

The following deductions can be made from the above boundary shear stress graphs

1. At the bend apex section A, given in figure 4.13.1, the shear stress carried by the inner wall is seen to be more as compared to the outer wall.
2. The highest shear stress at the inner bank of the section A is found to be around 3.44N/m^2, while a minimum of 2.67N/m^2 at the outer wall. The variation of shear stress in this section is seen to be erratic.
3. The sections B to F, i.e. from Fig. 4.13.2 to 4.13.6, the shear stress remains higher towards the inner wall. But, in these sections, the variation of shear stress between the inner and outer walls is observed to be gradual.
4. At the cross-over section G, the variation of boundary shear stress is seen to be more or less uniform throughout the channel section. The shear stress value remains close to 3N/m^2.
5. From the Fig. 4.13.1 through 4.13.13, it is observed that on moving from the initial bend apex section A; the boundary shear carried by the inner wall decreases and reaches a minimum at the cross-over. It then increases on the other bank (inner wall) while progressing towards the next bend apex section M.
6. From Fig. 4.13.8 to 4.13.12, it is observed that there is a gradual variation in boundary shear stress between the inner and outer walls, with higher stress remaining towards the left bank (inner wall).
7. Fig. 4.13.13 depicts drastic variation between the boundary shear stress values between the inner and outer walls of the channel section, with higher shear stress lying towards the inner wall.

4.5 BOUNDARY SHEAR FORCE DISTRIBUTION ALONG THE MEANDER PATH

Using the Preston tube technique, we have measured the boundary shear stress along the wetted perimeter of the channel at 13 different sections between one bend apex to the next bend apex.

At every section, the boundary shear distribution plots were shown in Fig. 13. At each section the boundary shear stress is integrated over the wetted perimeter to get the shear force at the inner wall, outer wall and bed separately.

$SF_{Inner}=\int_{Inner} \tau \, dP$ Eq. 4.1

$SF_{Outer}=\int_{Outer} \tau \, dP$ Eq. 4.2

$SF_{Bed}=\int_{Bed} \tau \, dP$ Eq. 4.3

$SF_{Inner} + SF_{Bed} + SF_{Outer} = SF_T$ Eq.4.4

Theoretically, $SF_T = \rho g A S$ Eq. 4.5

The total shear force is calculated by using the Eq. 4.4. The total theoretical shear force is calculated for each section by using Eq. 4.5. The total theoretical shear force is averaged and compared with the actual values. The error found between the values (which are less than 10%) is distributed proportionately among the bed and walls which give a new normalized value of shear force for the bed and walls.

The table 4.1 depicts the shear force distribution and the percentage of sharing of normalized shear force at the inner wall, outer wall and the bed of the channel section from the averaged total theoretical shear force.

After finding the shear force distribution in the inner wall, outer wall and bed, the boundary shear force distribution for the different sections are plotted and shown in Fig. 4.14 and 4.15

Table 4.1: Shear Force Distribution for Meandering Channel at Different Reaches

Section	Flow Depth (in m)	$Area_{MC}$ (in m^2)	SF_{Inner} (in Nm/s)	SF_{bed} (in Nm/s)	SF_{Outer} (in Nm/s)	SF_T' Experimental (in Nm/s)	SF_T Actual (in Nm/s)	SF_{Inner} as % of SF_T	SF_{Bed} as % of SF_T	SF_{Outer} as % of SF_T
A	0.035	0.012775	0.00690095	0.04039373	0.00450458	0.05179926	0.05029667	13.3224798	77.9813008	8.69621937
B	0.0377	0.01386229	0.00648843	0.04781314	0.00550344	0.05980501	0.05457745	10.849305	79.948384	9.20231096
C	0.0397	0.01467709	0.00696728	0.05045436	0.00470018	0.06212183	0.05778542	11.2155152	81.2184122	7.5660726
D	0.0415	0.01541725	0.00779788	0.05381132	0.00486157	0.06647077	0.06069951	11.7312916	80.9548561	7.31385231
E	0.044	0.016456	0.00782654	0.05026659	0.00340827	0.0615014	0.06478919	12.7257887	81.7324356	5.54177568
F	0.0422	0.01570684	0.00852204	0.05201762	0.00373357	0.06427323	0.06183966	13.2590836	80.9320131	5.80890329
G	0.04	0.0148	0.00553787	0.05042526	0.00705851	0.06302164	0.05826933	8.7872574	80.0126083	11.2001343
H	0.0373	0.01370029	0.00761981	0.04741461	0.00401603	0.05905044	0.05393964	12.903896	80.2950936	6.80101032
I	0.0363	0.01329669	0.00748323	0.04622744	0.00339398	0.05710465	0.05235062	13.1044107	80.9521422	5.94344712
J	0.0398	0.01471804	0.00905488	0.0522715	0.00461722	0.0659436	0.05794664	13.7312458	79.2669802	7.00177399
K	0.0354	0.01293516	0.00700224	0.04422857	0.00479621	0.05602702	0.05092724	12.497966	78.9415098	8.56052425
L	0.0361	0.01321621	0.00568623	0.04605451	0.00503772	0.05677846	0.05203376	10.0147723	81.1126371	8.87259066
M	0.0385	0.01418725	0.0066	0.04193355	0.00436462	0.05289463	0.05585686	12.4709341	79.2775215	8.25154446

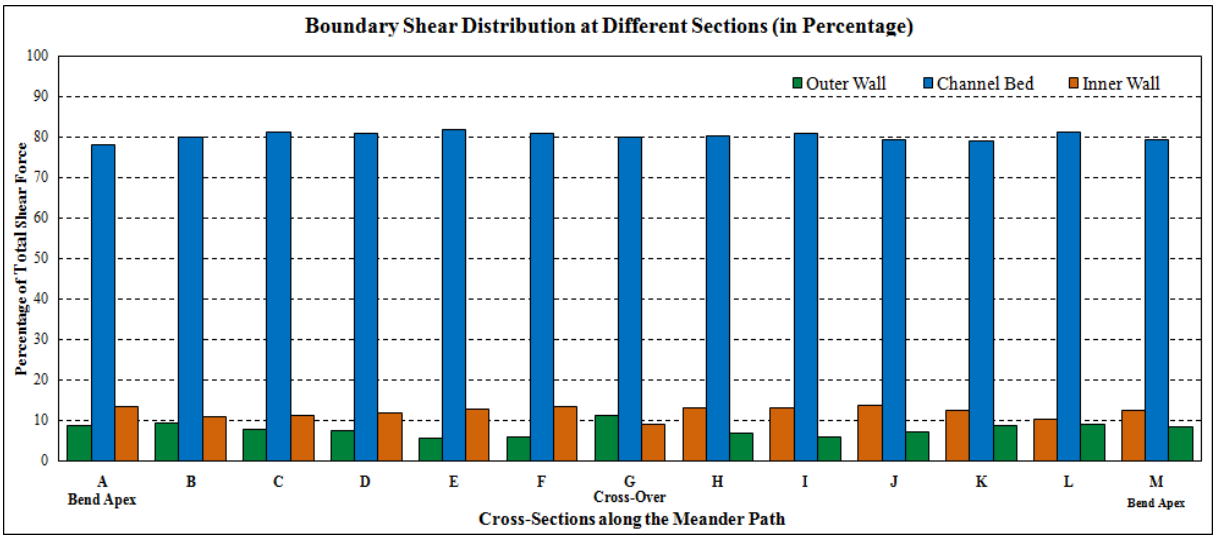

Figure 4.14: Boundary Shear Distribution at Different Sections (in %age) – Separately

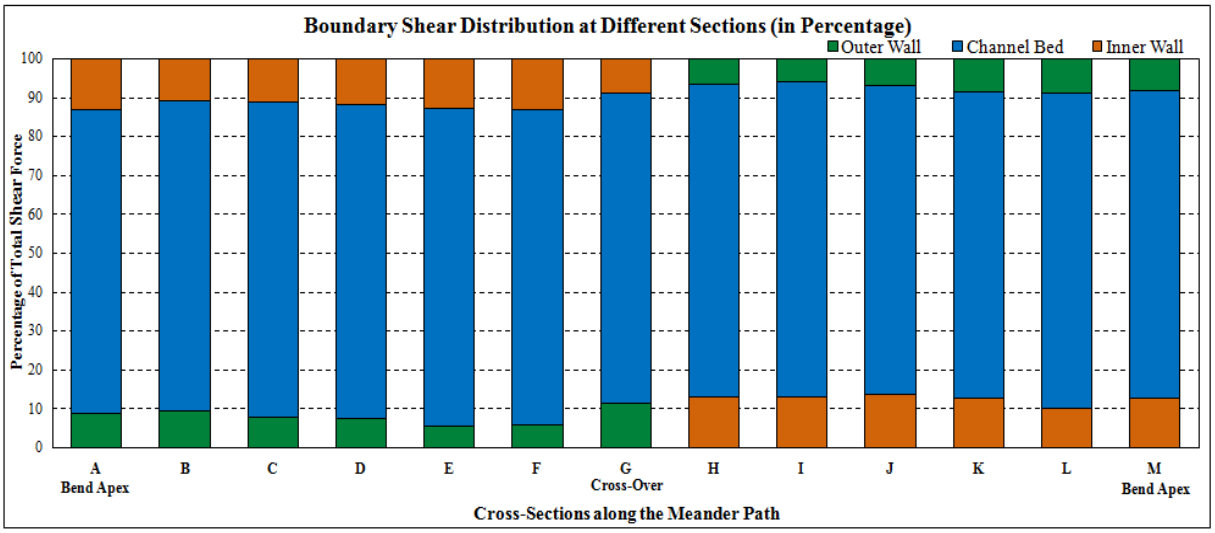

Figure 4.15: Boundary Shear Distribution at Different Sections (in %age) – In one Column

From the plots, the following findings are presented below:

1. From the Fig. 4.14 it is seen that, at the bend apex section A, the shear stress carried by the inner wall is more as compared to the outer wall. The inner wall carries about 13% of the total shear force while the outer wall carries about 8%.
2. While going from reach to reach from the bend apex, as seen in Fig. 4.15 the shear carried by the inner wall decreases and reaches a minimum at the cross-over (around 9% of the total shear force). Then the value goes on increasing towards the next bend apex.
3. Similarly as seen in Fig. 4.15, at the outer wall, the shear force carried by the bend apex is less (about 8% of the total shear force) which first slightly decreases and then increases to reach maximum value at the cross-over (about 11% of the total shear force).On moving from the cross-over, the shear force at the outer wall starts decreasing and then somewhat increases towards the other bend apex.
4. From Fig. 4.14, it is observed that there is a significant difference in the shear force sharing among the inner and outer walls of all the reaches. But, there is less variation among the inner and outer walls of the cross-over section G.
5. As seen in Fig. 4.14, the shear force carried by the bed of the channel throughout the meander path is found to remain more or less constant. The bed is observed to carry about 80% of the total shear force while the rest is being shared by the inner and outer walls.

CHAPTER 6
CONCLUSIONS

5.1 CONCLUSIONS

Experimental investigations are carried out on a highly sinuous meander path at different reaches. The different flow characteristics such as water surface profile, velocity distribution, shear stress distribution etc. are investigated Based on the analysis of the experimental investigations, certain conclusions are drawn which are discussed below:

1. The water surface profile remains higher on the outer wall than at the inner wall at every channel section across the meandering path.
2. The water surface profile levels itself at the cross-over section of the highly sinuous meandering channel, the results of which are similar to the case of straight channels.
3. The Sections closer to the cross-over regions, are found to have little variations in the water surface profile between their inner and outer walls.
4. Significant variations of water surface profile are found at the bend apex this may be due to presence of maximum curvature at those sections.
5. The results of Horizontal velocity profile shows higher velocity results at the inner wall of the channel section than outer wall and gradually decreases towards the outer wall.
6. Significant variation of water surface profile are seen at the bend apex sections which may be due to presence of maximum curvature at those sections
7. Horizontal velocity profile of a highly sinuous meandering channel remains higher at the inner wall of the channel section and decreases towards the outer wall.
8. At the bed of the cross-over section, the local maximum velocity is found to move towards the center of the section, with gradual variations towards the inner and outer walls.
9. Local maximum longitudinal velocity at the cross-over section are found to occur at the center of the channel section the highest value of which is at $0.6H$ level from the bed.

10. Maximum longitudinal velocity from the inner bank of the bend apex sections are found to move toward the central region sections. The maximum local velocity initially moves close to the surface, which later moves towards the bed.
11. Sections C and K (intermediate sections) have the highest maximum velocity throughout the meander path as seen in the longitudinal velocity contour plots for the entire path. Such observations are due to the curvature of the meander path moving towards the cross-over.
12. From the occurrence of maximum depth averaged velocity, It is observed, that the maximum velocity always remains towards the inner wall and moves even closer to the inner wall while approaching the cross-over.
13. The maximum depth averaged velocity is found to move through the center of the cross-over section from the inner wall of one curvature to the inner wall of the other inverse curvature of the meandering channel.
14. From the results of Shear stress measurements it is found that the shear stress at the inner wall always remains higher as compared to that at outer wall.
15. The boundary shear stress distribution at the cross-over sections is found to be more or less uniform throughout the channel section.
16. The shear force carried by the inner wall found to decreases up to the cross-over section and then goes on increasing. The shear force at the inner wall is also found to always remain higher than the shear force at the outer wall. The Shear force carried by the bed of the all the channel section is found to be nearly uniform throughout the meander path.
17. From the shear force distribution results, the sharing among the inner and outer walls is not uniform at all reaches along the meander path. Whereas there is very less variation between the shear force at inner and outer walls of the cross-over sections only.

5.2 SCOPE FOR FUTURE RESEARCH

The present research gives anextensive scope for future investigators to investigate other aspects of ameandering channel. The present research is limited to a single discharge flow analysis of the meander path. The research can be continued for different discharges to get an overall depiction about the flow characteristics.The future scope of the present research can be summarized as:

1. The flow analysis can be carried out at different discharges, giving the variation in surface profile and velocity profiles.
2. The work can be extended for meander paths with different rough surfaces.
3. Experimentation can be carried out for mobile bed meandering channels
4. Similar flow analysis can be carried out for meandering compound channels.
5. Experimental findings can be compared with data of other sinuous channels to carry out numerical modelling.
6. Mathematical modelling and numerical modelling can be carried out to predict the water surface profile, velocity profile and boundary shear stress distributions.

ACKNOWLEDGEMENT

The authors wish to acknowledge thankfully the support received by the second author from Department of Science and Technology, Government of India, under grant no.SR/S3/MERC/066/2008 for the research project work on compound channels at NIT, Rourkela.

REFERENCES

1. Absi, R. (2011). “An ordinary differential equation for velocity distribution and dip-phenomenon in open channel flows” *Journal of Hydraulic Research*, IAHR, Taylor and Francis, Vol. 49, N° 1, pp. 82-89
2. Ansari. K., Morvan. H. P. and Hargreaves. D. M. (2011),“Numerical Investigation into Secondary Currents and Wall Shear in Trapezoidal channels.” *Journal of HydraulicEngineering (ASCE)2011*; Vol.137 (4):432-440.
3. Baghalian, S., Bonakdari, H., Nazari, F., Fazli, M.(2012), “Closed-Form Solution for Flow Field in Curved Channels in Comparison with Experimental and Numerical Analyses and Artificial Neural Network”. *Engineering Applications of Computational Fluid Mechanics* Vo.6, No.4, pp. 514-526.
4. Bathurst, J. C., Hey, R. D., & Thorne, C. R. (1979). “Secondary flow and shear stress at river bends.”, *Journal of the Hydraulics Division*, *105*(10), 1277-1295.
5. Bhowmik, N. G., and Demissie, M. (1982), “Carrying capacity of flood plains”. *Journal of the Hydraulics Division*, *108*(3), 443-452.
6. Bonakdari, H., Baghalian, S., Nazari, F., Fazli, M.(2011), “Numerical Analysis and Prediction of the Velocity Field in Curved Open Channel using Artificial Neural Network and Genetic Algorithm”. *Engineering Applications of Computational Fluid Mechanics* Vo.5, No.3, pp. 384-396.
7. Boussinesq, J. (1868). Mémoiresurl’influence des frottementsdans les movement reguliers des fluids. J. Math. Pures Appl. (2me sér.), 13, 377-424.
8. Chang, H. H. (1984), “Variation of flow resistance through curved channels”, *Journal of Hydr. Engrg.,* ASCE, 110(12), 1772–1782.
9. Chow, V. T. (1959), “Open Channel Hydraulics”, McGraw-Hill Book Co, New York.
10. Coles, D. (1956). “The law of the wake in the turbulent boundary layer”. *Journal of Fluid Mechanics*, *1*(02), 191-226.

11. Cruff R.W. (1965), "Cross Channel Transfer of Linear Momentum in Smooth Rectangular Channels", *U. S. G. S Water Supply*, Paper 1592-B.
12. Dash, S. S. (2013), "Stage-Discharge Modelling of Meandering Channel". Thesis Presented to the National Institute of Technology, Rourkela, in partial fulfilment of the requirements for the Degree of Doctor of philosophy.
13. Ervine D. A., Koopaei K.B., and Sellin R. H. J. (2000)." Two-Dimensional Solution for Straight and Meandering Over-bank Flows." *Journal of Hydraulic Engineering*, ASCE, Vol. 126, No. 9, September, paper No.22144, 653-669.
14. Ghosh, S. N., Jena, S. B.(1971), "Boundary Shear Distribution in open Channel Compound", Proc. I. C. E, Vol. 49, August .
15. "Guide for selecting roughness coefficient "*n*" values for channels". (1963). Soil Conservation Service, *U.S. Dept. of Agric*., Washington
16. Guo, J., and Julien, P. Y. (2005). ''Boundary shear stress in smooth rectangular openchannels.'' Proc., 13th Int. Association of Hydraulic Research, APD Congress, Singapore, Vol. 1, 76–86.
17. "Hydraulic capacity of meandering channels in straight floodway" (1956), Tech.Memorandum No. 2-429, U.S. Army Corps of Engineers, Waterways Experiment Station, Vicksburg, Miss.
18. Inglis, C.C.(1947), "Meander and Their Bering on River Training.", *Proceedings of the Institution of Civil Engineers, Maritime and Waterways Engineering Div., Meeting, 1947.*
19. James, M., and Brown, R. J.(1977), "Geometric parameters that influence flood plain flow", U. S. Army Engineer Waterways Experimental Station, Vicksburg, Miss., June, Research report H-77.

20. Jarrett, R. D. (1984). ‘‘Hydraulics of high gradient streams’’, *Journal of Hydr. Engg., ASCE*, 110, 1519–1539.

21. Javid,S., and Mohammadi,M.(2012). ‘‘Boundary Shear Stress in a Trapezoidal Channel.” IJE TRANSACTIONS A: Basics Vol. 25, No. 4, (October 2012) 365-373.

22. Jin,Y.C.,Zarrati, A. R. andZheng,Y. (2004). “Boundary Shear Distribution in Straight Ducts and Open Channels” *J. Hydraul. Eng.*, ASCE, 130(9), 924-928.

23. Johannesson, H., & Parker, G. (1989). “Linear theory of river meanders.”, *Water Resources Monograph, 12*, 181-213.

24. Khatua, K. K. (2008), “Interaction of flow and estimation of discharge in two stage meandering compound channels”. Thesis Presented to the National Institute of Technology, Rourkela, in partial fulfilment of the requirements for the Degree of Doctor of philosophy.

25. Khatua, K.K and Patra, K.C,(2010). Evaluation of boundary shear distribution in a meandering channel.Proceedings of ninth International Conference on Hydro-Scienceand Engineering, IIT Madras, Chennai, India, ICHE 2010, 74.

26. Khatua K.K., Patra K.C., (2013) “stage–discharge prediction for meandering channels”, Int. J. Comp. Meth. and Exp. Meas., Vol. 1, No. 1 80–92

27. Khatua K.K., Patra K.C., Nayak P. (2012), “Meandering effect for evaluation of roughness coefficients in open channel flow” *Sixth* international conf. on river basin management, WIT Transactions on Ecology and the Environment (ISSN 1743-3541), CMEM, WIT Press., 146(6):213-227.

28. Knight, D. W. (1981). “Boundary shear in smooth and rough channels.” *J. Hydraul. Div., Am. Soc. Civ. Eng.*, 107(7), 839–851.

29. Knight D. W. and Demetriou J.D. (1983). “Floodplain and main channel flow interaction.” *J. Hydraul. Eng.*, ASCE, 109(8), 1073–92.

30. Knight, D. W., and MacDonald, J. A. (1979). "Open-channel flow with varying bed roughness." *J. Hydraul. Div., Am. Soc. Civ. Eng.,* 105(9), 1167–1183.
31. Knight, D. W., and Sterling, M. (2000), "Boundary shear in circular pipes running partially full.", *Journal of Hyd. Engg., ASCE* Vol.126, No.4.
32. Knight, D.W., Yuan, Y. M., and Fares, Y. R. (1992). "Boundary shear in meandering channels.", *Proceedings of the Institution Symposium on Hydraulic research in nature and laboratory,* Wuhan, China (1992) Paper No.11017, Vol. 118, Sept., pp. 151-159.
33. Langbein, W. B., & Leopold, L. B. (1966). "River meanders--Theory of minimum variance" (pp. 1-15). US Government Printing Office.
34. Leighly, J. B. (1932). "Toward a theory of the morphologic significance of turbulence in the flow of water in streams." Univ. of Calif. Publ. Geography,6(1), 1–22.
35. Mellor GL, Herring HJ. "A survey of mean turbulent field closure.", AIAA Journal 1973; 11:590 – 599.
36. Mohanty, L. (2013), "Velocity Distribution in Trapezoidal Meandering Channel". Thesis Presented to the National Institute of Technology, Rourkela, in partial fulfilment of the requirements for the Degree of Doctor of philosophy.
37. Mohanty, P.K., Dash, S. S. and Khatua, K. K. (2012). "Flow Investigations in a Wide Meandering Compound Channel." International Journal of Hydraulic Engineering 2012, 1(6) : 83-94
38. Myers, W. R. C. (1978). "Momentum transfer in a compound channel." *J. Hydraul. Res.,16(2),* 139–150.
39. Patel, V. C. (1965). "Calibration of the Preston tube and limitations on its use in pressure gradients.", *Journal of Fluid Mechanics*, *23*(01), 185-208.

40. Patnaik, M. (2013), "Boundary Shear Stress Distribution in Meandering Channels". Thesis Presented to the National Institute of Technology, Rourkela, in partial fulfilment of the requirements for the Degree of Doctor of philosophy.
41. Patra, K.C, and Kar, S. K. (2000), "Flow Interaction of Meandering River with Floodplains". *Journal of Hydr. Engrg., ASCE,* 126(8), 593–604.
42. Patra, K. C., and Kar, S. K., Bhattacharya, A. K. (2004). "Flow and Velocity Distribution in Meandering Compound Channels.", *Journal of Hydraulic Engineering, ASCE,* Vol. 130, No. 5. 398-411.
43. Preston, J. (1954). "The determination of turbulent skin friction by means of Pitot tubes.", *Journal of the Royal Aeronautical Society, 58*(518), 109-121.
44. Rajaratnam, N., and Ahmadi, R.M. (1979). "Interaction between Main Channel and Flood Plain Flows." *Journal of Hydraulic Division, ASCE,*Vol..105, No. HY5, pp. 573-588.
45. Rhodes, D. G., and Knight, D. W. (1994). "Distribution of Shear Force on Boundary of Smooth Rectangular Duct.",*Journal of HydralicEngg.*, 120-7, 787– 807.
46. Saine S. Dash, K. K. Khatua, P. K Mohanty (2013), "Energy loss for a highly Meandering open Channel Flow", *Res. J. Engineering Sci.,* Vol. 2(4), 22-27, April (2013).
47. Saine S. Dash, K. K. Khatua, P. K. Mohanty (2013), "Factors influencing the prediction of resistance in a meandering channel", *International Journal of Scientific & Engineering Research* ,Volume 4, Issue 5, May-2013.
48. Sellin R. H. J. (1961.), "A Study of the Interaction between Flow in the Channel of a River and that over its Floodplain", Ph. D Thesis, University of Bristol, Bristol, England
49. Sellin, R. H. J. (1964), "A Laboratory Investigation into the Interaction between the Flow in the Channel of a River and that over its Floodplain", La. Houille Blanche.

50. Shiono K., Al-Romaih I. S., and Knight D. W., (1999), "Stage-discharge assessment in compound meandering channels", *Journal of Hydraulic Engineering*, ASCE, 125 (1), 66-77, Mar., 45-54, and discussion in 1993, 101, Dec., 251-252.
51. Shiono, K., Muto, Y., Knight, D.W. & Hyde, A.F.L.(1999), "Energy Losses due to Secondary Flow and Turbulence in Meandering Channels with Overbank Flow.", *Journal of Hydraulic Research*, IAHR, Vol. 37, No. 5, pp. 641-664.
52. Shukry A. (1950), "Flow around Bends in an Open Flume", Transactions ASCE, Vol. 115, pp 75L788.
53. Thomson J. (1876), "On the origins of windings of rivers in alluvial plains, with remarks on the flow of water round bends in pipes", Proc. Royal Society of London,Vol. 25, 5-8.
54. Thomas TG. and Williams J.(1995a). "Large eddy simulation of a symmetric trapezoidal channel at Reynolds number of 430,000." *J. Hydraul. Res.*. 33(6), pp. 825-842.
55. Thomas TG. and Williams J.(1999). Large eddy simulation of flow in a rectangular open channel. *J. Hydraul Res.* 37(3), pp. 345-361.
56. Toebes, G.H., and Sooky, A.A. (1967),"Hydraulics of Meandering Rivers with Floodplains." *Journal of the waterways and Harbor Division, Proceedings of ASCE*, Vol.93, No.WW2, May, pp. 213-236.
57. Willetts B.B. and Hard Wick R.I. (1993), "Stage dependency for overbank flow in meandering channels", *Proc. Instn Civ. Engrs, Wat., Marit. & Energy*, 101.
58. Wormleaton, P.R., Allen, J., and Hadjipanos, P. (1982). "Discharge Assessment in Compound Channel Flow." *Journal of Hydraulic Engineering, ASCE*, Vol.108, No.HY9, pp. 975-994.
59. Yang, S. Q. and McCorquodale, John A. (2004) "Determination of Boundary Shear Stress and Reynolds Shear Stress in Smooth Rectangular Channel Flows." *Journal of Hydr. Engrg.*, Volume 130, Issue 5, pp. 458-462.

Publications from the Research

A: Journal

1. **Arpan Pradhan**, Saine S. Dash, K. K. Khatua (2014), "Water Surface Profile along a meander path of a Sinuous Channel", *IOSR Journal of Mechanical and Civil Engineering (IOSR-JMCE)* e-ISSN: 2278-1684, p-ISSN: 2320-334X, PP 48-52.
2. **Arpan Pradhan**, Kishanjit K. Khatua and Debashish Khuntia (2014), "Study of Variation in Velocity Profile along a 120° Meandering Path" *INROADS- An International Journal of Jaipur National University* Year: 2014, Volume: 3, Issue: 1s, pp 157-160 Print ISSN : 2277-4904. Online ISSN: 2277-4912.

B: Conference

1. **Arpan Pradhan**, Saine S. Dash, K. K. Khatua, "Transverse Water Surface Profile of a Meandering Channel", *Proceedings of Symposium on Integrated Water Resources Management* (*IWRM-2014*), CWRDM, Kozhikode, Kerela, India. Volume: I, pp: 3-8
2. S. S. Dash, K. K. Khatua, **Arpan Pradhan**, "Depth Average Velocity Prediction for Highly Sinuous Meandering Channel", *ISUD-9*, Aug. 27-29, 2014, France. (Accepted)
3. **Arpan Pradhan**, K. K. Khatua, Saine S. Dash, "Boundary Shear Force Distribution along different reaches of a Highly Meandering Channel" *HYDRO-2014 International, 19th International Conference on Hydraulics, Water Resources and Environmental Engineering*, Dec. 18-19, 2014, MANIT, Bhopal, India.
4. S. S. Dash, K. K. Khatua, **Arpan Pradhan**, "Roughness Variation in a Meandering Compound Channel" *HYDRO-2014 International, 19th International Conference on Hydraulics, Water Resources and Environmental Engineering*, Dec. 18-19, 2014, MANIT, Bhopal, India.